LATE WISCONSINAN GLACIAL HISTORY OF PLACENTIA BAY, NEWFOUNDLAND, AS INTERPRETED FROM SEABED GEOMORPHOLOGY AND STRATIGRAPHY

DENISE BRUSHETT

Late Wisconsinan glacial history of Placentia Bay, Newfoundland, as interpreted from seabed geomorphology and stratigraphy

By

Denise Brushett

A thesis submitted to the
School of Graduate Studies
in partial fulfillment of the
requirements for the degree of
Master of Science

Department of Geography
Memorial University

April 2008

St. John's Newfoundland

Abstract

This thesis reconstructs the glacial history of Placentia Bay, Newfoundland through the integration of seabed data and existing terrestrial records. Multibeam sonar data, augmented by seismic and coring data revealed a range of flow-parallel and flow-transverse glacial landforms on the Placentia Bay seabed. Flow-parallel landforms include drumlins, flutes, megaflutes and crag-and-tails. These landforms show a general trend of convergent flow, interpreted to represent fast-flowing ice converging into an ice stream down the axis of Placentia Bay. Flow-parallel landforms and striations from the surrounding land areas demonstrate that the convergent flow can be traced up-ice to regional ice dispersal centres. Flow-transverse landforms include De Geer moraines and grounding-line moraines. De Geer moraines occur in several fields throughout the bay marking the intermittent retreat of grounded ice up the bay. Radiocarbon ages from glaciomarine silt suggest that ice became ungrounded and glaciomarine sedimentation started ca. 16.1 cal ka BP and ended after 12.0 cal ka BP. This glacial landsystem is consistent with a conceptual model showing Late Wisconsinan ice advance to shelf edges with rapid calving retreat along deepwater channels and slower retreat of ice margins grounded in shallow water. The integrated approach used in this study represents an important development in mapping palaeo ice flows and the understanding of ice sheet behaviour during the transition from largely marine-based to land-based glacial conditions which may reflect deglacial scenarios in other bays in Newfoundland and elsewhere.

Acknowledgements

I extend my greatest thanks to my supervisor Dr. Trevor Bell who went above and beyond the expectations of any supervisor and for always encouraging me to think independently and question the data. I would like to thank my supervisory committee: Dr. John Shaw for his guidance on cruises, for providing data and assisting me in my interpretations and Dr. Martin Batterson for his patient positive witty feedback. I have been very fortunate to be surrounded by fellow students, in particular, Mariana Trinidade, Alison Copeland and Bryan Martin who have been there to provide much needed stress relief and editing. Finally thanks to my parents, sisters and Joe Rossiter for all their unending patience and support.

Table of Contents

List of Tables

List of Figures

List of Appendices

Chapter 1: Introduction

1.1 Introduction

This thesis reconstructs the glacial history of Placentia Bay, Newfoundland using both onshore and offshore glacial records. Traditionally, palaeo ice-flow mapping in Newfoundland and Labrador has had a predominantly terrestrial focus, combining surficial geology, striation data, and clast provenance studies. However, recent technological advances in both marine (multibeam bathymetric sonar) and terrestrial (Shuttle Radar Topography Mission (SRTM)) mapping have generated landscape and seabed imagery that permit a broader interpretation of glacial geomorphology and palaeo ice dynamics (*e.g.*, Liverman *et al.*, 2006; Shaw *et al.*, 2006a). In this thesis, recently generated multibeam bathymetric sonar data are integrated with existing terrestrial records to reconstruct the glacial history of Placentia Bay.

Recent interpretations of glacial geomorphology and palaeo ice dynamics of Newfoundland and Atlantic Canada represent an integrated research approach (*e.g.*, ACID Group, 2002), which has been important in shaping conceptual models of glaciation. According to these models, the most recent glaciation to have inundated the Newfoundland and Atlantic Canadian landscape occurred ca. 80-10 ka (*e.g.*, Shaw *et al.*, 2006a; Stea, 2004). Glacial cover had three general recurring characteristics: 1) almost complete ice coverage extending out to the shelf edge (*e.g.*, King, 1996; Shaw *et al.*, 2006a; Todd *et al.*, 1999); 2) multiple zones of ice dispersal in the form of peripheral ice caps that were present during the growth and decay of the Laurentide Ice Sheet (*e.g.*, Catto, 1998; Stea *et al.*, 1998; Stea, 2004); and 3) discrete zones of ice streaming and calving (*e.g.*, Shaw *et al.*, 2006a). Despite this new initiative, there remain many areas

that must be tested with field data or where ambiguous or conflicting interpretations have been proposed. In addition, limitations still exist in determining where on the seafloor the maximum ice extent was reached and in dating ice limits, both on the seabed and on land, where there is a general absence of organics for radiocarbon dating. As such, the maximum extent of ice at the last glacial maximum (LGM) is poorly known and precise reconstructions of the growth and decay of the Wisconsinan ice cover remains a future objective (Shaw, 2003).

In the past decade, more detailed palaeo ice reconstructions have been made possible largely by advances in multibeam bathymetric sonar imaging of the seafloor on which lies an important portion of the evidence for palaeo ice dynamics. Multibeam sonar data provide high-resolution digital bathymetry of the seabed which reveals a wealth of previously unmapped morphological features. The recognition of these features provides improved mapping of glacial landforms and delineation of offshore ice margins (*e.g.*, Shaw and Courtney, 1997; Shaw *et al.*, 1997).

In the present study, glacial landforms preserved on the seabed of Placentia Bay, Newfoundland, are mapped using recently acquired multibeam bathymetric data. It is anticipated that, based on similar nearshore studies (*e.g.*, Bedford Basin and Halifax Harbour, Nova Scotia; see Miller and Fader, 1995), the Placentia Bay seabed preserves a geomorphic record of equal or higher resolution than that of the adjacent terrestrial landscape. In addition, it is anticipated that the integration of these seabed data with existing onshore landform and striation data will permit onshore-offshore correlation of glacial geomorphology and palaeo ice flows. Previous studies have had to rely on stratigraphic correlations of terrestrial and marine glacigenic units, together with

inferences about glaciological behaviour of palaeo ice sheets (*e.g.*, Bell *et al.*, 1999). Thus, this combined ice-flow database represents a further development in the integration of onshore and offshore glacial records in Newfoundland.

This project also provides an opportunity to test the understanding of ice-sheet behavior across the transition from largely marine-based to land-based glacial conditions. For example, abrupt temporal and spatial shifts in ice-bed interactions of a marine-based ice sheet may produce a broad assemblage of subglacial landscapes reflecting conditions ranging from sustained fast flow to rapid disintegration and ice-marginal retreat. In the past decade, the understanding of subglacial landscapes has progressed substantially, largely as a result of research on contemporary ice sheets such as the West Antarctic ice sheet and those ice streams which drain the Siple Coast (*e.g.*, Evans, 2003; Vaughan, 2006). This body of research has shown that such ice streams display transient behavior at both spatial and temporal scales and are situated upon a bed of sediment that can be deformed and mobilized, in contrast to previous ideas which suggested that they formed on underlying bedrock (*cf.* Stokes and Clark, 2001). These findings have placed new emphasis on research relating to subglacial landforms and their importance to the interpretation of glacial events and palaeo ice dynamics. It is expected that the reconstruction of past glacial dynamics in Placentia Bay will provide insight into possible deglacial scenarios for other bays and inlets around Newfoundland and elsewhere.

1.2 Study Area

The study area includes all of Placentia Bay covering an area of approximately 6000 km^2. It is a glacially modified marine basin which lies on the southeastern coast of Newfoundland, opening to the Atlantic Ocean to the southwest. Placentia Bay has many islands, shoals, reefs and banks as well as three well-defined channels where maximum depths exceed 430 m. It is bordered by the Burin Peninsula to the west, the Avalon Peninsula to the east, and the Isthmus of Avalon to the north (**Figure 1.1**). In this thesis, the Placentia Bay study area is defined as the region extending from the head of the bay, around North Harbour, out to the mouth of the bay (approximately 120 km long). The bay is approximately 20 km at its head and widens to 90 km at its mouth.

Interpretation of multibeam data is placed within a general regional framework that includes adjacent parts of the surrounding peninsulas. This larger region includes the Burin Peninsula (bounded by Gisborne Lake to the north), the Isthmus of Avalon and the western Avalon Peninsula.

1.3 Context

This thesis uses seabed data made available by the Geological Survey of Canada's (GSC) *Geoscience for Ocean Management* (*GOM*) Program. Seabed mapping surveys were carried out in 2004, 2005 and 2006, building upon earlier surveys in 1995 and 1999. These surveys were undertaken in cooperation with the Canadian Hydrographic Service (CHS) and with the support of the *SMARTBAY* project (a pilot project within Canada's *Oceans Action Plan* (OAP)).

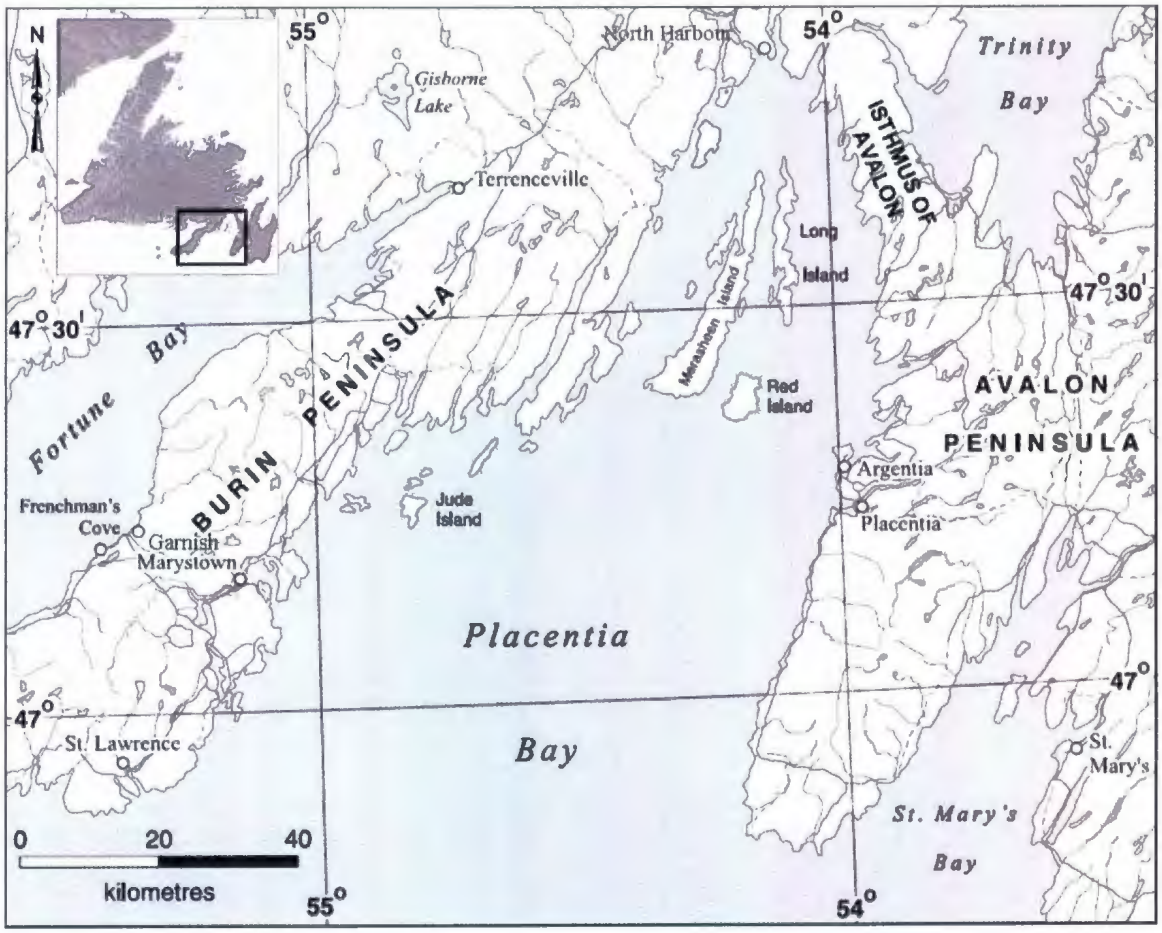

Figure 1.1 Location map of Placentia Bay, Newfoundland, bordered by the Burin Peninsula to the west and the Avalon Peninsula to the east. Place names referred to in the text are labeled.

Multibeam bathymetric data exist for most of the bay with the exception of some shallow areas at the coast and surrounding islands. These surveys revealed areas of rugged topography with northeast-southwest trending bedrock ridges, deep channels and other areas with complex glacial landform assemblages (Brushett *et al.*, 2007; Batterson *et al.*, 2006; Shaw *et al.*, 2006b). Follow-up activities, including subbottom profiling, bottom photography, grab sampling and piston coring, were carried out in two subsequent surveys (Shaw *et al.*, 2006b; 2006c). Together, these data will be used by the *GOM* program to produce maps of bathymetry, acoustic backscatter and surficial geology for Placentia Bay, similar to those recently published for St. George's Bay, southwest Newfoundland (Shaw *et al.*, 2006d; 2006e; 2006f).

The Department of Fisheries and Oceans and *SMARTBAY* are using these data to improve management and sustainable development of the diverse coastal and ocean resources in the bay. The high level of research interest from these programs stems from the identification of Placentia Bay as an environmentally sensitive area that hosts an abundant and diverse marine ecosystem combined with the highest potential for an oil-related accident in Canada. The presence of an oil refinery (and plans for a new refinery) and transshipment terminal has increased tanker traffic and the risk of accidents, necessitating the need for increased research and improved management of resources (Canadian Centre for Marine Communications, 2004).

1.4 Research rationale

The data generated from the *GOM* program are an important contribution to the understanding of the glacial history of this region and provide geomorphic and

sedimentologic links between the terrestrial and marine environments. Placentia Bay has a complex palaeo ice-flow history, draining ice from the surrounding Burin and Avalon peninsulas, both of which also preserve a complex record of glacial movements (*e.g.*, Catto, 1998; Batterson *et al.*, 2006). However, there are few published data pertaining to its glacial history, with the exception of the most recent conceptual model of glaciation (Shaw *et al.*, 2006a). According to this model, Placentia Bay was a conduit for ice which extended out of the bay towards the continental shelf edge. Thus, an interpretation of the seabed data provides a fuller understanding of glacial events in Placentia Bay and also provides a test of the recent conceptual model by Shaw *et al.* (2006a).

Details regarding the ice-flow history of the surrounding terrestrial areas also remain uncertain. For the most part, the ice-flow history of the Avalon and Burin peninsulas is based on complex cross-cutting relationships of striations (*e.g.*, Batterson *et al.*, 2006). Previous work on the glacial history of the Burin Peninsula, detailed in the following chapter, has had very different interpretations ranging from an ice-free peninsula (with the exception of limited local ice) (Tucker and McCann, 1980; Tucker, 1979) to multiple ice-flow phases during the last glaciation (Batterson *et al.*, 2006). The seabed data from Placentia Bay provide additional details on the surrounding glacial history and may resolve these previous palaeo ice flow discrepancies.

In order to reconstruct the pattern of late Wisconsinan glacial dynamics in Placentia Bay, several research tasks were devised: 1) an analysis of the glacial geomorphic evidence on the seabed of Placentia Bay from the multibeam sonar data and groundtruthing data; 2) the development of a relative and absolute chronology of glacial events, using morphostratigraphic relationships of glacial landforms and ^{14}C data from

marine cores, respectively; 3) an interpretation of ice-flow events and the pattern of ice retreat in Placentia Bay; and 4) an integration of the seabed glacial history with the surrounding terrestrial glacial records.

1.5 Thesis Structure

The thesis is organized to reflect the research tasks outlined in 1.4. Chapter 2 discusses previous studies and research questions stemming from these studies. This is followed by a description of the study area and methods used to address the research questions in Chapter 3. Chapter 4 describes the surficial geology and glacial landforms preserved on the seabed of Placentia Bay. Chapter 5 details the ice-flow events and pattern of ice retreat in Placentia Bay and discusses the local and regional ice flow history in the context of these new data. It concludes with a summary of the contributions made to understanding this ice flow history as well as the advantages and limitations that come from using onshore and offshore glacial records.

Chapter 2: Previous Work and Research Questions

2.1 Outline

This chapter begins with a review of ideas concerning glaciation in Newfoundland and in regions surrounding Placentia Bay. It starts with a review of models of glaciation in Newfoundland and Atlantic Canada, followed by a discussion of the glacial history, both on land and offshore. The latter includes a discussion of conflicting interpretations that have been proposed in the past and knowledge gaps that have yet to be tested with field data. Finally, research questions stemming from this discussion are listed.

2.2 Glacial History

2.2.1 Changing models of glaciation

Several models of glaciation of Atlantic Canada and Newfoundland have been developed over the past century. Traditionally, these models were divided into those that supported either a minimum or maximum ice extent (**Figure 2.1**) (see discussion in Grant, 1989). The minimum model, based primarily on terrestrial morphology and stratigraphy, had late-Wisconsinan ice restricted to lowland terrestrial areas, with ice margins near the present day coast, leaving many areas ice-free (Dyke and Prest, 1987; Grant, 1989). The maximum model, based primarily on offshore stratigraphy, suggests that ice extended out to the continental shelf break (Dyke *et al.*, 2002; Grant, 1989). This model also included a series of Newfoundland-hosted ice dispersal centres as part of the Newfoundland Ice Cap, separate from the Laurentide Ice Sheet, with the exception of ice that flowed across the tip of the Great Northern Peninsula from southern Labrador (Grant, 1989).

Figure 2.1. Models of ice extent over Atlantic Canada. The maximum model (indicated by gray dotted line) has ice margins at the continental shelf edge. The minimum model (indicated by black dashed line) has ice margins close to the present day coasts (modified from Grant, 1989). Box indicates location of study area.

More recently, Stea (Stea *et al.*, 1998; Stea, 2004) proposed an intermediate model of ice extent which described the growth and convergence of local ice dispersal centres, together with Laurentide ice that drained down the Laurentian Channel producing an extensive ice cover that reached near the continental shelf edge.

The most recent conceptual model of deglaciation in Atlantic Canada proposed by Shaw *et al.* (2006a) supports an intermediate model of ice extent. This model, derived from both onshore and offshore evidence, suggested that multiple local ice dispersal centres produced almost complete ice coverage extending out to the continental shelf edge and also included discrete zones of ice streaming and calving.

Shaw *et al.* (2006a) believed that ice streams played a critical role in the ice sheets that covered Atlantic Canada. Ice streams are regions in a grounded ice sheet in which the ice flows much faster than in regions on either side (Stokes and Clark, 1999). Stokes and Clark (1999) summarized a number of geomorphic criteria for identifying former ice streams: 1) landform assemblages display highly convergent flow patterns; 2) subglacial landforms are highly attenuated (length:width > 10:1), indicative of rapid velocity; 3) ice streams are marked by abrupt lateral shear margins; 4) deformable bed conditions are present as ice stream marginal moraines or deformed till; and 5) focused sediment delivery is present as submarine accumulation of sediment (*e.g.*, trough mouth fans or till deltas).

2.2.2 Glacial history of Newfoundland

A brief glacial history of Newfoundland is presented below and incorporates ideas discussed by Shaw *et al.* (2006a) in the most recent conceptual model of deglaciation. A

location map of Newfoundland with place names discussed below is provided in **Figure 2.2**. **Figure 2.3** shows the locations of offshore banks and channels discussed below.

During the last glacial maximum (LGM), Newfoundland supported its own ice cap that was mostly independent of the Laurentide Ice Sheet (Grant, 1989). Ice reached its maximum extent with the eastern and southern margins close to the continental shelf edge at approximately 21 ka BP (**Figure 2.4**). A major ice stream in the Laurentian Channel was fed by converging ice, originating mostly north of the Cabot Strait, including the western ice margin of Newfoundland. This necessitated a first-order ice divide that extended south and southeast across Newfoundland along the axis of the Long Range Mountains, and east through central Newfoundland and the Avalon Peninsula. Second-order ice divides extended over southwest Newfoundland and over the Cape Freels Peninsula which separated ice-flow into the Notre Dame Basin from flow in Trinity Basin (Shaw *et al.*, 2006a).

The conceptual model suggests that early ice retreat was facilitated by calving along deeper channels (Shaw *et al.*, 2006a). By 20 ka BP, calving was occurring in the Laurentian Channel Ice Stream, the largest calving margin in the region. By 18 ka BP, the evacuation of ice from calving lowered ice elevations further inland and ice margins began to retreat inland from the continental shelves (**Figure 2.5**). Ice streams occupied basins and troughs and it was along these that calving proceeded. As deeper areas were evacuated, ice margins developed on shallower banks where there was no mechanism for rapid removal. Shaw *et al.* (2006a) suggests that these margins were likely ice walls which retreated slowly.

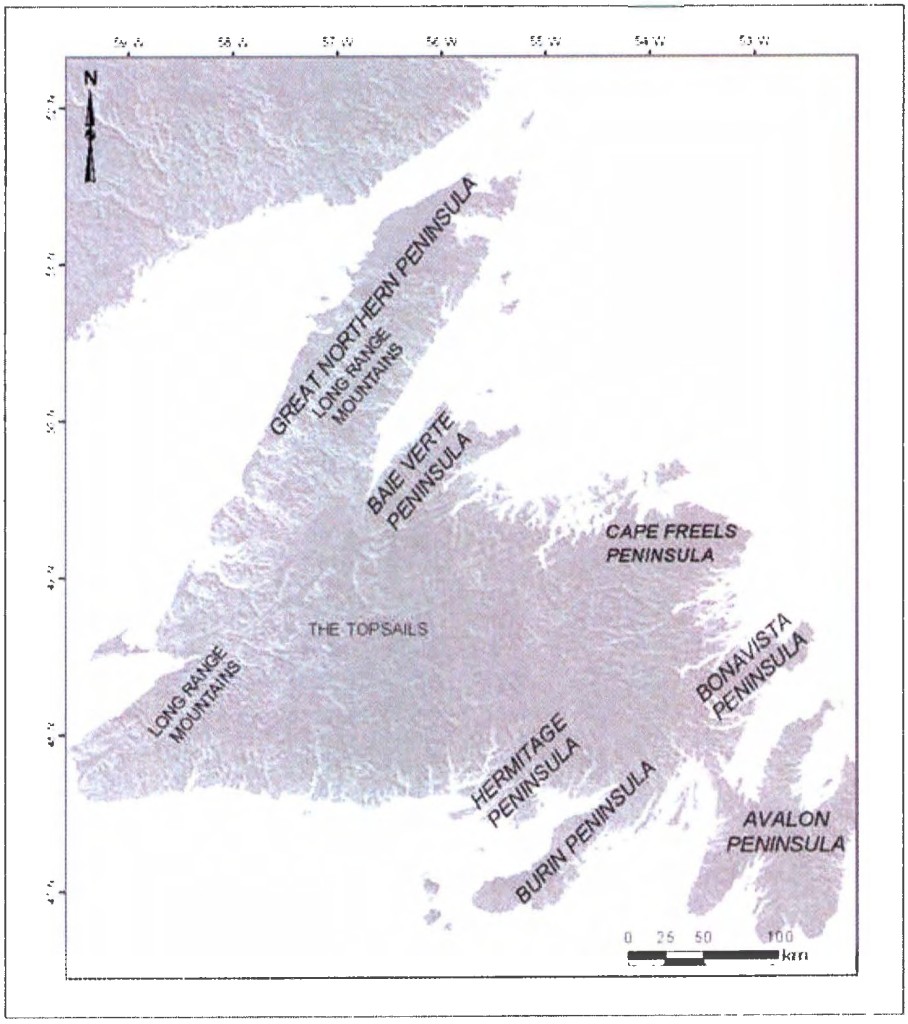

Figure 2.2 Location map of Newfoundland. Place names mentioned in the text are included.

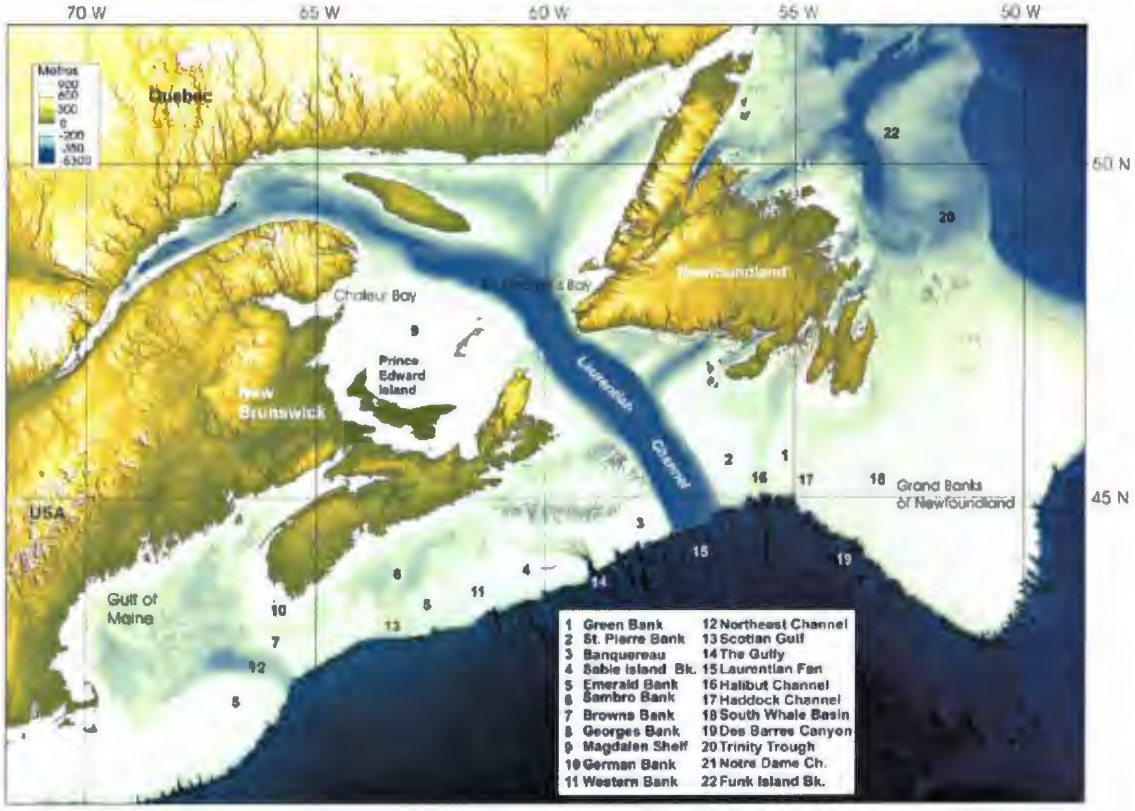

Figure 2.3 Digital elevation model of Atlantic Canada with offshore banks and channels indicated (from Shaw *et al.*, 2006a).

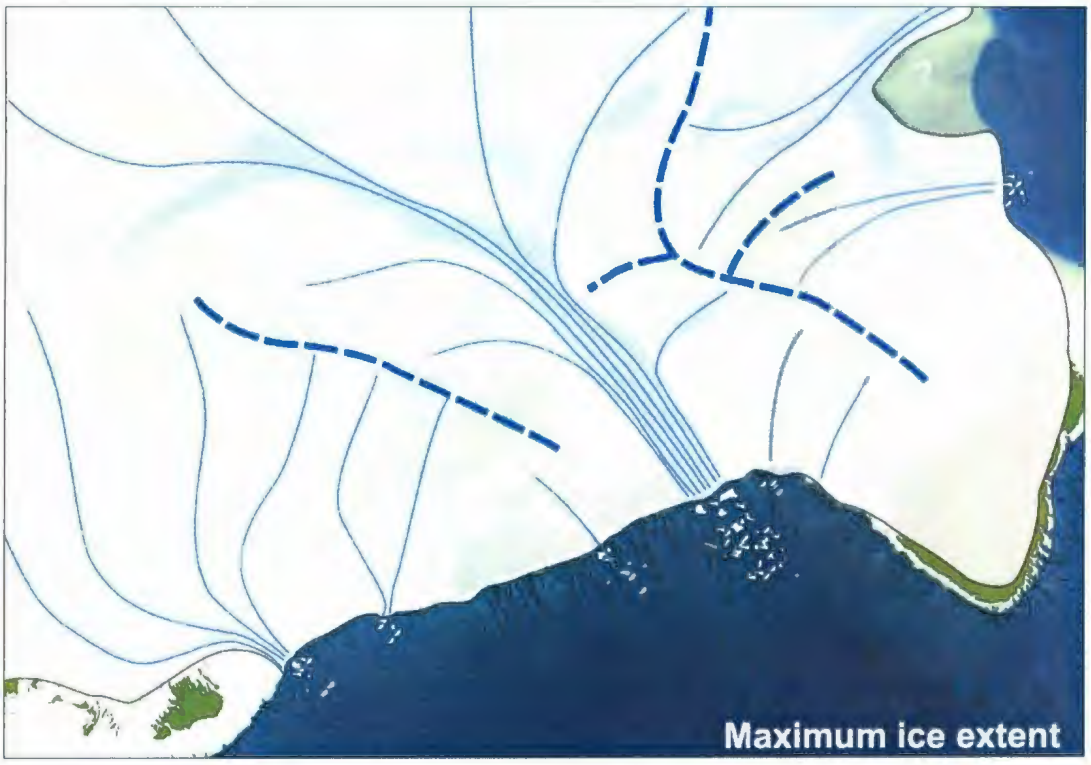

Figure 2.4 Last glacial maximum in Atlantic Canada. Generalized flow lines are indicated by thin blue lines. Major ice divides are shown with thicker blue dashed lines. The underlying digital elevation model shown here and in Figures 2.5- 2.7 is only an approximation that depicts the distribution of land and water at 13 ka BP (from Shaw *et al.*, 2006a).

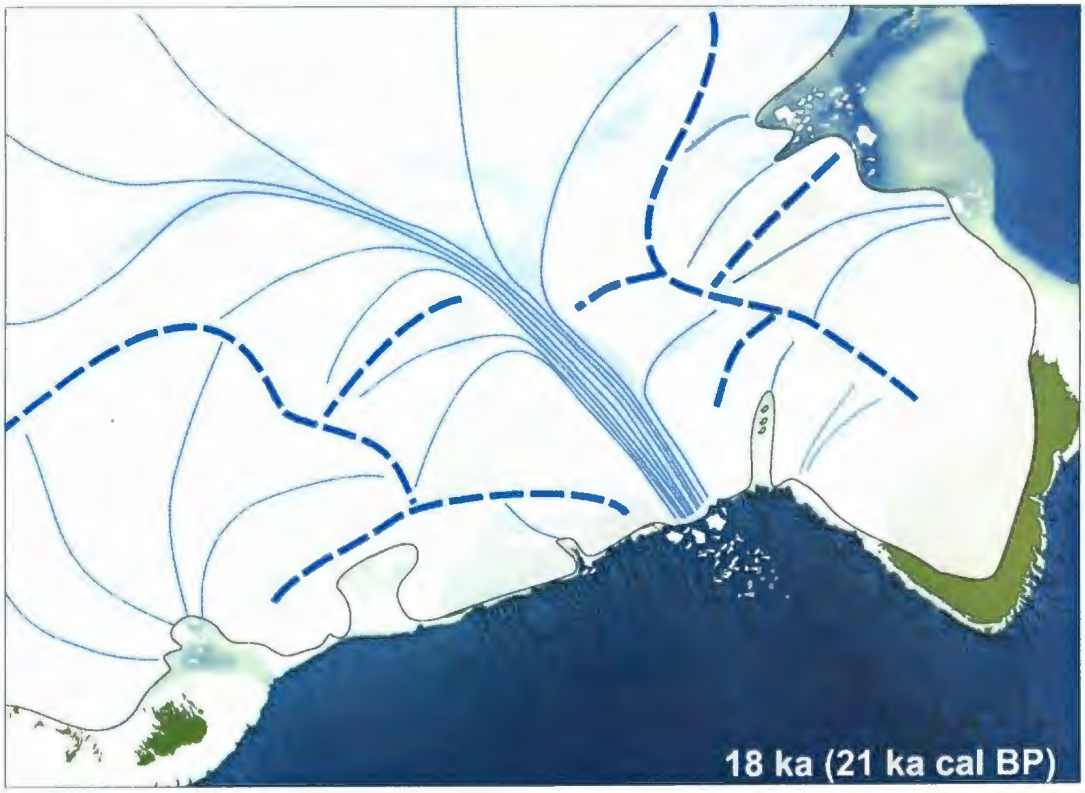

Figure 2.5 Glacial extent at 18 ka BP (from Shaw *et al.*, 2006a).

Calving was most prevalent in Notre Dame Bay and Halibut Channel where the rapidly retreating ice generated glaciomarine sedimentation on the seafloor (Miller *et al.*, 2001; Moran and Fader, 1997). Miller *et al.* (2001) suggest that sedimentation in Halibut Channel began prior to 19 ka BP and the channel was likely free of grounded ice by 18 ka BP. Dates off northeast Newfoundland associated with palynological data suggest that the margin of an ice stream in Trinity Bay had retreated with open waters off the northeast coast by this time (Scott *et al.*, 1989). In Bonavista Bay, radiocarbon dates from glaciomarine sediments overlying diamicton suggest that ice had retreated from the outer bay by ~ 13.5 ka BP (Cummings *et al.*, 1992).

By 16 ka BP, ice that had been flowing into Notre Dame Bay no longer converged with ice flowing into White Bay, leading to an ice lobe on the Baie de Verte Peninsula (**Figure 2.6**). Evidence comes from striations which indicate that this ice lobe separated ice-flow into either of the two calving margins (Liverman and St. Croix, 1989; Taylor, 2001). On the Newfoundland Shelf, open water extended up Halibut Channel and a lobe of thin grounded ice persisted over Grand Bank (Miller *et al.*, 2001; King *et al.*, 2001). North of Grand Bank, the retreating ice margin had grounded on a sill leading to the formation of the Trinity moraine which is dated ca. 15 ka BP (King *et al.*, 2001; King and Sonnichsen, 2000).

By 14 ka BP massive and rapid disintegration of the ice sheets was underway. Continued calving led to the isolation of the Newfoundland ice cap and smaller offshore ice caps (on the Grand Banks, St. Pierre Bank and St. Mary's Bay) and inter-stream ice lobes on peninsulas, including the Burin Peninsula (Shaw *et al.*, 2006a; Shaw, 2003) (**Figure 2.7**). The Newfoundland ice cap, now isolated from shelf ice, drained into fiords

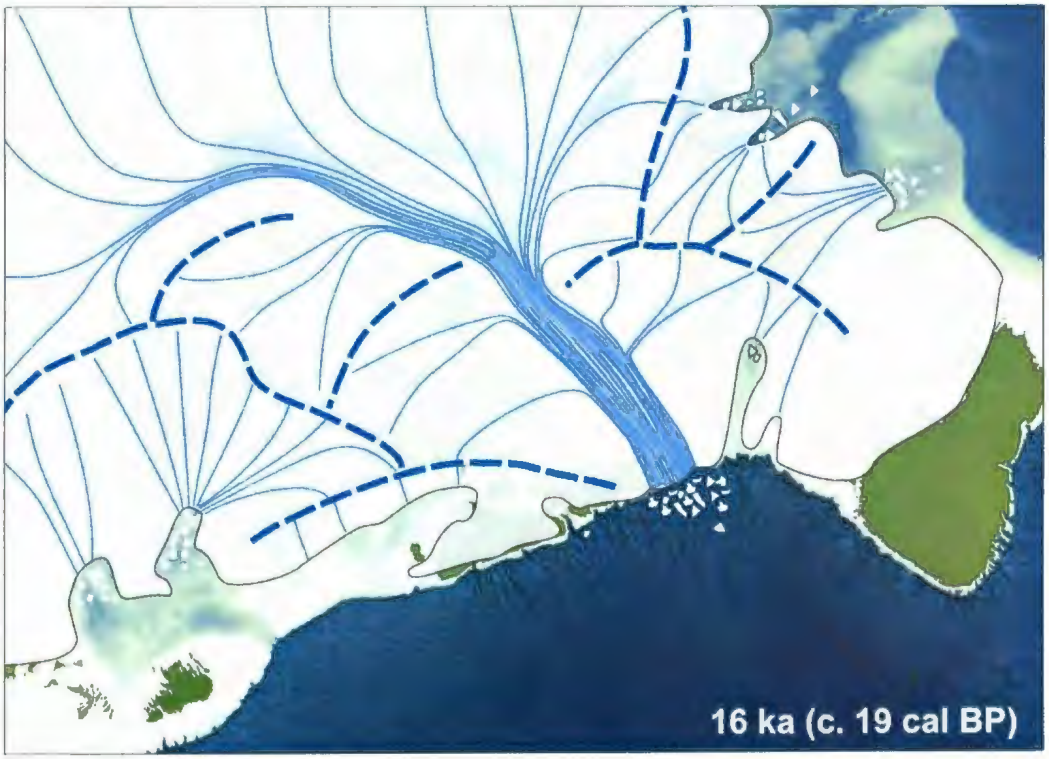

Figure 2.6 Glacial extent at 16 ka BP (from Shaw *et al.*, 2006a).

Figure 2.7 Glacial extent at 14 ka BP (from Shaw *et al.*, 2006a).

with ice-flow directions becoming increasingly controlled by local physiography. By ~12.5 ka BP ice had retreated up to the fiord heads (Shaw, 2003). Offshore, grounded ice created till tongues around St. Pierre Bank which are dated between 11 and 13 ka BP (Miller *et al.*, 2001). Bonifay and Piper (1988) suggested that ice lingered on St. Pierre Bank, followed by a late glacial surge in the vicinity of Halibut Channel out to the shelf edge at 11.5 -12.0 ka.

By 12 ka BP most of the ice on the island had retreated to the modern coasts in most areas (Shaw, 2003). Once on land, ice retreat (ablating by melting) was much slower. Deglacial ice dispersal centres were located over the Long Range Mountains, The Topsails, Middle Ridge and the Avalon Peninsula (Gosse *et al.*, 1995; Grant, 1989).

2.2.3 Glacial history of Placentia Bay

Few published data exist on the glacial history of Placentia Bay; interpretations of its glacial history, which are included in recent conceptual models, remain to be tested with field data. Before this study, data were limited to striations that occur on Merasheen and Long islands, where cross-cutting striation relationships suggest that at least two ice-flow events were present in the bay. Both of these ice-flow events are also recorded on the surrounding peninsulas and described in more detail below (Batterson *et al.*, 2006; Taylor, 2001). Important data pertaining to the glacial history of Placentia Bay are found southeast of the Burin Peninsula, where the Burin Moraine was identified during marine surveys (Fader *et al.*, 1982), detailed below.

The glacial history of Placentia Bay was influenced by several ice-flow events originating from the surrounding Burin and Avalon peninsulas; however the chronology

of events remains uncertain. Previous interpretations of the last glaciation on the Burin Peninsula have had very different interpretations ranging from a largely ice-free peninsula (Grant, 1975; Tucker and McCann, 1980; Tucker, 1979) to multiple ice-flow phases described in more detail below (Batterson *et al.*, 2006; Batterson and Taylor, 2007). For example, Tucker and McCann (1980) considered that the last ice flow to cross the peninsula was pre-Wisconsinan (**Figure 2.8**) whereas Batterson *et al.* (2006) proposed that all ice-flow events could be assigned a late Wisconsinan age based on the fresh and unweathered appearance of striations and the consistency of flow records with the main part of Newfoundland (**Figure 2.9**).

Three ice-flow events on the Burin Peninsula may have affected Placentia Bay. The oldest and most pervasive event originated from the northwest, likely the central Newfoundland ice divide and flowed across the Burin Peninsula into Placentia Bay. The record of this ice-flow is preserved in an extensive striation record (*e.g.*, Taylor, 2001), glacial erratic distributions (*e.g.*, Batterson and Taylor, 2007) and streamlined landforms including drumlins, flutes and crag-and-tails (*e.g.*, Batterson *et al.*, 2006) (**Figure 2.10**).

A second ice-flow, predominantly westward on the Burin Peninsula, appears to have originated in Placentia Bay and is clearly recorded on the younger event in cross-cutting striation records. This flow appears to have had little influence on sediment dispersal but remoulded bedrock in the central part of the peninsula (Batterson and Taylor, 2007). The distribution of striations necessitates that any source of ice must have been of sufficient thickness to have crossed the entire peninsula, which is over 170 m asl

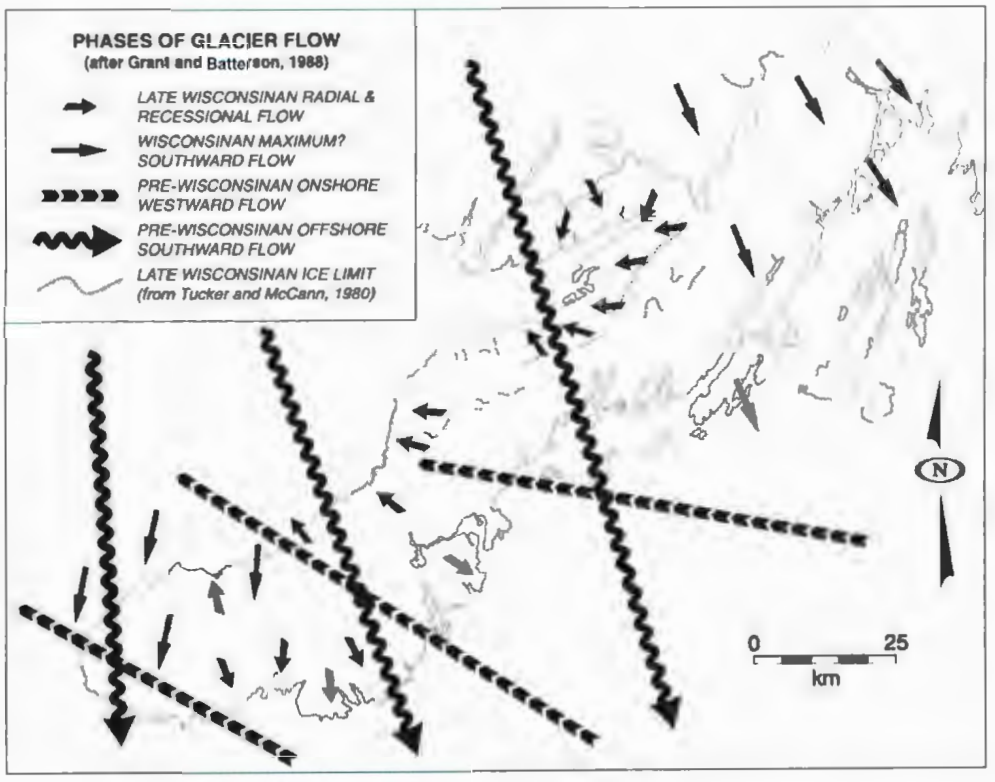

Figure 2.8 Glacial flow phases on the Burin Peninsula, as published in the 1980s (from Batterson *et al.*, 2006, after Grant and Batterson, 1988; Tucker and McCann, 1980).

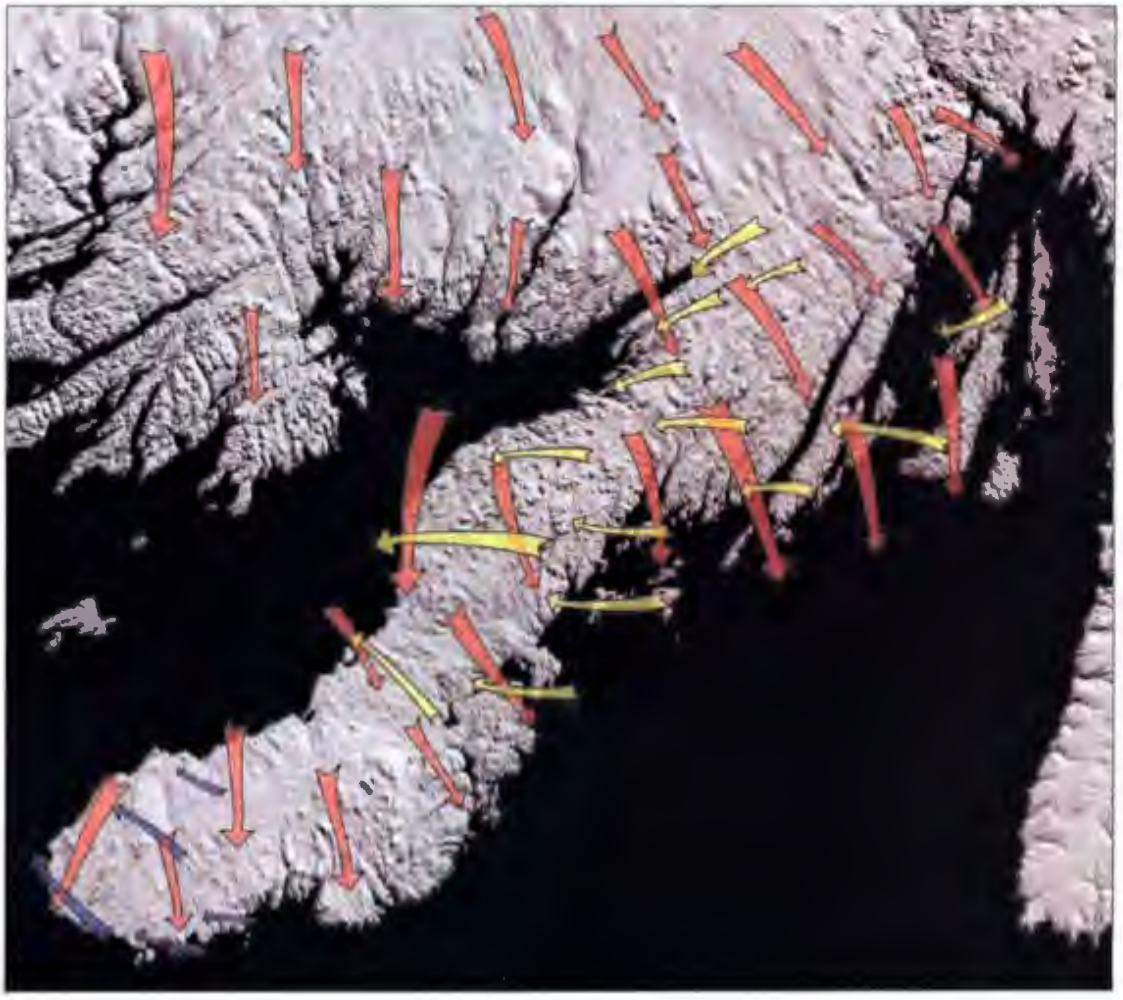

Figure 2.9 Glacial flow phases on the Burin Peninsula. Red arrows represent an ice-flow event that is relatively older than the ice-flow events represented by the yellow and purple arrows, which have the same relative age (after Batterson *et al.*, 2006).

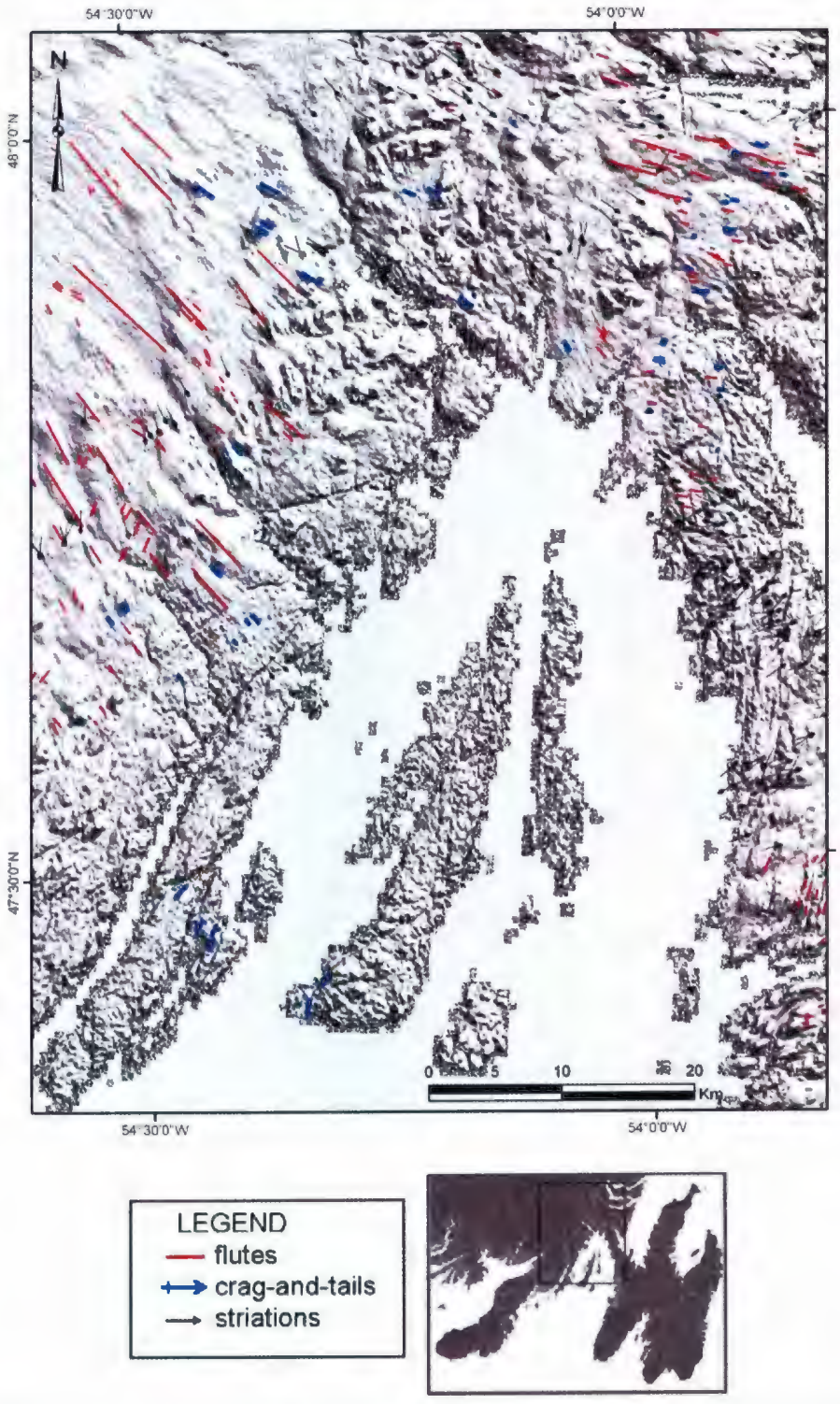

Figure 2.10 Large scale streamlined landforms identified from SRTM imagery in northern Burin Peninsula and the Isthmus of Avalon. Flutes and crag-and-tails parallel the orientation of striations measured in this area.

in the centre of the peninsula and reaches a maximum elevation of approximately 320 m asl.

The source of this westward flow is uncertain and several hypotheses have been proposed to explain its source. One hypothesis is that ice originated from an ice centre which resulted from the isolation of the Burin Peninsula inter-stream lobe by calving along deep water on either side of the peninsula (Shaw, 2003). Shaw *et al.* (2006a) suggest that this ice cap was sustained for a long time and grew in size. The conceptual model by Shaw *et al.* (2006a) shows an ice cap extending down the Burin Peninsula and onto St. Pierre Bank (shown in **Figure 2.7**) coinciding with the location of the Burin Moraine (Fader *et al.*, 1982).

Another hypothesis is that this ice originated from an ice centre over St. Mary's Bay (Batterson and Taylor, 2007). They suggested that the westward flow from the Avalon Peninsula during the late Wisconsinan was confluent with Newfoundland ice, flowing southward down Placentia Bay. During deglaciation and following retreat of Newfoundland ice, ice crossed Placentia Bay and the Burin Peninsula.

A third ice flow, though perhaps only spatially and not temporally distinct from the second flow, is found on the southern tip of the peninsula and records a northwestward flow onto land from an offshore source (Tucker, 1979; Tucker and McCann, 1980; Batterson and Taylor, 2007).

On the eastern side of Placentia Bay, the Avalon Peninsula supported an independent ice cap during the last glaciation (*e.g.*, Henderson, 1972; Catto, 1998). The main ice centre was located over St. Mary's Bay with smaller ice centres over the sub-peninsulas (**Figure 2.11**). Striation and streamlined landforms along the east coast of

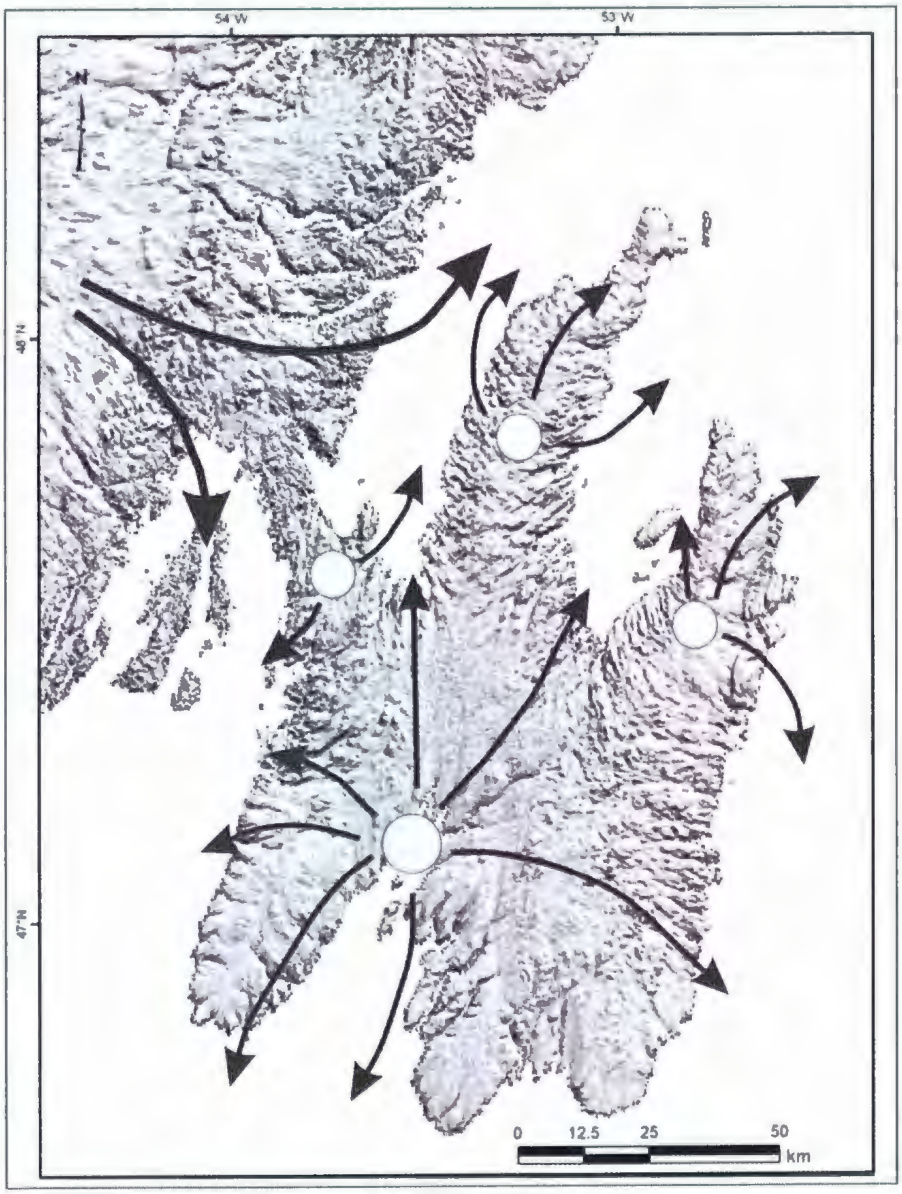

Figure 2.11 Ice-flow directions and ice dispersal centres on the Avalon Peninsula during and following the last glacial maximum. The largest ice centre was over St. Mary's Bay with smaller ice centres located over the Isthmus and sub-peninsulas (modified from Catto, 1998).

Placentia Bay suggest that an earlier ice flow crossed the coast and flowed southwest into the bay whereas a later flow flowed directly westward into the bay (Catto, 1998; Taylor, 2001).

The apparent convergence of southeastward flow on the Burin Peninsula and southwestward flow from the Avalon Peninsula, together with preliminary mapping of seabed features in Placentia Bay prompted Shaw *et al.* (2006a) to hypothesize the occurrence of an ice stream in the bay during the last glacial maximum. The idea of an ice stream in Placentia Bay is not new and was discussed in earlier studies from the Laurentian Channel (*e.g.*, Fader *et al.*, 1982) and Halibut Channel (*e.g.*, Miller *et al.*, 2001) based on sub-bottom and coring data.

2.3 Research Questions

To address knowledge gaps and discrepancies in the glacial history of Placentia Bay, mapped glacial landforms on the seabed were compared to existing terrestrial data and used to address the following research questions:

What do the morphology, orientation and spatial distribution of glacial landforms preserved on the seabed reveal about ice-flow events in Placentia Bay?

The morphology, orientation and spatial distribution of the landforms are described and used to determine the nature and number of ice-flow events recorded in Placentia Bay. Morphostratigraphic relationships of glacial landforms are used to build a relative chronology of ice-flow events.

What was the style and timing of ice retreat from Placentia Bay?

The morphology, orientation and spatial distribution of glacial landforms interpreted to be deposited during the retreat of ice from Placentia Bay are analyzed. Radiocarbon ages from marine cores are used to provide minimum dates for ice retreat.

Are the ice-flow events and pattern of ice retreat in Placentia Bay consistent with onshore records?

The ice flow events and the pattern of retreat in Placentia Bay, interpreted from the seabed landform assemblages, are compared to existing glacial records on the Burin and Avalon peninsulas. The westward ice-flow event recorded on the Burin Peninsula, in particular, has been difficult to explain and multiple hypotheses have been offered for the source of this ice-flow event. Seabed data provide additional details on the surrounding glacial history and may resolve discrepancies in previous interpretations.

Is there landform evidence to support the concept of ice streaming as proposed by Shaw *et al.* (2006a)?

The presence of southward-oriented landforms on the surrounding peninsulas converging into Placentia Bay may indicate the presence of an ice stream, as discussed by Shaw *et al.* (2006a). The type and distribution of glacial landforms on the seabed will be critical to determine if they are consistent with an ice stream.

3.0 Study Area and Methods

3.1 Outline

The first section describes the general physiography of the study area including the bathymetry of the bay and topography of the surrounding peninsulas. The surficial and bedrock geology of both marine and terrestrial areas are discussed. This is followed by a description of the methods used to address the research questions.

3.2 Study Area

3.2.1 Physiography

The bathymetric relief of Placentia Bay exceeds the surrounding topographic relief (**Figure 3.1**). Northeast-southwest trending bedrock ridges form shoals, reefs and islands which are dissected by deep channels reaching depths greater than 430 m. This northeast-southwest structural trend is the result of compression during the Appalachian Orogeny (570 to 650 Ma) which resulted in the formation of large structural domes and basins. The large bays, which include Placentia, Conception, St. Mary's and Trinity bays, are the result of water infilling structural basins (King, 1990). These bays vary in depth from 210 m in St. Mary's Bay to 580 m in Trinity Bay. The surrounding sub-peninsulas of the Avalon Peninsula form the domes, where maximum heights reach over 330 m above sea level (asl).

The structure of the Burin Peninsula also trends southwest to northeast. The topography can be divided into three sections: the lower peninsula (90-120 m asl), Marystown-Garnish lowland (30-75 m asl) and the upper Burin Peninsula (150-180 m asl) (Grant, 1989; Tucker, 1979). The highest elevations occur at White Hills on the

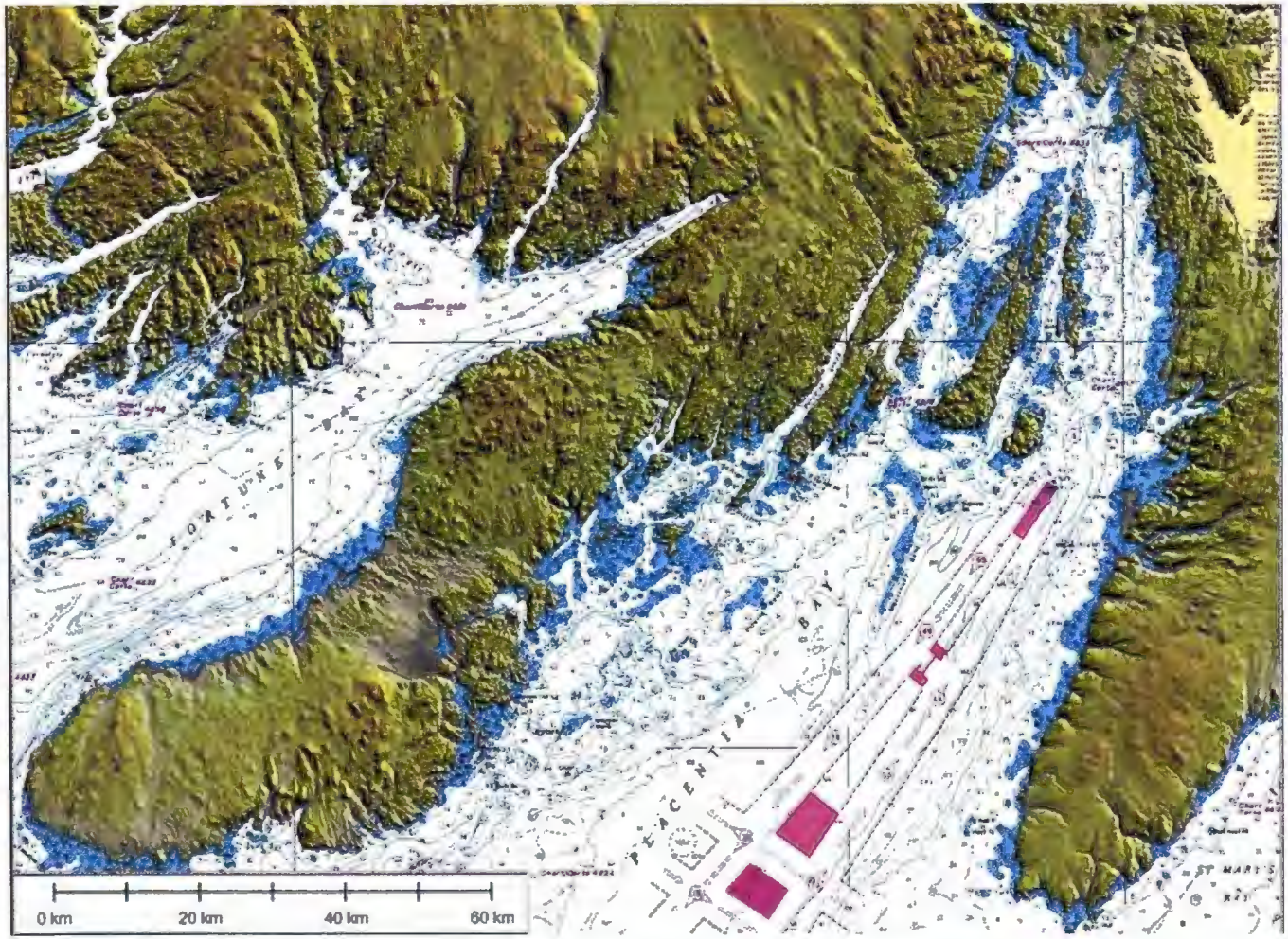

Figure 3.1 Nautical Chart of Placentia Bay with SRTM imagery of the surrounding land areas. Bathymetric contours are shown at 20 m intervals. Purple lines outline the shipping lanes (Canadian Hydrographic Service Chart 4016).

northeast coast (335-365 m asl) and at several volcanic plugs that outcrop along the lower south coast (230-245 m asl). The coast is mostly steep and jagged, particularly along Placentia Bay where vertical cliffs reach up to 60 m asl (Tucker, 1979).

Several banks occur farther offshore: St. Pierre Bank and Green Bank to the south of Placentia Bay, and Whale and Grand banks farther east on the continental shelf (**Figure 2.2**). These banks are separated by deep channels: Halibut Channel, between St. Pierre and Green banks and Haddock Channel between Green and Grand banks off Newfoundland. Halibut Channel connects Placentia Bay in the north with the continental shelf edge in the south. The Laurentian Channel, the largest and deepest channel on the Atlantic Canadian margin, extends out from the St. Lawrence River valley through the Gulf of St. Lawrence, across the continental shelf between Nova Scotia and Newfoundland and terminates at the shelf edge. Extensive local overdeepening of these channels is the result of glacial erosion (Fader *et al.*, 1982; Miller *et al.*, 2001).

3.2.2 Bedrock geology

3.2.2.1 Bedrock geology of Placentia Bay

Two types of bedrock were interpreted from seismic records and rock core drill samples collected from earlier surveys in Placentia Bay (Fader *et al.*, 1982; King *et al.*, 1986). The lowermost unit forms the basement, which has minimal acoustic penetration. Areas where this bedrock outcrops on the seabed are most prominent in the northern part of Placentia Bay where there are many shoals and islands separated by deep channels and basins. This unit was interpreted to be Precambrian to Devonian volcanic, sedimentary, metamorphic and granitic rocks.

A second type of bedrock observed in sub-bottom profiles is acoustically stratified and gently dipping. This sequence defines a syncline, oriented sub-parallel to the bathymetric axis of Placentia Bay. Based on rock core samples, this bedrock was interpreted to be Carboniferous conglomerate, sandstone, siltstone, and limestone. Carboniferous bedrock occurs extensively throughout Placentia Bay as shown in **Figure 3.2**.

3.2.2.2 Bedrock geology of areas surrounding Placentia Bay

The bedrock geology of the areas surrounding Placentia Bay falls within the Avalon Zone and consists of Late Proterozoic marine and non-marine volcanic and sedimentary rocks, overlain by Neoproterozoic to Carboniferous shallow marine sediments (**Figure 3.3**). Sandstone, siltstone and shale turbidites of the Neoproterozoic Connecting Point Group are the oldest of the sedimentary rocks. They are found exposed along the eastern Burin Peninsula, underlying Long Island in Placentia Bay and much of eastern Avalon Peninsula. These rocks are overlain by sedimentary rocks, mostly sandstone and siltstone (Musgravetown Group) and volcanics (Marystown Group). Higher in the sequence are late Neoproterozoic volcanic rocks (rhyolite flows and tuffs) of the Long Harbour Group. Devonian to Carboniferous non-marine sedimentary and volcanic rocks also occur; however, most rocks younger than Ordovician have been removed by erosion (Colman-Sadd *et al.*, 1990).

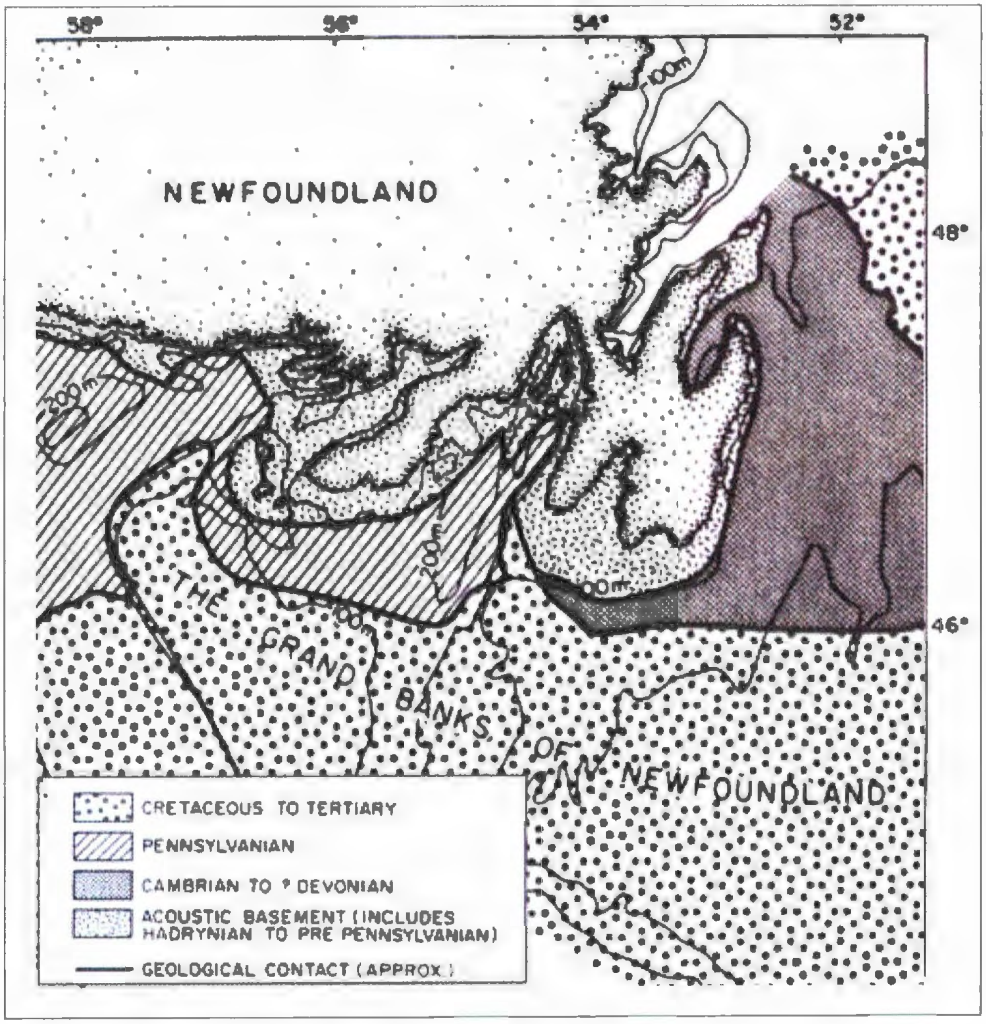

Figure 3.2 Simplified bedrock geology map of Placentia Bay (modified from Fader and Miller, 1986).

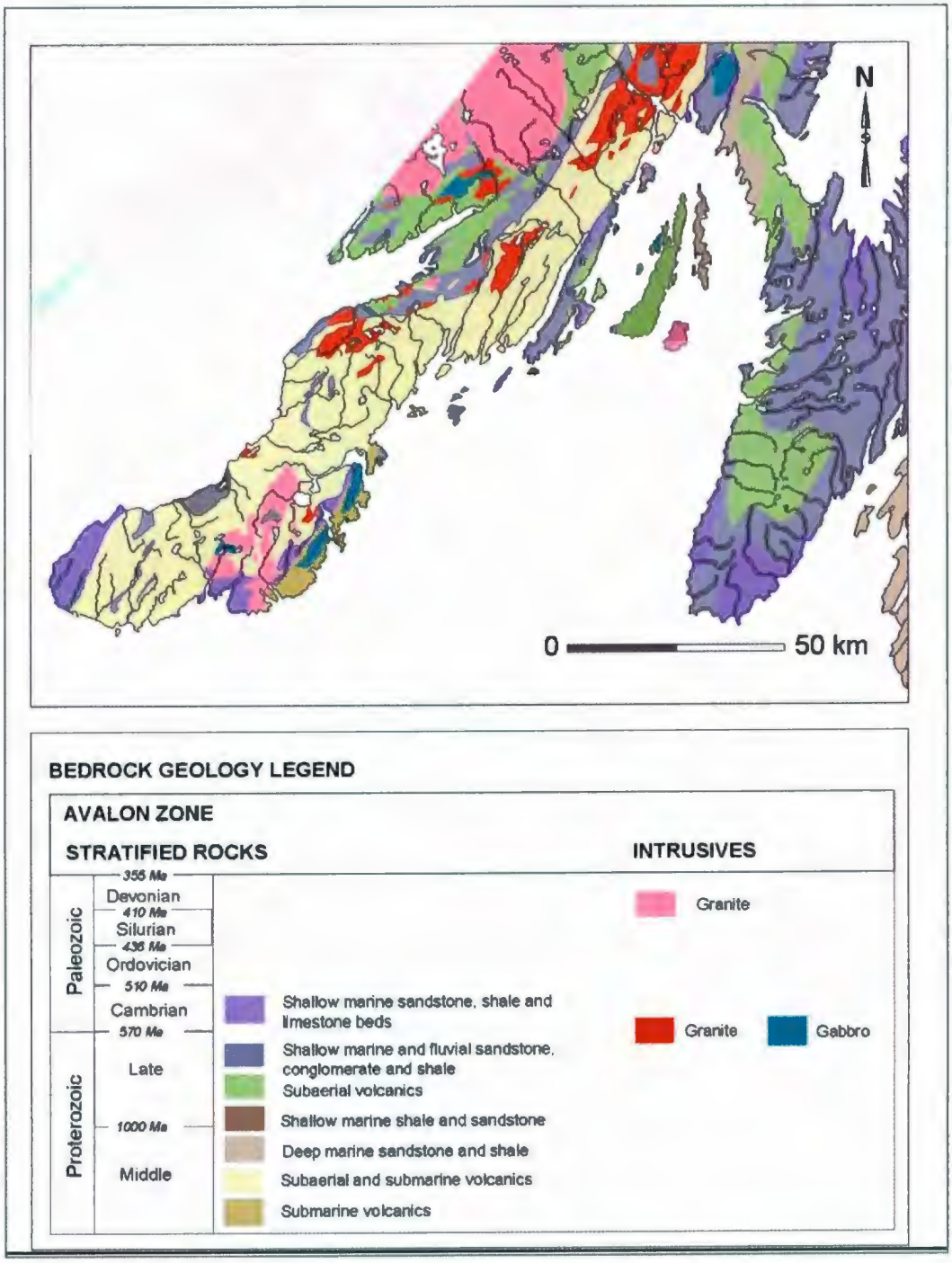

Figure 3.3 Simplified Bedrock Geology Map of areas surrounding Placentia Bay (modified from Colman-Sadd *et al.*, 1990).

These rocks are intruded by Devonian granitic plutons which outcrop around Placentia Bay and include: Red Island granite, Bar Haven granite, Ragged Islands Intrusive suite and Ackley Granite (Colman-Sadd *et al.*, 1990). Ackley granite is the most common and extensive granite present in the northern part of the Burin Peninsula. It is a pink, coarse-grained, massive biotite granite that is easily recognized in hand specimen and has been used in drift mapping (Batterson *et al.*, 2006).

3.2.3 Surficial Geology

3.2.3.1 Surficial Geology of Placentia Bay

Little published data exists on the surficial geology of Placentia Bay; however, surficial geology maps of large areas of the eastern Canadian continental shelves were produced by the Geological Survey of Canada during the 1970s and 1980s (*e.g.*, MacLean and King, 1971) using echograms obtained by the Canadian Hydrographic Service, augmented by data on Quaternary sediment thickness and bedrock characteristics obtained using air gun seismic systems. Later research used high resolution seismic reflection systems, including Huntec DTS and Seistec (*e.g.*, Fader *et al.*, 1982). Fader *et al.* (1982) described the surficial geology of the St. Lawrence Channel and western Grand Banks of Newfoundland, including the southernmost part of Placentia Bay. Surficial units were interpreted and correlated with five key surficial formations that were first described by King (1970; 1980) on the Scotian Shelf. Fader and Miller (1986) and Miller *et al.* (2001) described the equivalency of these surficial units on the southeastern Grand Banks of Newfoundland and in Halibut Channel (**Table 3.1**). The distribution and

Table 3.1 Quaternary surficial formations on the Scotian and Newfoundland shelves (after Fader and Miller, 1986 and Fader *et al.*, 1982).

Scotian Shelf	Grand Banks of Newfoundland	Acoustic character and material composition
LaHave Clay	Placentia Clay	Acoustically transparent Mud Pleistocene-Holocene basin deposits
Sable Island Sand and Gravel	Grand Banks Sand and Gravel	Acoustically stratified –incoherent Sand and gravel Transgressive deposits in water depth < 100 m
Sambro Sand	Adolphus Sand	Acoustically stratified Fine sand Sub-littoral deposit, below 100 m
Emerald Silt	Downing Silt	Acoustically stratified Gravelly sandy mud Glaciomarine sediment
Scotian Shelf Drift	Grand Banks Drift	Acoustically incoherent Gravelly sandy mud Till

stratigraphic relationships of these formations were controlled by the advance of an ice sheet across the shelf together with late glacial and postglacial isostatic and eustatic fluctuations.

3.2.3.1a Grand Banks Drift

Grand Banks Drift is an olive-gray to reddish-brown, poorly sorted gravelly sandy mud with angular to sub-rounded pebbles, cobbles and boulders throughout. In seismic records, it appears acoustically incoherent (Fader *et al.*, 1982). Bottom photographs where this unit is exposed on the seafloor showed many cobbles and boulders within a sandy mud (Fader *et al.*, 1982). This unit was interpreted as till by Fader *et al.* (1982) and was considered the equivalent of the Scotian Shelf Drift deposited on the Scotian Shelf, described by King (1970). Till occurs in three forms: thin blankets of ground moraine, infillings in channels and thick moraine ridges (up to 115 m) which were derived from subglacial melt-out debris from a neutral to negatively buoyant active ice shelf that was in direct contact with the seabed (King and Fader, 1986).

Till in the southwestern part of Placentia Bay forms the Burin moraine, the easternmost extension of the submarine end moraine system on the Scotian Shelf (**Figure 3.3**). The Burin Moraine has been observed in sub-bottom profiles along the southwest coast of Placentia Bay where it is continuous for at least 97 km and may extend farther to the northeast. It was described by Fader *et al.* (1982) as occurring in a series of ridges (up to 42 m high) connected by a thinner continuous sheet of ground moraine. At its southeastern margin, till is interbedded with glaciomarine silt at the front of the moraine

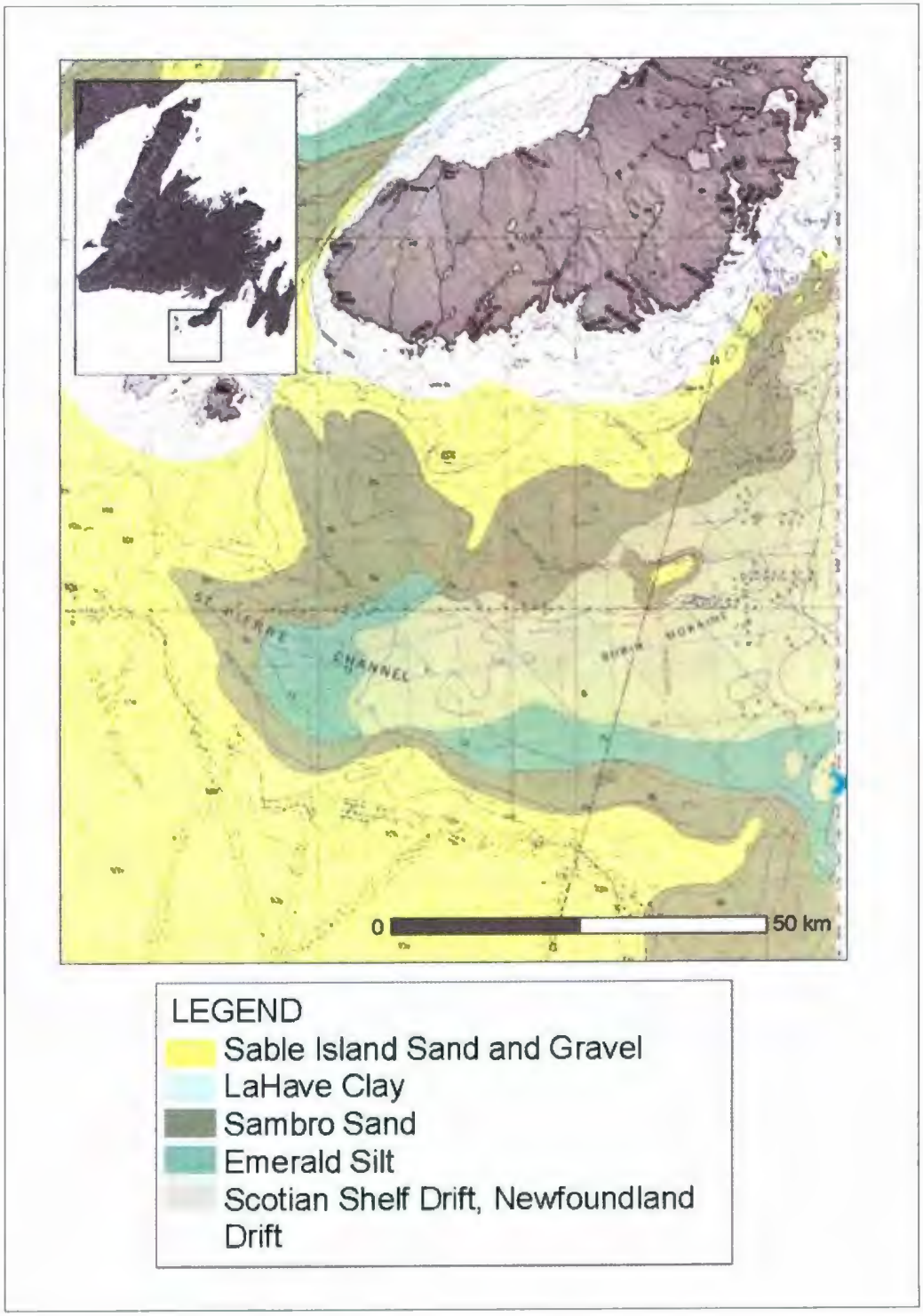

Figure 3.3 Surficial geology south of the Burin Peninsula and the Laurentian Channel. The Burin moraine is also shown. (modified from Map 4015-G from Fader *et al.*, 1982).

to form till tongues, interpreted to be the position where grounded ice became buoyant (Fader *et al.*, 1982).

3.2.3.1b Downing Silt

Downing Silt is described as a dark grayish brown to greenish brown clayey and sandy silt which contains minor angular gravel. It is commonly found in depressions and overlying till surfaces and interbedded with till at the distal sides of moraines or overlying it as a thin blanket (Fader *et al.*, 1982; Fader and Miller, 1986). Thicknesses vary from thin blankets to 120 m. In sub-bottom profiles, one of the dominant characteristics of this formation is the conformabilty of the reflections which parallel the underlying surface morphology. This unit was interpreted to be a proglacial muddy sediment that was deposited from floating ice in front of a grounded ice sheet. As this sediment settled through the water column it formed conformable, rhythmically banded deposits which mimic the underlying substrate (King and Fader, 1986).

3.2.3.1c Placentia Clay

Placentia Clay is a homogenous dark grayish brown to dark olive silty clay which grades locally to clayey silt and silty clayey sand. It was deposited in basins and depressions on the shelf during the Late Pleistocene-Holocene transgression from reworking of Grand Bank Drift and Downing Silt that had previously been deposited on shallow bank and inner shelf areas. Placentia Clay overlies Downing Silt. In sub-bottom profiles these units are easily differentiated; the clay is acoustically transparent, whereas the silt shows many continuous coherent parallel reflections. This formation is mostly confined to

basins and local depressions on the shelf, reaching maximum thicknesses of 30 m. It is the dominant surficial formation exposed along the bottom of the Laurentian Channel and along the south coast of Newfoundland, where it is found very close to shore and likely extends inland within fiords in this area (Fader *et al.*, 1982; Fader and Miller, 1986).

3.2.3.1d Adolphus Sand

Adolphus Sand is a dark, grayish-brown, poorly sorted, fine to coarse-grained sand containing smaller amounts of silt, clay and gravel. Foraminifera and shells are common throughout. It is a generally thin deposit but reaches maximum thicknesses of 20 m and is commonly found fringing bank and nearshore zones and along the edges of channels. In some areas it is derived from reworking of Grand Banks Drift and Downing Silt. North of the Burin moraine, Adolphus Sand has a high gravel content from erosion of Grand Banks Drift (Fader *et al.*, 1982; Fader and Miller, 1986).

3.2.3.1e Grand Banks Sand and Gravel

Grand Banks Sand and Gravel consists of reddish to grayish-brown, fine to coarse-grained, well sorted sand which may grade laterally to sub to well-rounded gravel with large boulders. It is differentiated from Adolphus Sand as it does not contain silt and clay-sized sediment (Fader *et al.*, 1982). This deposit is generally thin but reaches thicknesses up to 20 m and is found along the bank and inner shelf areas, in depths less than 115 m (Fader and Miller, 1986). It was formed by erosion of Grand Banks Drift and proglacial sediments (Fader *et al.*, 1982).

3.2.3.2 Surficial Geology of areas surrounding Placentia Bay

A brief overview of the surficial geology of the areas surrounding Placentia Bay, covering the Burin and southwestern Avalon peninsulas, is described here and shown in **Figure 3.4**. The most common surficial deposit on both peninsulas is diamicton which is found as thin discontinuous veneers in bedrock-dominated terrain, glacial landforms and blankets up to several metres thick. The lithology and characteristics of diamicton vary depending on the area, and commonly reflects the underlying bedrock geology (Catto, 1992; Batterson *et al.*, 2006).

The northern part of the Burin Peninsula contains the greatest variety and concentration of glacial landforms, which include flutings, drumlins, eskers and arcuate morainal ridges (Tucker, 1979; Tucker and McCann, 1980). Streamlined landforms in this area trend either north-south or northwest-southeast and are clearly evident on SRTM imagery, particularly in the Gisborne Lake area extending southeast to the Terrenceville area (Batterson *et al.*, 2006; Batterson and Taylor, 2007) (shown in **Figure 2.10**).

South to the Marystown-Garnish area, the surficial geology is predominantly bedrock outcrop with few glacial depositional landforms preserved. The lowlands between Marystown and Garnish have thicker sediment cover (> 5m). Southeast-northwest oriented flutes are common here. Thick sediment cover occurs along the southern and southwestern coasts; however, few glacial depositional landforms are preserved. Southward-oriented landforms are common in the St. Lawrence area to the southeast. Wetlands are also common in the central part of the peninsula, particularly in the south. Glaciofluvial sediments occur in many of the major valleys and are commonly

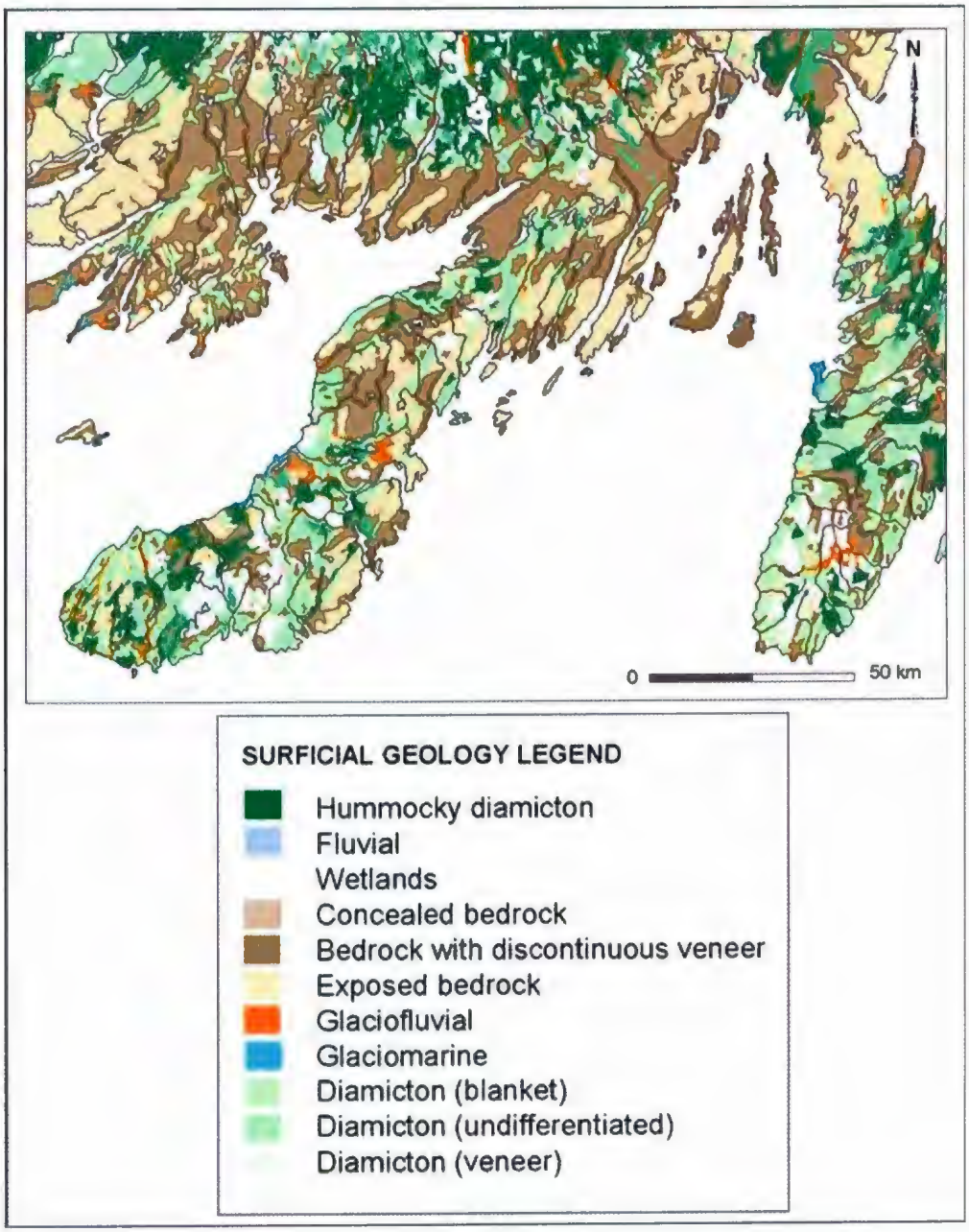

Figure 3.4 Surficial Geology Map of the areas surrounding Placentia Bay (modified from the Geosciences Resources Atlas: http://gis.geosurv.gov.nl.ca/).

graded to the postglacial sea level (higher than present) (Batterson *et. al.*, 2006; Batterson and Taylor, 2007; Tucker and McCann, 1980).

North of Placenta Bay, along the Isthmus of Avalon, the most common surficial deposit is diamicton which occurs in blankets. There is a distinct change in lithology from coarse sandy diamicton to fine, silty sand diamicton as well as a lack of granitic or mafic clasts from rock groups west of the Isthmus (Catto, 1998; Henderson, 1972).

On the eastern side of Placentia Bay, the southwestern portion of the Avalon Peninsula, the most common surficial deposit is diamicton. In coastal areas, these deposits are commonly blanketed by marine, fluvial, colluvial, or aeolian deposits (Catto, 1992). Diamicton is found as thin veneers and blankets over bedrock, and also forms a range of glacial landforms, including flutings, drumlins, hummocks, and Rögen moraines. Flutings are present in several parts of this region and are most prevalent in the Argentia area and around Dildo. They reach a maximum height of 8 m, width of 20 m and length greater than 300 m. Drumlins are also present, but less common than flutings. They are relatively poorly developed and may have bedrock cores. Drumlins reach a maximum height of 7 m and a width of 15 m (Catto, 1992).

Large areas of ridged and hummocky till also occur and become more prevalent towards the central part of the peninsula. The ridged till commonly occurs as sub-parallel ridges up to 30 m high with wetlands commonly occurring between them (Marich *et al.*, 2005; Catto and Taylor, 1998). Hummocky till may also be found in these areas as a series of knobs, mounds, ridges and depressions. Till is either thin or absent towards Conception Bay, St. Mary's Bay and to the east and west of the central lowland.

Glaciofluvial sediments consisting of fine sand to cobble gravel occur near St. Mary's Bay occur as plains, ridges, hummocks, and terraces (Catto and Taylor, 1998).

3.3 Methods

3.3.1 Outline

Data collection and analysis for this study included two GSC marine surveys (Shaw *et al.*, 2006b; Shaw *et al.*, 2006c). The primary data source used to interpret glacial landforms was multibeam bathymetric data provided by the GSC (Atlantic). Other data provided by the GSC (Atlantic) to assist in interpreting the multibeam data included: Huntec sub-bottom profiles, sidescan sonograms, vanVeen grab samples, bottom photographs, and piston cores.

Using the above data sources, glacial landforms were interpreted and mapped using ArcGIS software (ESRI 2004, ArcGIS 9.0). These landforms were then compared with existing terrestrial data from the onshore surficial sediment and landform digital databases of the Newfoundland and Labrador Geological Survey (Taylor, 2001) and SRTM data. Finally, the ice-flow and ice retreat patterns found both onshore and offshore were compared and mapped.

3.3.2 Introduction to Multibeam Sounder Systems

Multibeam bathymetric systems offer opportunities for the recognition and interpretation of seafloor features and have become one of the most important tools for ocean mapping (Lurton, 2002). In Atlantic Canada, the use of multibeam sonar systems began when the Canadian Hydrographic Service invested in high resolution multibeam sonar for

surveying the continental shelf in the late 1980s (Courtney and Shaw, 2000). This work started by mapping the marine geology and geomorphology of Halifax Harbour (*e.g.*, Fader *et al.*, 1991) and the offshore banks on the inner Scotian Shelf (*e.g.*, Loncarevic *et al.*, 1994) and has expanded to cover shallower coastal areas, including fjords and bays in Newfoundland (*e.g.*, Shaw *et al.*, 1997).

The basic principles behind multibeam echo sounders are similar to other sonar systems that emit beams of sound which contact a target and are reflected back to a receiver (Lurton, 2002). Unlike other sonar devices (*e.g.*, single beam, normal incidence sonar) multibeam echo sounders emit many beams of sound from an array of transducers which are typically mounted on the hull of the survey ship (**Figure 3.5**). These beams span a fan-shaped arc below and to the sides of the vessel. Each of these beams contacts the seabed at a slightly different angle creating a cone of sound that covers a swath of the seabed. The width of the beam on the seafloor – the footprint of the system – expands with the distance between the transducer and seabed. As water depth increases the area of the seafloor covered by the sonar swath increases and the resolution decreases. The attenuation of the signal becomes more unpredictable in deeper water because different water masses may have different acoustic properties. The width and number of beams depends on the multibeam manufacturer and model and may be changed depending on the users needs (Shaw and Courtney, 1997).

Multibeam echo sounders record the two-way travel time of the emitted sound through the water column to the target (seabed) and back to the transducer array to calculate the distance to each seafloor footprint. Using this two-way travel time and

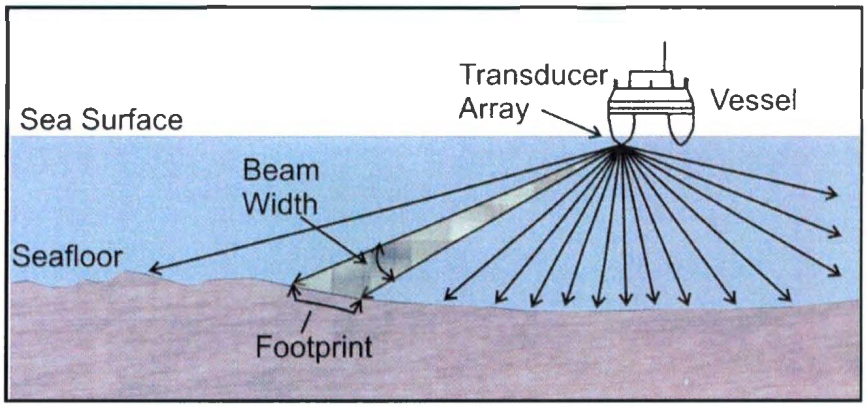

Figure 3.5 Principles of multibeam sonar systems. The sounder sends sound out and receives it back. Sound is projected toward the seabed in cone-shaped beams formed using an array of transducers mounted on the hull of a vessel. These beams span a fan-shaped arc below and to the sides of the vessel. The arc is divided into a number of distinct and separate beams. The beam width on the seabed determines the footprint of the system. The footprint expands with the distance between the transducer and the seabed. By measuring the transit time of a pulse projected from the transducer array and reflected from each seafloor footprint back to the array, an estimate of the distance to each seafloor footprint can be calculated (modified from Shaw and Courtney, 1997).

measurements of acoustic velocity variations in the water column, the water depth can be calculated. The system also records the angle from which the return signal arrives, which gives the location of the beam across the survey track. Water depth is calculated for each beam and combined to give a continuous record of water depth so that when the data are mapped topographic features can be observed due to changes in water depth, and hence elevation, across the seabed (Lurton, 2002; Shaw and Courtney, 1997).

There are three main sources of error in multibeam bathymetric measurements for which corrections must be made. The first important source of error is beam loss that occurs at the edges of the arc. The area of the seafloor ensonified by each beam depends on the position of the beam in the arc and the angle it contacts the seabed. Those beams closest to the point directly below the ship (nadir) will travel a straight path from the sonar head, through the water column to the seabed and back to the receiver. However, the beams on the outer edges of the arc must travel to the seabed at an angle so their return echo must be corrected for ray bending.

The second factor that must be accounted for is vessel movement. The vertical movement of a ship, changes in the tide or changes in the forward speed of the ship all effect the accuracy of water depths obtained from the sounder (Hughes Clarke *et al.*, 1996; Lurton, 2002). This problem is reduced by using attitude sensors which continuously measure the roll, pitch, yaw and heave of the vessel.

The third factor is inaccuracies in sound velocity corrections. Sound velocity profiles modify the acoustic paths and thus affect the positions of depth measurements. All multibeam sounders account for this. This factor can be further reduced by making

additional sound velocity measurements in areas where hydrological conditions vary (Lurton, 2002).

The EM1102 sounder on the *CCGS Matthew* was replaced by the EM710 and used primarily for mapping in deeper water. It has a swath width up to 5.5 times the water depth, with a maximum survey depth of 1700 to 2000 meters (Kongsberg Maritime, 2006b).

3.3.3 Multibeam Sonar Surveys

Multibeam sonar surveys covering most of Placentia Bay were conducted in several cruises from 1995 to 2006. Most of Placentia Bay was surveyed in 2005 and later. The pre-2005 surveys were primarily in the southeast quadrant of the bay (*CCGS Creed*, 2004) and up into Eastern Channel leading north into Come By Chance (*CCGS Matthew* and *Plover*, 2000; *Plover*, 1997) and Argentia (*CCGS Creed*, 1995). The vessels and multibeam sonar systems used in the different surveys are shown in **Table 3.2.**

The EM1000 sounder (95 kHz) mounted to the hull of the *CCGS Creed* produces 60 beams covering an arc of 150°. The width of the seafloor imaged on each survey line is 7.5 times the water depth. Line spacing is about three to four times water depth to provide ensonification overlap between adjacent lines (Kongsberg Maritime, 2006a).

The Simrad EM1002 sounder (95 kHz) originally mounted on the hull of the *CCGS Matthew*, produces 111 beams arrayed over an arc of 150°. The width of the seafloor imaged on each survey line is 7.4 times the water depth in shallow water and up to 1500 m in deeper water. Line spacing is about three to four times the water depth to provide ensonification overlap between adjacent lines.

Table 3.2 Vessels and sounders used to collect multibeam data in Placentia Bay.

Vessel	Sonar System
Creed (pre-2005)	SIMRAD EM1000
Matthew (pre-2005)	SIMRAD EM1002
Creed (2005 and later)	SIMRAD EM1002
Matthew (2005 and later)	SIMRAD EM710
Plover (launch in shallow water)	SIMRAD EM3000

A hydrographic launch, the *Plover*, was also deployed to carry out surveys in the shallower areas (1 to 150 m). The *Plover* was equipped with a Simrad EM 3000 system (300 kHz) which has a swath capability of ten times the water depth, but only up to a swath width of 200 m (Kongsberg Maritime, 2006c). In order to obtain 100% bottom coverage it was necessary to run a larger number of survey lines close together.

The survey data for the different cruises were processed by the Canadian Hydrographic Service. The raw bathymetric data were manually cleaned using HIPS (Hydrographic Information Processing System) software to remove erroneous depth values. The cleaned data (HDCS format) were imported into GRASS (Geographic Resources Analysis Support System) and gridded at 5 m resolution. Vertical resolution is on the order of centimeters. The data were also colour-shaded by depth and artificially illuminated from two angles, 45 and 315° from an azimuth of 45° (Patrick Potter, GSC Atlantic, Oct 11, 2006, *pers. comm.*). Geotiffs were created for the two different illumination angles and imported into the ArcMap module of ArcGIS (9.0) as separate raster layers.

3.3.4 Seismic and Sidescan Sonar Surveys

Seismic data provide information regarding the nature of the material both on and below the surface of the seafloor and are necessary for a complete interpretation of the seabed. Seismic data were collected in Placentia Bay during surveys from 1989 to 2006 using the Huntec deep-towed seismic reflection system (cruise 2005-051 (Shaw *et al.*, 2006b) and 2006-039 (Shaw *et al.*, 2006c)) and the Knudsen 320 BR Sub Bottom profiler (Shaw *et al.*, 2006b). The Huntec seismic system shows geological structure to approximately 40

m beneath the seabed. The Knudsen 320 BR Sub Bottom Profiler was used to image the subsurface when the bottom was soft enough to penetrate; however, it did not allow deep penetration of the sediments. Details regarding these systems are included in Shaw *et al.* (1989, 1999, 2006b, and 2006d).

To provide the best quality output, the acoustic delay and sweep were changed as depths within the bay changed. Using the sweep rate, the thickness of sediment layers in seismic records can be calculated. Time markers on the seismic records were imported into ArcMap using the position recorded at the time of the survey and used to aid in the interpretation of seabed features evident from the multibeam data.

Sidescan sonograms were collected concurrently with seismic data to show the distribution and morphology of large-scale bottom features and materials on the seafloor. Sidescan sonar systems used include the Simrad MS992 neutral tow sidescan sonar system (Shaw *et al.*, 2006b) and the Klein 3000 system (Shaw *et al.*, 2006d).

3.3.5 Groundtruthing

Grab samples and bottom photographs were also collected to aid in the interpretation of the surficial geology. Where possible, both grab samples and bottom photographs were taken at the same site to provide a more complete interpretation.

Seafloor sediment samples were obtained using a vanVeen grab sampler. The sampler has a strong closing mechanism that allows the jaws to excavate relatively undisturbed sediments when it makes contact with the seafloor. Samples were only retrieved from soft bottoms where the seafloor was not too hard to penetrate. Bottom

photos were taken using a camera that triggered when a lead weight hanging below the camera hit the seafloor.

3.3.6 Coring

Piston cores were collected as part of CCGS Hudson Cruise # 2006-039 in Placentia Bay and on the Burin Moraine, south of Placentia Bay. The cores were collected using the AGC#2 piston corer. The corer was able to penetrate soft glaciomarine and postglacial sediments, but not harder surfaces such as glacial diamicton. Core lengths ranged from 4.2 to 7.6 m. Cores were logged at the Bedford Institute of Oceanography and were described on the basis of grain size (using the Wentworth size class scheme), colour (using the Munsell scale), texture, and internal sedimentary structures. Shells and shell fragments were collected from the cores, cleaned and sent for AMS radiocarbon dating at the Beta Analytic Radiocarbon Dating Laboratory (Miami, Florida) where the conventional radiocarbon ages (*i.e.*, delta ^{13}C = 25 ‰) were calibrated in IntCal04 using the MARINE04 marine radiocarbon age calibration curve (Hughen *et al.*, 2004). This calibration curve takes into account the global reservoir effect; local reservoir corrections were not made. Median probability ages and calibrated age ranges (2σ) are presented in the text.

3.3.7 Terrestrial Mapping

Terrestrial data were provided from the digital databases of the Newfoundland and Labrador Geological Survey. These databases include sediment and landform data, and striation data (Taylor, 2001). These data were collected from field mapping which

included air photo analysis and field verification by helicopter and foot. Striation measurements were made to determine ice-flow directions. Direction was also determined by stoss/lee relationships, cross-cutting relationships, and the preservation of older striae in the lee of younger ones. Exotic clasts were also used to support the ice-flow data (*e.g.*, Batterson and Taylor, 2007). The SRTM data (available at http://seamless.usgs.gov/) were used to construct a digital elevation model for Newfoundland. Large-scale glacial features have been mapped using these data (*e.g.*, Liverman *et al.*, 2006) and are now part of the provincial surficial sediment and landform database.

3.4 Approach

3.4.1 Glacial landform classification

Seabed landforms observed from the multibeam bathymetric data were classified and digitized in ArcMap. Preliminary interpretation of the multibeam data showed several types of glacial landforms on the seabed. Based on analogy with terrestrial landforms, submarine landforms were divided into two general categories: flow-parallel and ice-marginal landforms (Benn and Evans, 1998; Rose, 1987).

3.4.1.1 Classification of flow-parallel landforms

Flow-parallel landforms in Placentia Bay were classified using the classification scheme discussed by Rose (1987). He described flow-parallel longitudinal landforms as part of a landform continuum which developed in response to ice moving across deformable or erodable bed materials under a range of stress levels. Stress is determined by ice

thickness and velocity, interacting with a range of bed materials that have different levels of resistance. Different landforms are defined primarily by size; differences in size are attributed to the dimensions of the moving ice that reflect flow cells within the ice. Elongation of landforms varies according to whether flow within these cells is converging or diverging. For example, drumlins that are relatively equant and displaying high relief are typically a response to a dominantly converging flow, whereas elongated, low relief flutes are a response to a dominantly diverging flow (Rose, 1987).

Three primary flow-parallel landforms are reported in this study: drumlins, megaflutes and flutes. These landforms show diversity in size and form and can be distinguished on the basis of their length and elongation ratios. The elongation ratio is determined by:

$$E = l/w \qquad \text{(Equation 1)}$$

where E is the elongation ratio, l is length, and w is the width of the landform (Rose, 1987). Typical morphologic characteristics of these landforms are described below.

Flutes

Flutes are narrow, regularly-spaced ridges that generally occur in groups of sub-parallel ridges. They are normally less than 5 m high and wide. They are generally less than 100 m long, although individual ridges may be larger. The elongation ratio of flutes is variable and falls under the range of 2 to 60 or even more (Benn and Evans, 1998; Rose, 1987) (**Table 3.3**). They are generally straight or very gently curving, but may swerve abruptly around boulders before a resuming a straight course (Gordon *et al.*, 1992).

Drumlins and megaflutes

Drumlins occur in different forms that range from the typical oval-shaped mounds to long narrow spindle forms and more asymmetrical drumlins known as parabolic forms. More complex forms also exist where longitudinal ridges are superimposed on transverse or oblique hills. Drumlins are typically higher and wider near their up-ice stoss end and narrow and thin down-ice. They commonly have long axes greater than 200 m long, heights ranging from 5 to 50 m and reasonably consistent elongation ratios ranging from 2 to 4 (although higher ratios exceeding 6 have been recorded). Drumlins grade into megaflutes with increasing elongation ratios; however, there is no clear spatial segregation between drumlins and megaflutes (Benn and Evans, 1998; Rose, 1987). Based on Rose (1987), the following dimensions were used to differentiate drumlins and megaflutes: landforms with long axes greater than 200 m, heights greater than 5 m and elongation ratios less than 4 were classified as drumlins; landforms with long axes greater than 1000 m and elongation ratios greater than 4 were classified as megaflutes (**Table 3.3**).

3.4.1.2 Classification of ice-marginal landforms

Ice-marginal landforms identified in this study include De Geer moraines and grounding-line moraines which were formed during overall ice retreat.

A classification of moraine ridges in subaquatic/subglacial environments was proposed by King and Fader (1986) who distinguished three major ridge groups: linear, tabular and hummocky, and lift-off. Typically moraine ridges in the first two categories are dimensionally large and formed in deep water, whereas lift-off moraines are formed

Table 3.3. Classification of flow-parallel landforms (modified from Rose, 1987).

Landform	Typical length (m)	Typical height (m)	Typical elongation ratios
flute	< 100	< 3	> 4
drumlin	> 200	> 5	< 4
megaflute	> 1000	> 5	> 4

in water depths less than 100 m. Lift-off moraines, first recognized from sidescan sonograms and high resolution seismic reflection profiles from the Scotian Shelf, were described as sub-parallel roughly evenly spaced ridges up to 3 m high and 20-80 m wide (Gipp, 2000; King and Fader, 1986). Sub-bottom profiles showed that these ridges were deposited contemporaneously with glaciomarine sediments where glaciomarine sediments occur between and generally conformably overly the ridges. This succession was thought to develop as a grounded ice shelf lifted off the seabed (King and Fader, 1986).

With the advent of multibeam sonar, subsequent studies interpreted ridges of a similar morphology as De Geer moraines. For example, De Geer moraines identified on German Bank of the coast of Nova Scotia, have variable dimensions but are generally less than 5 m high and 30 to 50 m wide (Todd *et al.*, 2007).

These moraines show different spatial patterns depending on how they were deposited and fall under two possible depositional processes. First, they may be formed at or close to the grounding line, marking former ice-marginal positions, where sediment was deposited or pushed up during brief stillstands or minor readvances (Blake, 2000; Todd *et al.*, 2007). These moraines typically show a regular spatial pattern with regular horizontal spacing that suggests that the rate of ice front retreat was consistent from one cycle of formation to the next (Todd *et al.*, 2007). Second, De Geer moraines may form as a result of squeezing of substrate into basal crevasses behind the ice margin. In this scenario, ice retreat is affected by thinning, loss of contact of the ice with the seafloor and by the breaking of the ice sheet along crevasses which results in the formation of tabular ice bergs (Gipp, 2000; Lundquist, 1989). Several specific conditions must be met:

isolated water-filled crevasses penetrate to the base of the ice, ice is less than 22 m thick, or basal water pressure is higher than the ice overburden pressure (Todd *et al.*, 2007). Given these conditions, material may squeeze into crevasses from below. Such ridges would display a different morphology from those described above such as a more randomly-oriented criss-crossing pattern. The preservation of these ridges would require that ice either melted in-situ or lifted off the seafloor once the crevasse fills formed (Todd *et al.*, 2007).

Grounding-line moraines

The dimensions of grounding-line moraines are consistently larger than De Geer moraines, thought to mark larger stillstands or readvances of a grounded ice margin. They also have a more complex morphology; instead of a single ridge they are usually composed of a suite of curvilinear ridges that may continue for hundreds of metres. These curvilinear elements are interpreted as reflecting processes occurring at the ice front during moraine deposition (Menzies, 2001).

3.4.2 Mapping and compilation

Processed multibeam data were imported into ArcMap 9.0 to provide 3-dimensional bathymetric images of the seafloor (projected in UTM zone 21 using the NAD 1983 datum). Images were sun-illuminated using two illumination angles at 90° to each other (azimuths of 45° and 315°), a sun inclination angle of 45° and a vertical exaggeration of 10. The recognition of features depends on the illumination angle chosen to view the

image. Typically, the optimal angle is perpendicular to the orientation of the seabed feature.

Using the above classification schemes, seabed landforms were classified on the basis of their morphological and sedimentological characteristics. The morphology of the seabed landforms was described using multibeam data. Length, width, height and orientation were measured from the digitized landforms in ArcMap. These dimensions were calculated for each field of landforms taken from a sample (n = 30) from within that field. Their sedimentology was described using sub-bottom profiles, bottom photos, grab samples, and cores.

Glacial landforms were digitized separately for each of the two illumination angles and then compiled into a single layer in ArcMap. Where landforms were defined in both illumination angles, they were redigitized into one representative landform. Where available, data from sub-bottom profiles, sidescan sonograms and grab samples were used to support sediment and landform interpretations. Ice-flow patterns were mapped from the flow-parallel landforms. The pattern of retreat was mapped from the distribution of ice-marginal landforms. This imagery was matched with the SRTM data, also illuminated from the same angles. The ArcScene extension of ArcMap was also used to generate 3-D images to aid in interpretation of landforms. The mapped seafloor landforms were then viewed in combination with the Newfoundland and Labrador digital landform and striation database from adjacent land areas (Taylor, 2001). Ice-flow patterns and ice-marginal patterns were then examined using both the seabed and terrestrial data sets. Ice-flow patterns were mapped for ice-flow events that could be extended on land.

4.0 Results

4.1 Outline

This chapter begins with a description of the surficial units identified from sub-bottom profiles, sidescan sonograms, piston cores, bottom photographs and van Veen grab samples (location of seismic tracks, sampling and coring stations are shown in **Figure 4.1**). Next, the morphology of glacial landforms is described and interpreted from the multibeam data on the Placentia Bay seabed. Sedimentologic descriptions are used to support these interpretations. The spatial distribution and orientations of these landforms are discussed.

4.2 Seabed sediments

4.2.1 Surficial units

Four main units were identified: bedrock, glacial diamicton, glaciomarine silt and postglacial mud. These units and their stratigraphic relations are discussed and correlated to formations described by Fader and Miller (1986) and Fader *et al.* (1982) (see section 3.2.3.1). Descriptions of grab samples and piston cores are presented in Appendices A and B, respectively. The general spatial distribution of surficial units within Placentia Bay is presented and illustrated with examples from sub-bottom profiles.

4.2.1.1 Bedrock

Two types of bedrock were identified in sub-bottom profiles from Placentia Bay. The lowermost unit forms the basement, which has minimal acoustic penetration. Areas where this bedrock outcrops on the seabed are most common in the northern part of

Figure 4.1 Locations of seismic tracks (from cruise 2005-051 (Shaw *et al.*, 2006b), sampling and coring stations (from cruises 2005-051 and 2006-039(Shaw *et al.*, 2006c)). Sub-bottom profiles described in subsequent figures are indicated with red lines.

Placentia Bay where there are many shoals and islands separated by deep channels and basins. Based on previous research by Fader *et al.* (1982), Fader and Miller (1986) and King *et al.* (1986), this unit was interpreted as Ediacaran to Pre-Pennsylanian bedrock comprising volcanic, sedimentary, metamorphic and granitic rocks.

A second type of bedrock observed in sub-bottom profiles is acoustically stratified. Dipping layers indicating the presence of anticlines and synclines are common throughout Placentia Bay and are most prominent around bedrock ridges on the western side of the bay. Bedrock ridges follow the structural trend found on surrounding land and generally trend northeast-southwest. This bedrock was interpreted to be Carboniferous conglomerate, sandstone, siltstone, and limestone based on sub-bottom profiles and rock core drill samples (Fader *et al.* 1982; Fader and Miller, 1986; King *et al.*, 1986).

4.2.1.2 Glacial diamicton

At the base of the surficial succession, unconformably overlying the bedrock is an acoustically structureless unit with few internal coherent reflections. This acoustic character is typical of non-sorted to poorly-sorted sediments. Sub-bottom profiles also show that the thickness of this unit varies, reaching a maximum of 30 m, and occurs as blankets or ridges overlying bedrock.

Bottom grab samples of this unit where it outcrops at the seafloor typically show a dark grayish-brown sediment (5Y 3/2) with a silty sand to clayey sand matrix and subangular to subrounded gravel to boulder clasts (**Figure 4.2a**). The larger size of some of the clasts in this unit prevented the van Veen grab sampler from closing completely

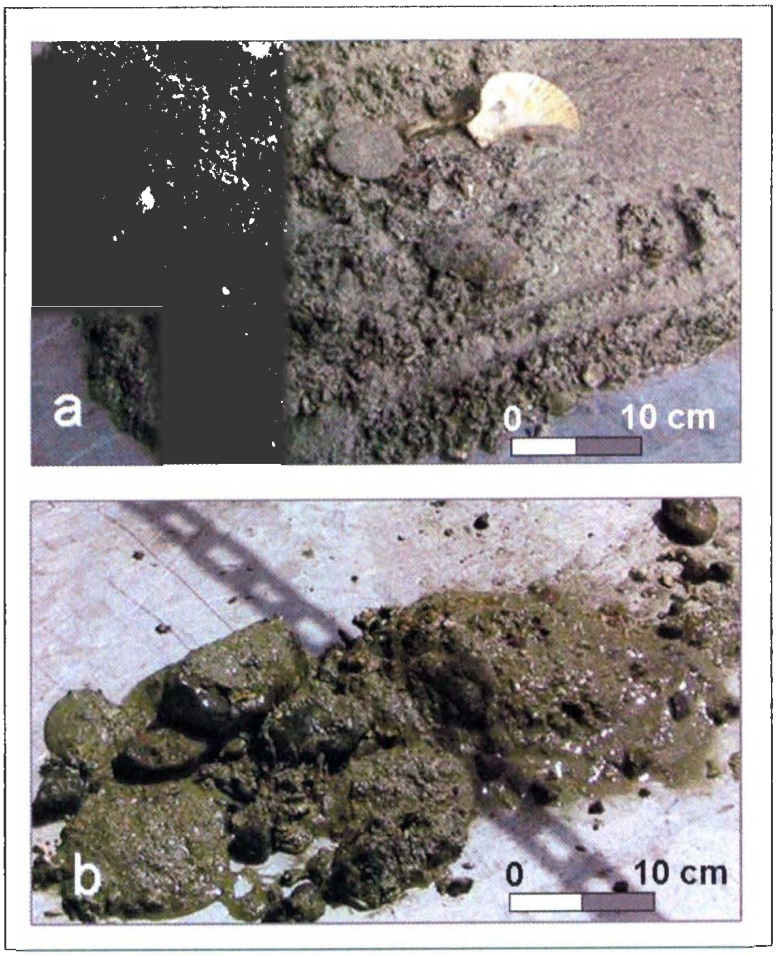

Figure 4.2. Photographs of glacial diamicton obtained from van Veen grab samples from a morainal area in ~85 m water depth. Samples of this unit typically consist of dark grayish-brown (5Y 3/2) sediments with a silty sand to clayey sand matrix and subangular to subrounded gravel clasts as shown in Photo a. Shell fragments, sand dollar and scallop shell are also present in Photo a. Photo (b) shows a grayish-brown (5Y 4/2) sediment with a silty to clayey sand matrix and subangular to subrounded gravel and boulder clasts. Some of the material was lost during this grab because the boulders prevented the grab from closing completely. Samples were collected during CCGS cruise 2006-039 (sample #s: 0045 (a), 0041 (b) in Appendix A).

and some to all of the material was lost in these cases (**Figure 4.2b**). Piston cores were unable to penetrate through this substrate.

This unit is interpreted as glacial diamicton primarily based on its acoustic character which is similar to that described in other areas, including outer Placentia Bay (Fader *et al.*, 1982) and the Grand Banks of Newfoundland (Fader and Miller, 1986; Miller *et al.*, 2001). The description of this unit is consistent with that of Fader and Miller (1986) for the Grand Banks Drift formation (**see 3.2.3.1a**).

4.2.1.3 Glaciomarine silt

In sub-bottom profiles this unit appears acoustically stratified with continuous coherent parallel reflections. This unit occurs throughout the bay, generally draped over underlying material. In areas where this unit is thin and overlies rough surfaces, the morphology of the surface is mimicked by the surface of this unit. It also shows some degree of ponding in deep channels and basins. This unit occurs overlying and interbedded with glacial diamicton; contacts between these units are readily distinguished by sharp boundaries.

Grab samples where this unit is exposed on the seafloor are described as a stiff dark olive gray (5Y 3/2) silty mud with scattered worm tubes and shell fragments (**Figure 4.3a**). A brown (7.5YR 4/2) surface veneer was found on several grab samples (**Figure 4.3b**).

Piston cores intersecting this unit show that it is a dark gray (5Y 4/1) to olive-gray (5Y 3/2) silty clay to clayey silt with rhythmically banded dark silty laminae and minor

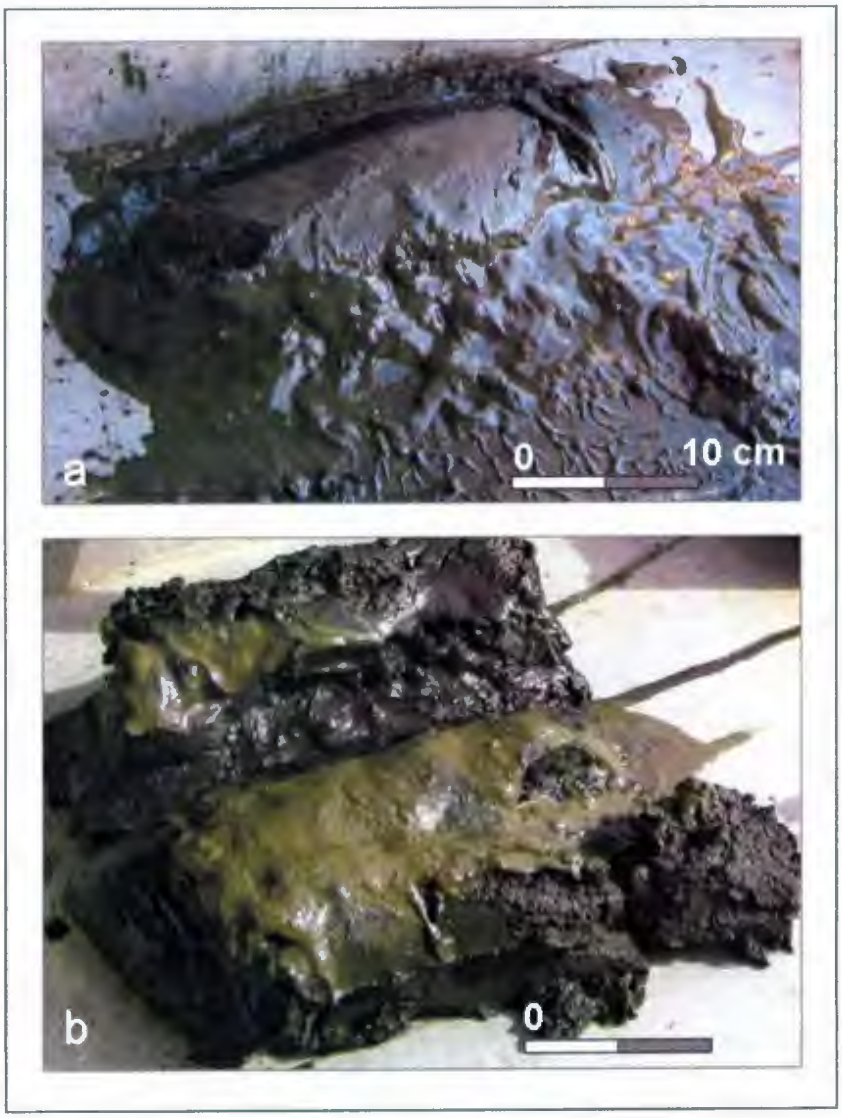

Figure 4.3 Photographs of glaciomarine silt obtained from van Veen grab samples. Samples are described as stiff dark gray (5Y 3/2) silty mud with scattered worm tubes and shell fragments. A brown (7.5YR 4/2) surface veneer was found on several grab samples as shown in Photo (b). These samples were collected during CCGS cruise 2006-039 (sample #s: 033 (a), 006 (b) in Appendix A).

very fine sand (See **Figures B.1** to **B.5** in **Appendix B**). Reddish gray (10YR 5/1) clayey layers 10 to 50 mm thick are also present but are less common than the silty laminae. Extensive mottling from bioturbation occurs throughout. Angular to sub-rounded gravel clasts and marine shells are common and occur scattered throughout the unit. The angular gravel clasts are interpreted as dropstones.

This unit is interpreted as glaciomarine silt. Its description, depositional style and acoustic character are comparable to the Downing Silt described by Fader and Miller (1986) and Fader *et al.* (1982).

Radiocarbon ages were obtained from marine shell fragments, valves and articulated bivalves throughout this unit (median probability ages are presented in text, dated material, its location as well as conventional and calibrated age ranges are provided in **Table 4.1**). Core locations are shown in **Figure 4.1**. Ages from Placentia Bay range from 9690 to 16280 cal BP. Radiocarbon ages closest to the base of the glaciomarine unit around the mouth of the bay are: 15,820 cal BP (495 cm depth from core 013, **Figure A.2**), 16,080 cal BP (514 cm depth in core 015, **Figure A.3**) and 14,650 cal BP (644 cm depth from core 019, **Figure A.4**). A sample from a similar stratigraphic position towards the middle of the bay is 14,010 cal BP (458 cm depth from core 032, **Figure A.5**). Radiocarbon ages closest to the top of the glaciomarine unit around the mouth of the bay are: 12,020 cal BP (169 cm depth from core 13) and 12,680 cal BP (302 cm depth from core 019).

Three samples were collected outside Placentia Bay, on the eastern flank of the Burin Moraine (core 007, **Figure A.5**). Here the Downing Silt is interbedded with the glacial diamicton forming till tongues, previously identified by Fader *et al.* (1982). Cores

Table 4. 1 Piston cores collected as part of Hudson Cruise 2006-039 (Shaw *et al.*, 2006c). Locations of cores are shown in **Figure 4.1.** Conventional dates were calibrated using the marine calibration curve (MARINE04), taking into account the global reservoir effect. Median probability ages are reported in text. All samples were collected from the glaciomarine unit.

Core #	core depth (cm)	sample depth in core (cm)	Dated material	Conventional ^{14}C age (BP)	Calibrated age range (cal BP, 2σ)	Median probability age (cal BP)
007	644.5	109	*Nuculana tenuis*	13680 +/- 40	16060 to 15460	15730
007	644.5	300	*Yoldia sp.*	13710 +/- 40	16070 to 15500	15780
007	644.5	558	*Portlandica arctica*	14090 +/- 40	16600 to 16020	16280
013	243.0	169	*Nuculana pernula*	11000 +/- 40	12800 to 12570	12680
013	243.0	245	*Nuculana pernula*	12650 +/- 40	14220 to 13980	14100
013	243.0	248	*Buccimim tenue*	12540 +/- 40	14110 to 13840	14000
013	243.0	271	*Nuculana pernula*	12710 +/- 40	14390 to 14040	14160
013	243.0	495	*Nuculana tenuis*	13740 +/- 40	16120 to 15550	15820
015	174.0	167	*Nuculana tenuis*	12870 +/- 40	14930 to 14190	14610
015	174.0	332	*Portlandica arctica*	13610 +/- 40	15910 to 15360	15630
015	174.0	514	*Portlandica arctica*	13930 +/- 40	16380 to 15810	16080
019	199.0	041	Unidentified fragment	9020 +/- 40	9890 to 9540	9690
019	199.0	125	*Nuculana pernula*	10010 +/- 40	11150 to 10760	11080
019	199.0	270	Unidentified fragmented bivalve	10620 +/- 40	12100 to 11720	11940
019	199.0	302	*Nucula expansa*	10670 +/- 40	12190 to 11860	12020
019	199.0	495	*Nuculana sp.*	12010 +/- 40	13600 to 13320	13420
019	199.0	644	*Mytelis trossulis*	12890 +/- 40	14950 to 14220	14650
032	211.0	267	*Nuculana pernula*	11620 +/- 40	13220 to 13000	13110
032	211.0	458	*Nucula tenuis*	12560 +/- 40	14130 to 13870	14010

penetrated the Downing Silt facies but were unable to intersect the upper surface of the till tongue. The age closest to the top of the till unit is 16,280 cal BP.

4.2.1.4 Postglacial mud

In sub-bottom profiles, this unit appears semi-transparent to transparent and in places is faintly laminated. This unit overlies glaciomarine silt and generally occurs ponded in basins and depressions where it reaches thicknesses up to 20 m. This unit is absent or thin over ridges.

Grab samples of this unit are described as olive to dark olive gray (5Y 5/2 to 5Y 3/2) gravelly sandy mud (**Figure 4.4a**). Bottom photographs typically show a dark gray brown muddy surface with biogenic trails and burrows and siphon pits (**Figure 4.4b**). This unit grades to a coarser sand and gravel in shallow water where it commonly forms a surface veneer of sub-rounded to sub-angular gravel embedded in a muddy to sandy matrix. Shells, shell fragments, sand dollars and sea urchins are also evident in bottom photographs from these areas (**Figure 4.4c**).

Cores from this unit consist of a dark gray (5Y 4/1) clayey silt to silty clay with few clasts and shell fragments (See piston cores 010, 013, 015, 019 and 032 in **Appendix B**). Cores show a fining downwards with sandy mud near the top and increasing clay content towards the bottom. There is generally a sharp contact with the overlying glaciomarine silt with a thin lens of sand or gravel marking an erosional unconformity.

This unit is interpreted as postglacial mud. The description, depositional style and acoustic character of this mud is consistent with that of the Placentia Clay Formation, which was derived by winnowing during transgression of glacial diamicton and

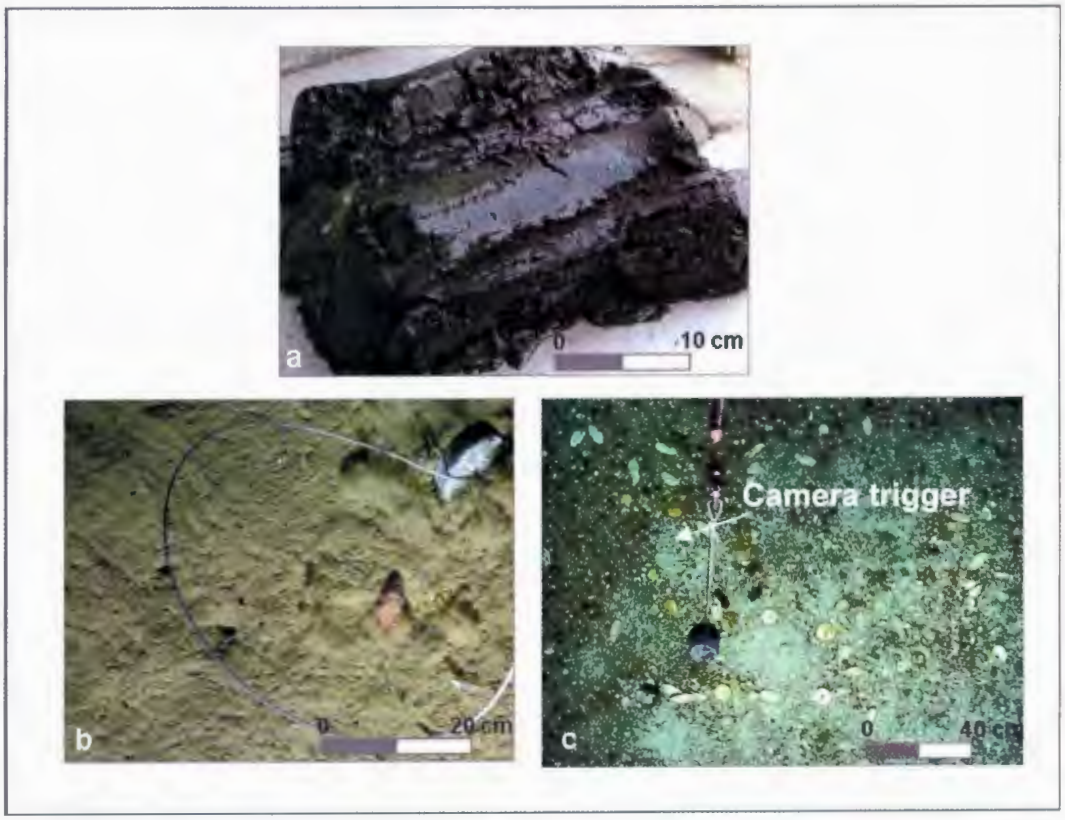

Figure 4.4 Photographs of postglacial mud obtained from van Veen grab samples and bottom photographs. Samples of this unit are described as olive to dark olive gray gravelly sandy mud (a). Bottom photographs typically show a dark gray brown muddy surface with biogenic trails and burrows and siphon pits, as shown in Photo b. In shallower water, this unit grades to a coarser sand and gravel which commonly has a surface veneer of sub-rounded to sub-angular gravel embedded in a muddy to sandy matrix. Shells, shell fragments, sand dollars and sea urchins are also evident (c). These samples were collected during CCGS cruise 2006-039 (sample #s: 033 (a), 006 (b) in **Appendix A**).

glaciomarine silt during the late Pleistocene-Holocene (Fader and Miller, 1986; Fader et *al.*, 1982).

4.2.2 Spatial Distribution

The spatial pattern of surficial units varies throughout Placentia Bay. However, there are several important relationships which are discussed below and illustrated with examples from sub-bottom profiles (locations of sub-bottom profiles shown in **Figure 4.1**).

In the northernmost part of the bay, sub-bottom profiles reveal areas where bedrock either crops out on the seafloor or has very thin sediment cover. Isolated areas of thicker sediment cover are made up of acoustically incoherent sediments, interpreted as glacial diamicton (up to 14 m thick). Several small basins contain acoustically stratified sediments, interpreted as glaciomarine silt. The glaciomarine unit is overlain by a nonstratified unit interpreted as postglacial mud. Combined sediment thicknesses in these basins are commonly 8 m. In the deeper channels, including Western, Central and Eastern channels, bedrock ridges and basins are draped by glaciomarine silt with postglacial mud thickening in the basins (combined thicknesses up to 60 m) and thinning or absent on the ridges (**Figure 4.5**). At the bottom of Central Channel, an area with ridges of glacial diamicton (15-38 m thick) is overlain by glaciomarine silt (averaging 6 m thick) and postglacial mud (averaging 8 m thick) (**Figure 4.6**). The bottom of Eastern Channel also shows small ridges of glacial diamicton (4-9 m thick) which are draped by glaciomarine silt (up to 19 m thick).

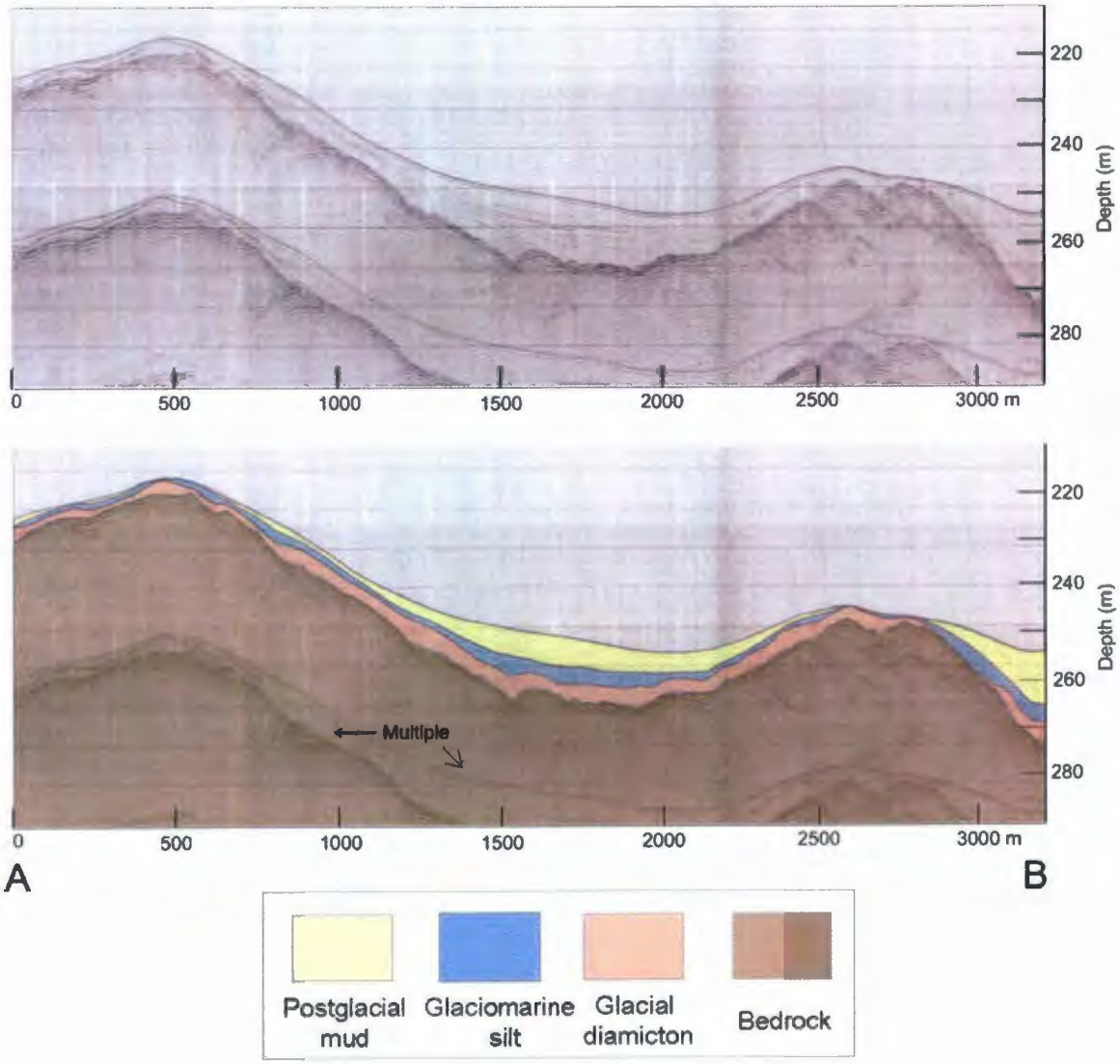

Figure 4.5 Huntec sub-bottom profile and interpreted geological cross-section from Central Channel (Line 40, daytime 3081318 from cruise 2005-051). Glacial diamicton blankets bedrock ridges and is draped by glaciomarine silt and postglacial mud which thickens in basins. Acoustically stratified bedrock is interpreted to be Carboniferous bedrock. Location of profile is shown in Figure 4.1.

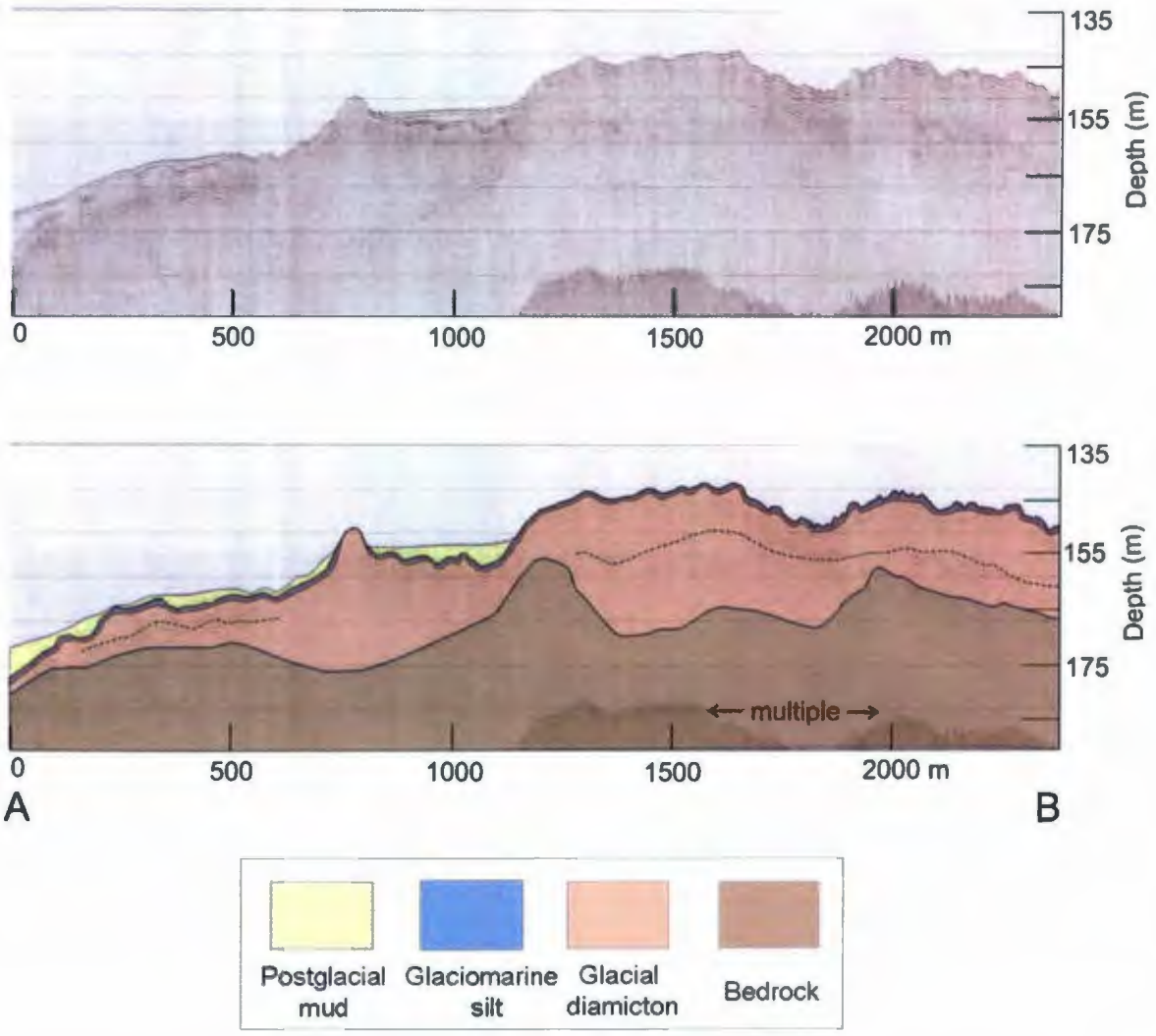

Figure 4.6 Huntec sub-bottom profile and interpreted geological cross-section from southern Central Channel (Line 43, daytime 3081558 from cruise 2005-051). Glacial diamicton occurs in ridges and is overlain by glaciomarine silt and postglacial mud occurs in basins. At ~1500 m ridges appear at the surface of the seafloor. Bedrock shows no acoustic stratification and is interpreted to be acoustic basement. Location of profile is shown in Figure 4.1.

In western Placentia Bay, south of Western Channel, in water depths of 40-250 m, there is a large area of glacial diamicton occurring in ridges (up to 12 m thick). These ridges are draped by glaciomarine silt (up to 6 m thick) and may also have postglacial mud occurring in basins (**Figure 4.7**). East and southeast of Jude Island, northeast-southwest trending bedrock ridges and basins are draped by glaciomarine silt with postglacial mud thickening in the basins (up to 21 m) and thinning or absent on the ridges. No glacial diamicton was apparent in the sub-bottom profiles around these bedrock ridges. South of this area, east of Marystown, another large area with ridges of glacial diamicton is present. Ridges are commonly 15-28 m thick (**Figure 4.8**). Glaciomarine silt either drapes the ridges or occurs in inter-ridge basins (up to 8 m thick).

Along the eastern coast of Placentia Bay, south of Eastern Channel, in water depths of 45-130 m, sub-bottom profiles show ridges of glacial diamicton (11-15 m thick) overlying bedrock (acoustic basement). These ridges are draped by glaciomarine silt, which thicken in basins and thin on ridge crests (5-8 m thick) (**Figure 4.9**).

Further off the east coast, in water depths of ~150-195 m, blankets of glacial diamicton (up to 10 m thick) are overlain by glaciomarine silt (reaching thicknesses of 20-28 m thick) which in turn is overlain by postglacial mud (up to 18 m thick). There are several areas where part of the glaciomarine and postglacial unit has been truncated (up to 10 m), strongly suggesting erosion of these sediments (**Figure 4.10**).

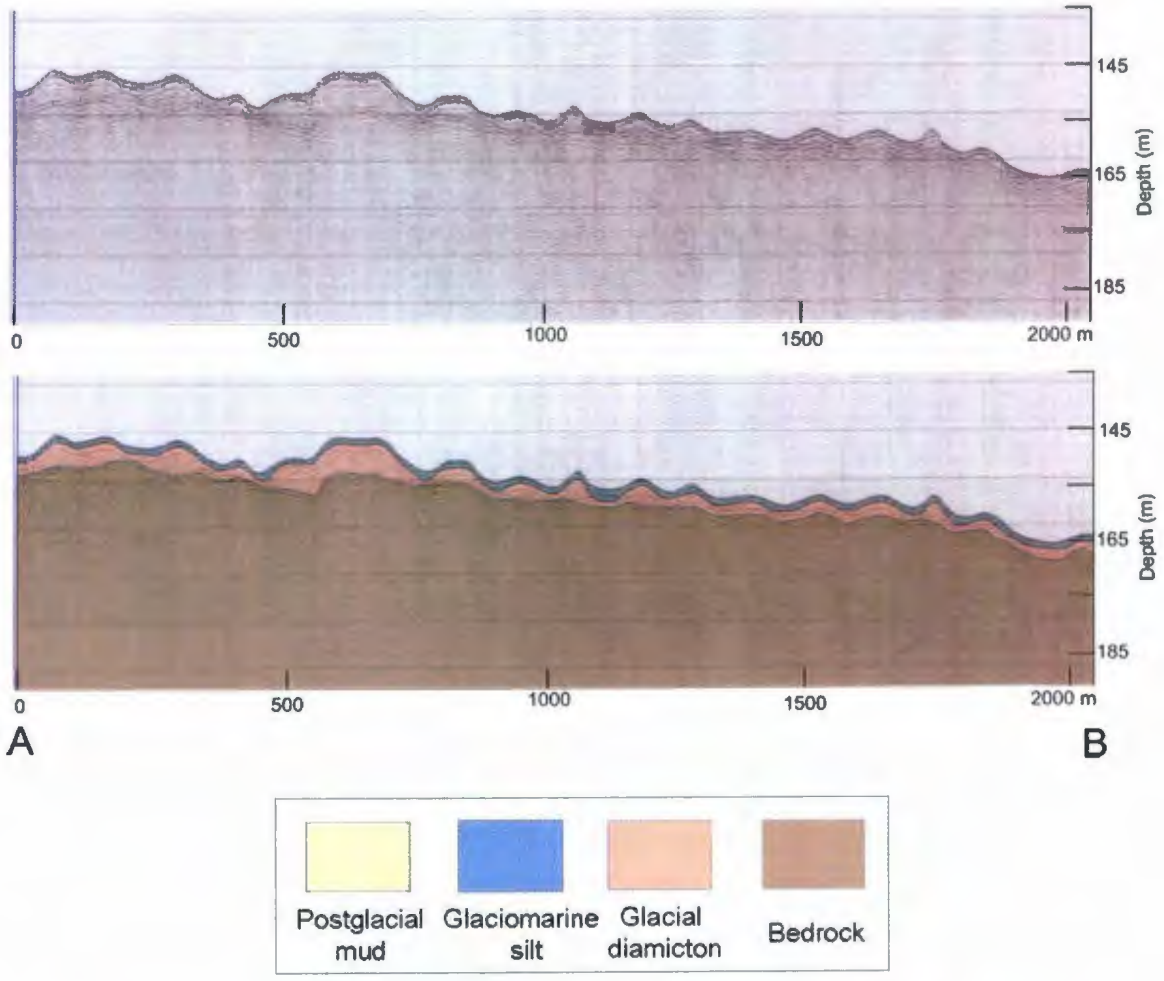

Figure 4.7 Huntec sub-bottom profile and interpreted geological cross-section from western Placentia Bay, south of Western Channel (Line 19, daytime 3021848 from cruise 2005-051). Glacial diamicton occurs in ridges draped by glaciomarine silt. Location of profile is shown in Figure 4.1.

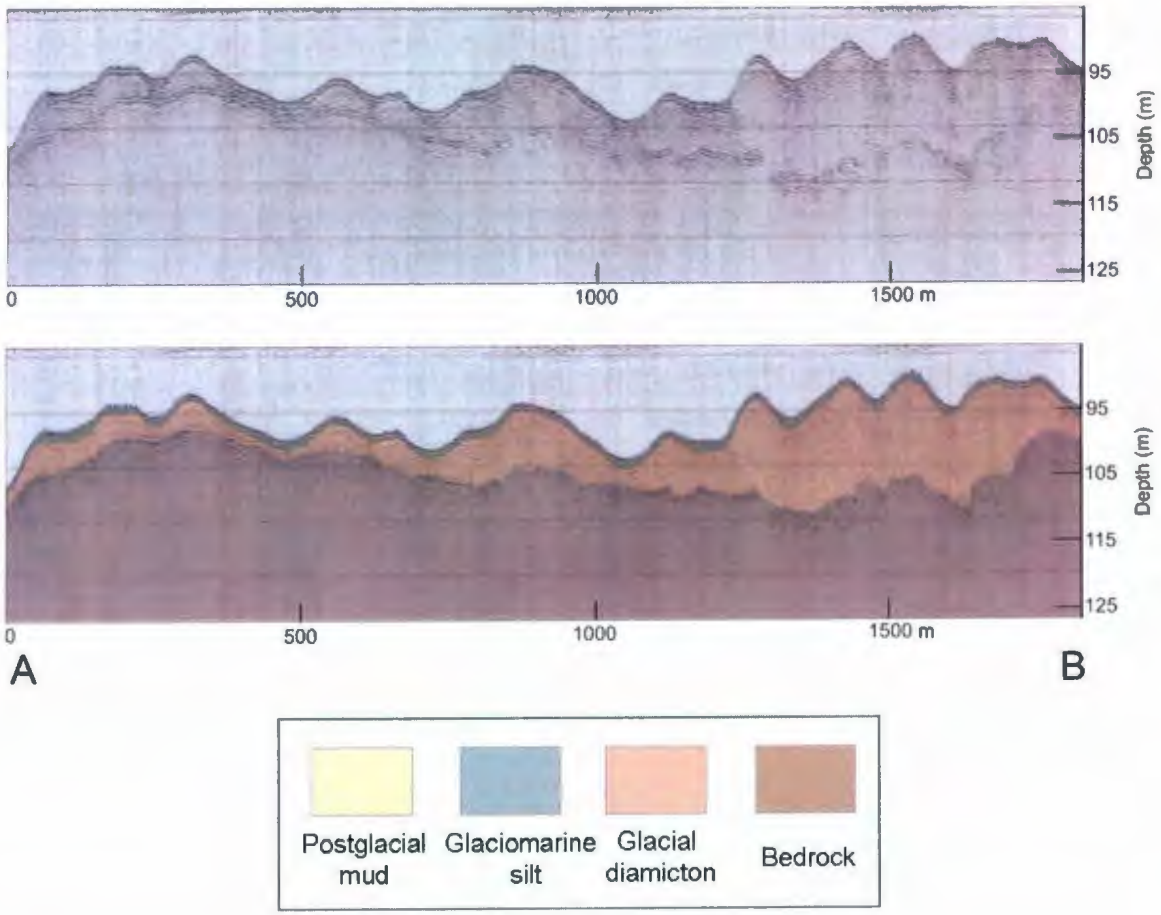

Figure 4.8 Huntec sub-bottom profile and interpreted geological cross-section from western Placentia Bay (Line 21, daytime 3022230 from cruise 2005-051). Glacial diamicton occurs in ridges overlying bedrock. A thin drape of glaciomarine silt overlies the glacial diamicton unit. Location of profile is shown in Figure 4.1.

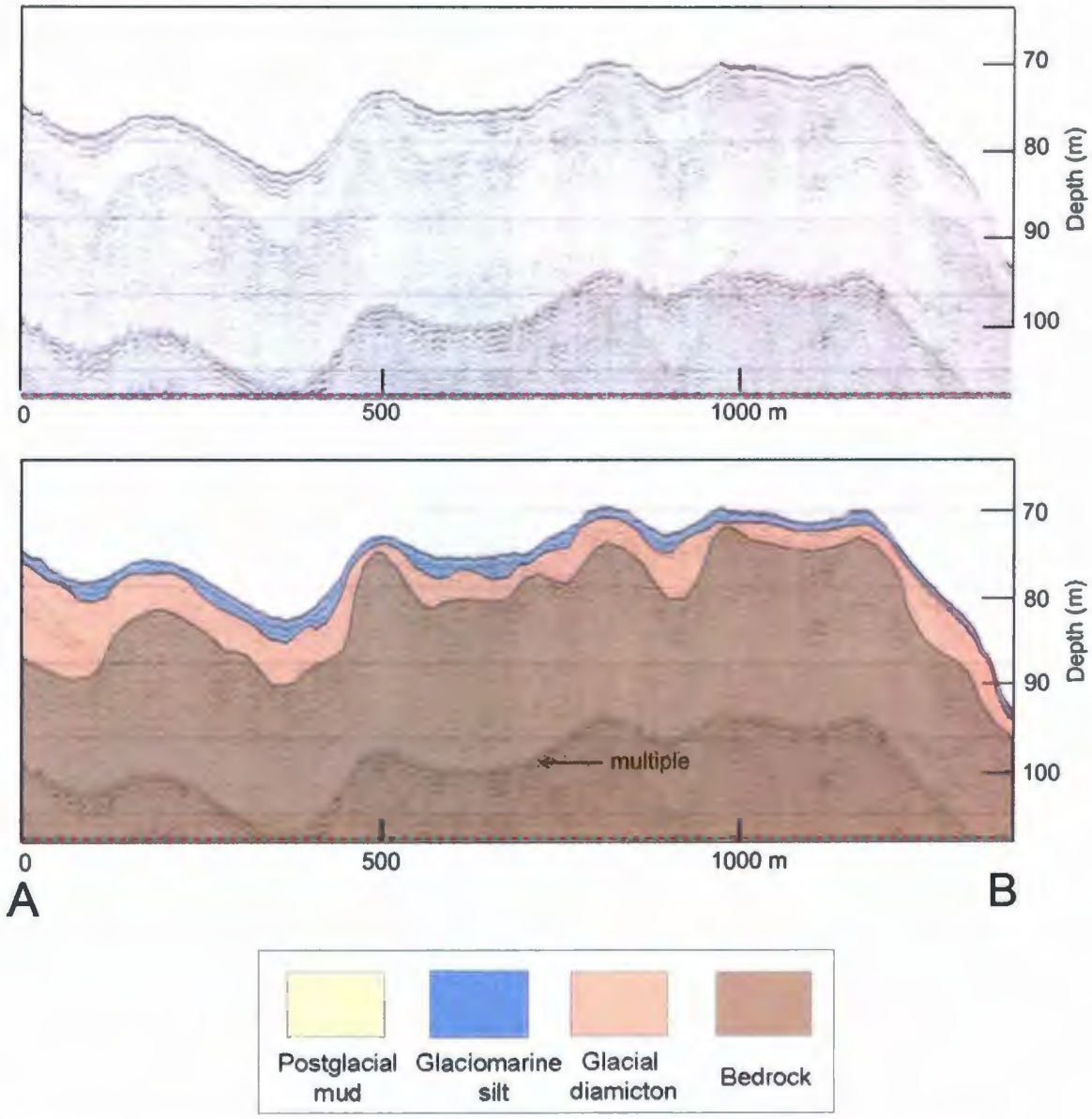

Figure 4.9 Huntec sub-bottom profile and interpreted geological cross-section from eastern Placentia Bay (Line 1, daytime 2981250 from cruise 2005-051). Glacial diamicton occurs in ridges overlying Carboniferous bedrock and is draped by glaciomarine silt which thickens in inter-ridge basins. Location of profile is shown in Figure 4.1.

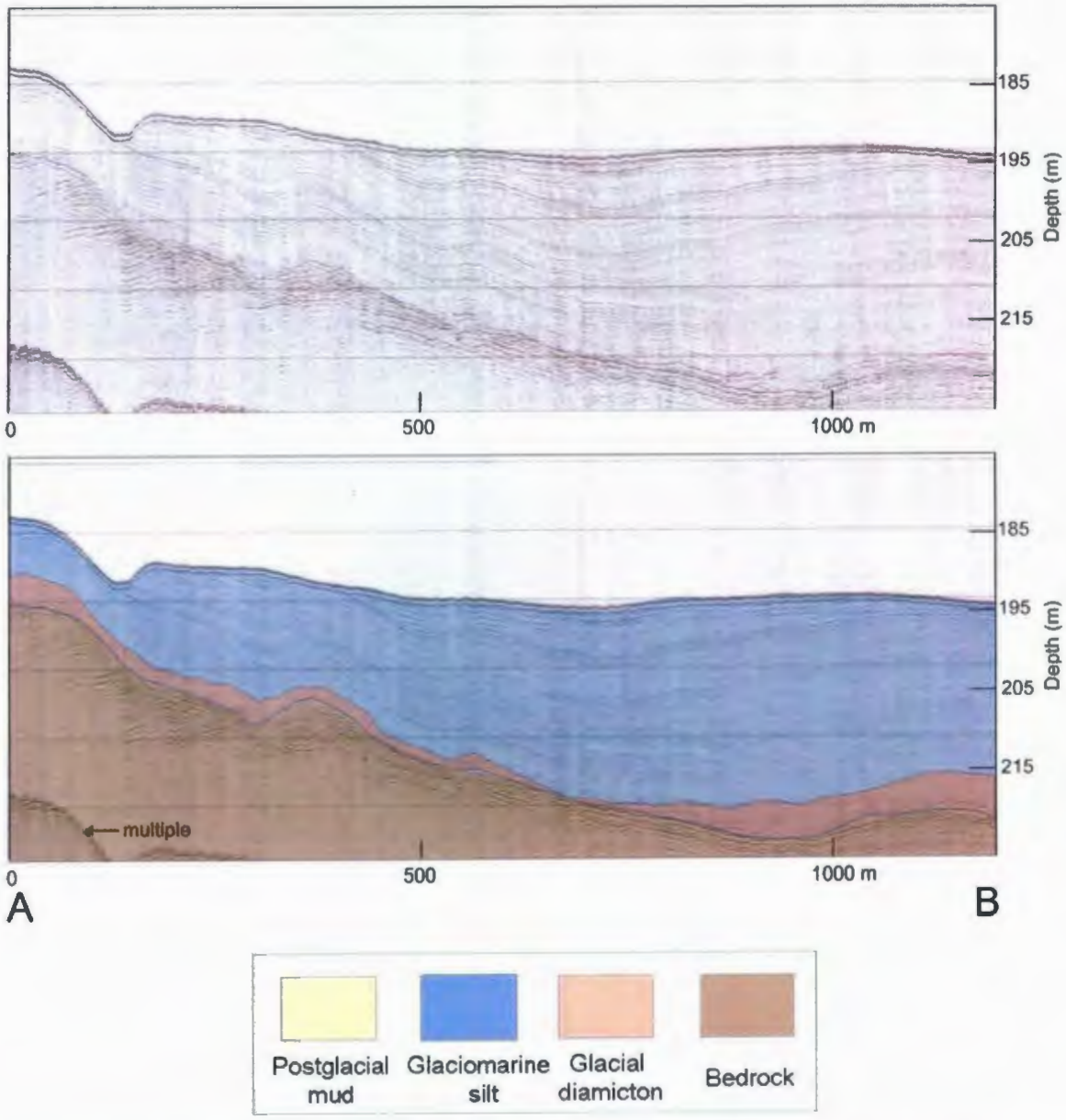

Figure 4.10 Huntec sub-bottom profile and interpreted geological cross-section from eastern Placentia Bay (Line 2, daytime 2981411 from cruise 2005-051). Glaciomarine silt overlies a thin blanket of glacial diamicton which overlies acoustically stratified bedrock interpreted to be Carboniferous bedrock. Up to 10 m of the upper sediments have been removed in this section (escarpment in left of section). Location of profile is shown in Figure 4.1.

In the central part of the bay, in water depths of 195-240 m, acoustically stratified glaciomarine silt thickens (up to 15 m) and is draped over glacial diamicton (9-14 m thick). In water depths greater than 300 m, sediment packages thicken where the glaciomarine silt is up to 30 m thick overlain by postglacial mud up to 8 m thick.

4.3 Seabed landforms

Glacial landforms occur in several fields throughout Placentia Bay and are divided into two categories: flow-parallel landforms and ice-marginal landforms. Flow-parallel landforms include flutes, drumlins, megaflutes, and crag-and-tails. Ice-marginal landforms include De Geer moraines and grounding-line moraines. Landforms are described and illustrated with examples from the multibeam data (location of figures shown in **Figure 4.11**). The dimensions of individual landforms are presented in **Appendix 3.**

4.3.1 Flow-parallel landforms

4.3.1.1 Drumlins and megaflutes

Drumlins preserved on the Placentia Bay seabed are identified based on their morphology, which ranges from egg-shaped parabolic mounds to elongated spindle forms that grade into megaflutes. Drumlins have average elongation ratios of ~4.0. They become more elongated at greater water depths, where they grade into megaflutes with average elongation ratios of ~7.0. Drumlins and megaflutes occur in several fields discussed below.

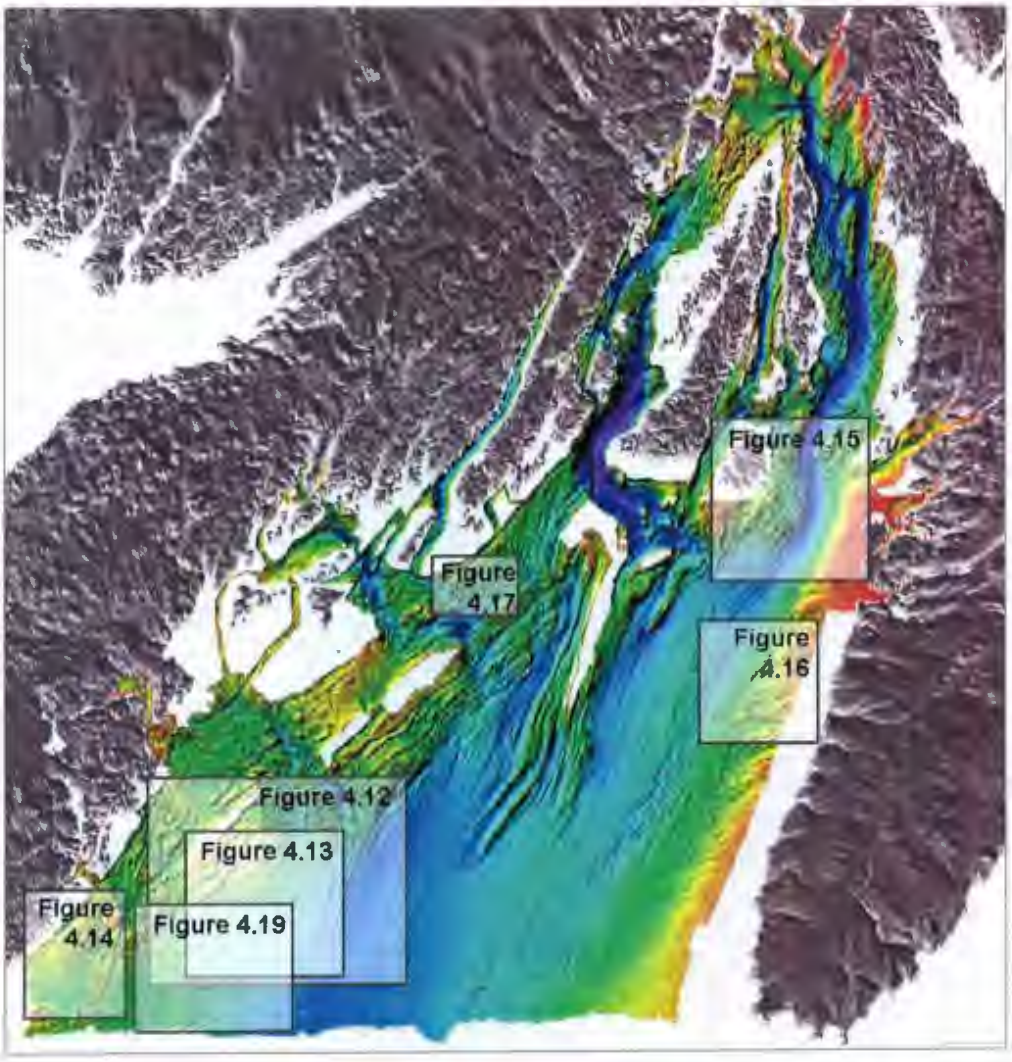

Figure 4.11 Multibeam shaded-relief image showing the extent of multibeam survey area and locations of subsequent figures.

Sub-bottom profiles through these landforms show acoustically incoherent reflections interpreted as glacial diamicton. Van Veen grab samples show a gravelly sandy mud with sub-rounded to sub-angular gravel up to 15 cm in diameter, interpreted as glacial diamicton. Drumlins are commonly draped by varying thicknesses of glaciomarine sediments that mimic the surface of the drumlins. Postglacial mud commonly occurs ponded in basins and inter-ridge crests.

Drumlins are common in southwestern Placentia Bay, which has the most extensive field of drumlins observed in offshore Atlantic Canada (Shaw *et al.*, 2006a). This field is approximately 22 km wide and occurs in water depths of ~55-200 m (**Figure 4.12**). Drumlins from western and southwestern Placentia Bay typically show a steeper, blunt stoss side and a gentler lee slope, pointed southeast into the central bay. Drumlins average 795 m long (SE (standard error): 38 m), 10 m high (SE: 0.5 m), 230 m wide (SE: 8.4 m) with elongation ratios of ~3.5 (SE: 0.1). Drumlins grade into megaflutes at water depths greater than ~140 m. Megaflutes average 1970 m long (SE: 116 m), 10 m high (SE: 0.79 m), 285 wide (SE: 8.2 m) with elongation ratios of ~ 7.0 (SE: 0.4). Megaflutes curve southwest, with an average orientation of 140°, into the central part of the bay, as shown in **Figure 4.13**.

Another field of drumlins in the southwesternmost corner of the bay have dimensions averaging 700 m long (SE: 26 m), 10 m (SE: 2.0 m) high, 235 m wide (SE: 9.0 m) with elongation ratios of ~ 3.1 (SE: 0.1) (**Figure 4.14**). Compared to other drumlins surrounding this field, there are subtle differences in form; however these differences are not reflected in dimensions and may be explained by post depositional reworking (see below).

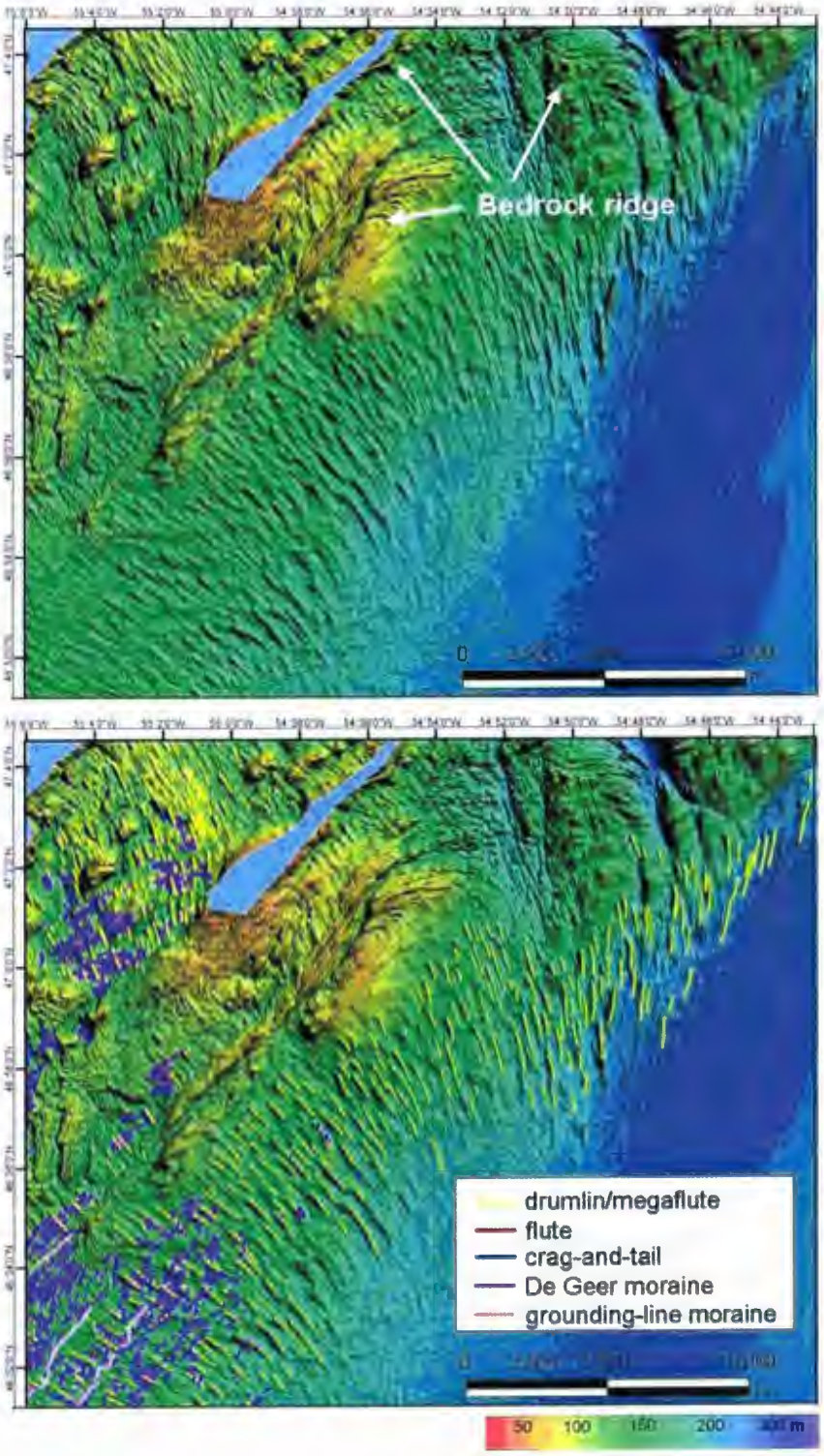

Figure 4.12 Multibeam shaded-relief image of drumlinized terrain in southwestern Placentia Bay. Interpretation (shown in lower image) shows drumlins which grade into megaflutes with increasing depths. Image is sun-illuminated from the northeast (45°) with a vertical exaggeration of 10 times and a horizontal resolution of 5 m. See Figure 4.11 for location.

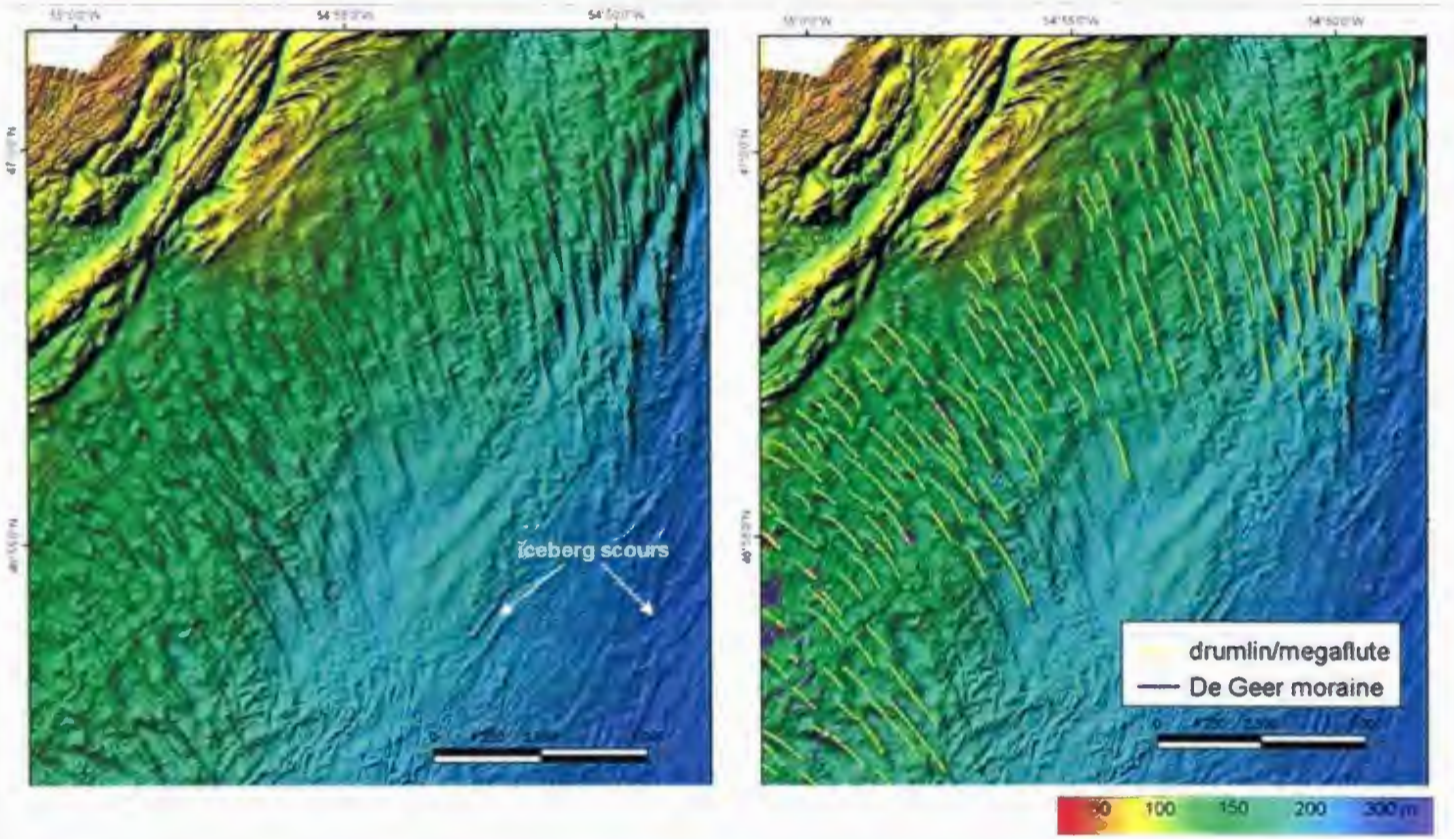

Figure 4.13 Multibeam shaded-relief image of megaflutes in southwestern Placentia Bay. Interpretation (shown in right image) shows megaflutes curving down the axis of Placentia Bay. Image is sun-illuminated from the northeast (45°) with a vertical exaggeration of 10 times and a horizontal resolution of 5 m. See Figure 4.11 for location.

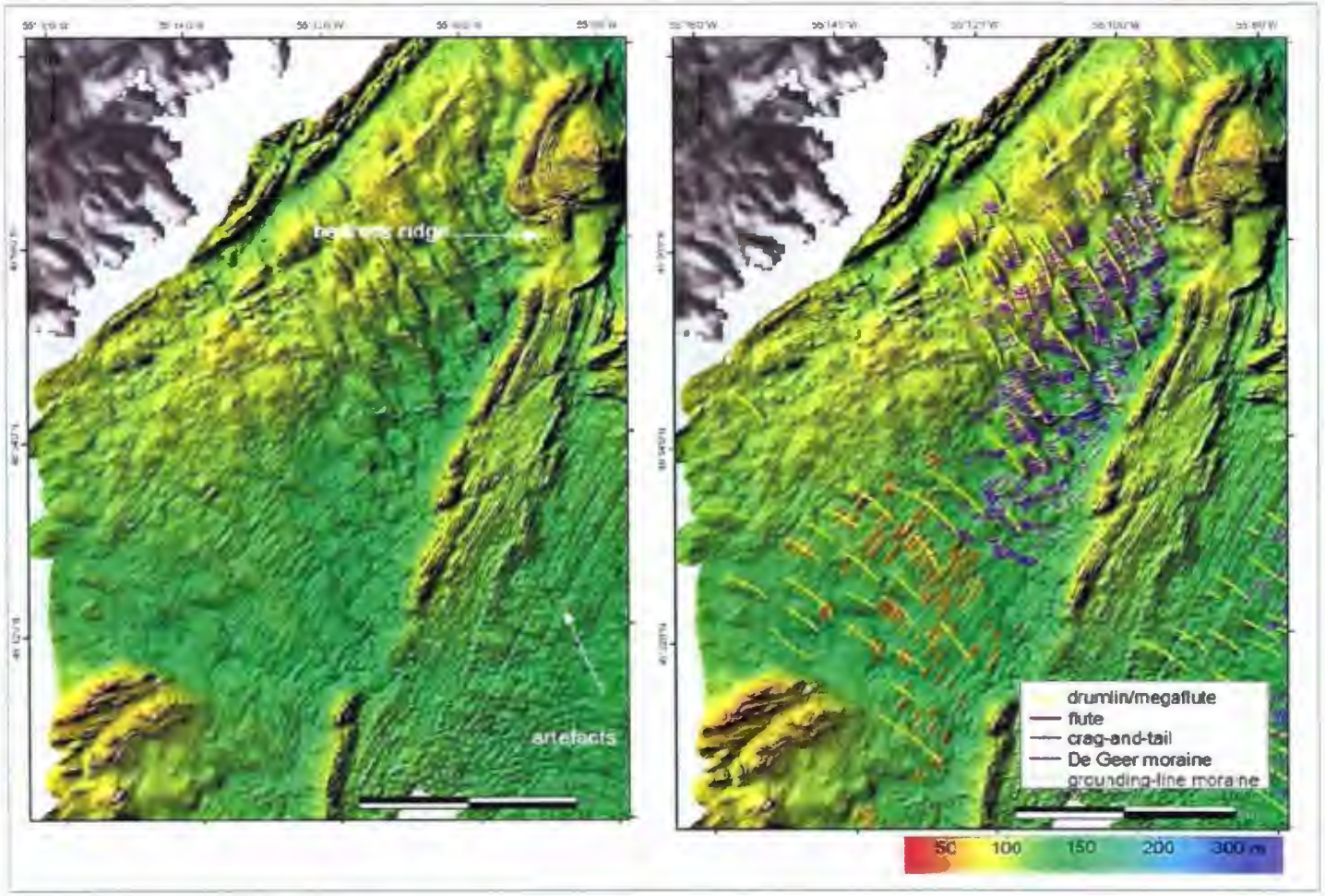

Figure 4.14 Multibeam shaded-relief images of drumlins and fluted terrain in southwestern Placentia Bay. Interpretation (shown in right image) shows drumlins in the extreme southwest which have been fluted. These drumlins appear lower and wider than those to the north; however, measured dimensions are similar. Image is sun-illuminated from the northeast (45°) with a vertical exaggeration of 10 times and a horizontal resolution of 5 m. See Figure 4.11 for location.

Drumlins and megaflutes also occur on the eastern side of Placentia Bay. Drumlins are elongated spindle-shaped forms with average lengths of 1040 m (SE: 72 m), widths of 320 m (SE: 28 m), and heights of 10 m (SE: 1.6 m). Drumlins grade into megaflutes in water depths greater than ~80 m. The long axes of these landforms curve down Eastern Channel with an average azimuth of 225° (**Figure 4.15**).

South of Red Island the seafloor morphology becomes much more complex with ridges of different sizes and orientation, giving the area a 'corrugated' appearance (**Figure 4.16**). Sub-bottom profiles in this area indicate 20-27 m of glacial diamicton overlying bedrock. Drumlins average 1350 m long (SE: 51 m), 430 m wide (SE: 71 m), 15 m high (SE: 3 m), and have a similar orientation (240°, southwest into the bay) as those north of this area (described above). Superimposed on these drumlins are smaller ridges, also consisting of glacial diamicton. The smaller ridges, interpreted as drumlins, average 500 m long (SE: 111 m), 205 m wide (SE: 28 m) and 10 m high (SE: 1.63 m). They have distinct stoss and lee sides with an average azimuth of 285° and start to curve into the bay with greater water depths (>150 m).

4.3.1.2 Crag and tails

Streamlined landforms occur south of Red Island. Sub-bottom profiles were unable to penetrate these landforms, suggesting that they are bedrock. These landforms are interpreted as crag-and-tails composed of bedrock which has been moulded by ice. South of Red Island, crag-and-tails are 1984 m long (SE: 439 m), 21 m high (SE: 4.2 m)

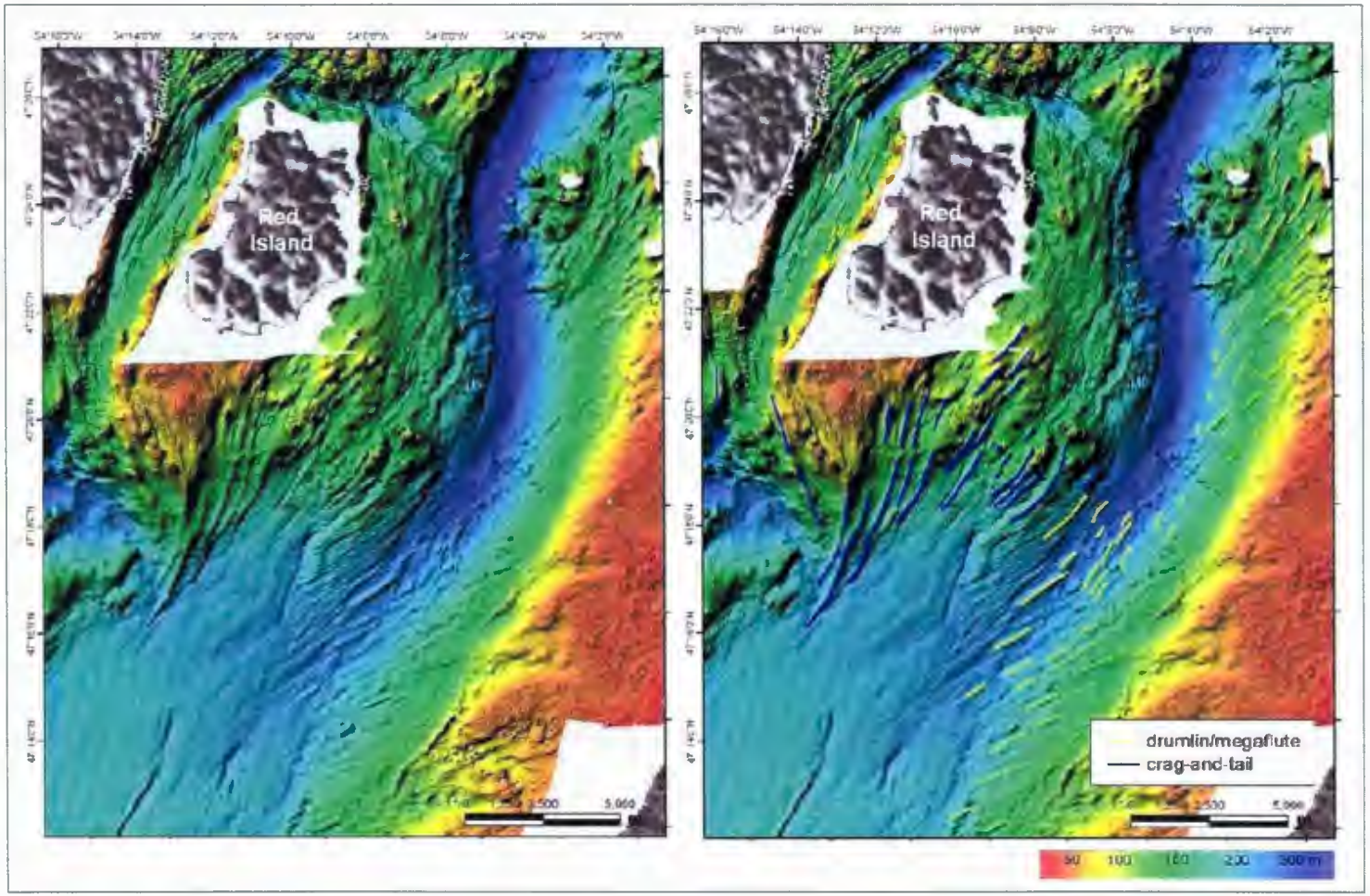

Figure 4.15 Multibeam shaded-relief image of flow-parallel landform assemblage in eastern Placentia Bay. Interpretation (shown in right image) shows drumlins, megaflutes and crag-and-tails curving down Eastern Channel into the bay. Image is sun-illuminated from the northwest (315°) with a vertical exaggeration of 10 times and a horizontal resolution of 5 m. See Figure 4.11 for location.

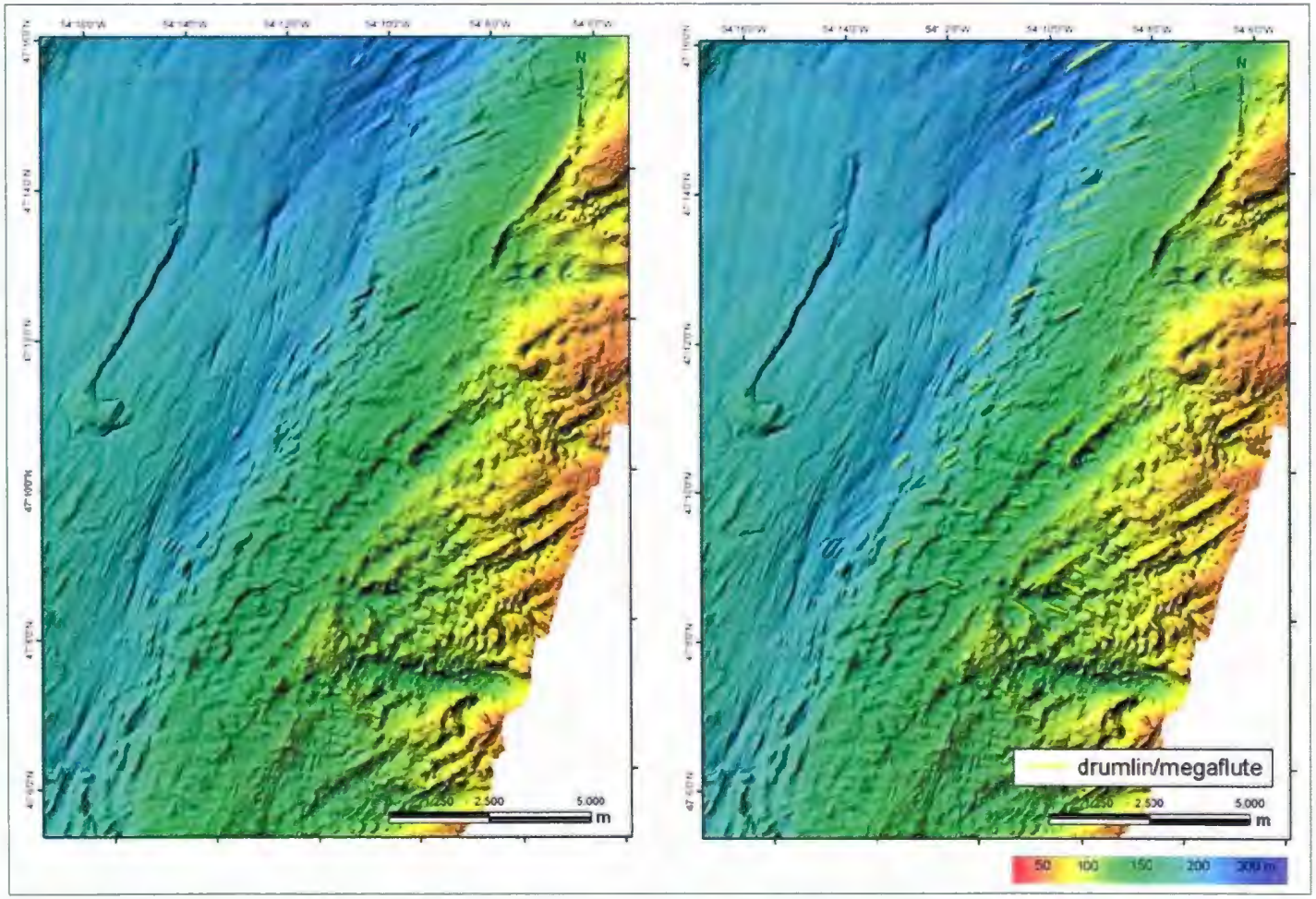

Figure 4.16 Multibeam shaded-relief image of drumlins in eastern Placentia Bay. Interpretation (shown in right image) shows drumlins of different orientations including larger southwest-trending drumlins and smaller westward-trending drumlins. Image is sun-illuminated from the northwest (315°) with a vertical exaggeration of 10 times and a horizontal resolution of 5 m. See Figure 4.11 for location.

and 417 m wide (SE: 57 m). Their orientation varies but curves down Eastern Channel into the bay, similar to the drumlins and megaflutes in this area (shown in **Figure 4.16**).

4.3.1.3 Flutes

The flutes observed in Placentia Bay are small, linear ridges which average 3 m high (SE: 0.14 m), 425 m long (SE: 20.4 m) and 60 m wide (SE: 3.2 m). They are spaced 40-60 m apart and have an average elongation ratio of 7.1 (**Figure 4.14**). Flutes are found only in one field (~ 100 km²) in the southwesternmost part of the bay. They are oriented northeast-southwest (40°-220°). They occur superimposed on much larger ridges, which are interpreted to be drumlins.

No subbottom profiles, photos or samples are available from this area to determine flute composition; however, it is thought likely that they are composed of remobilized drumlin material which elsewhere has been interpreted as glacial diamicton.

4.3.2 Ice-marginal landforms

Glacial landforms aligned transverse to the interpreted ice-flow direction are divided into De Geer moraines and grounding-line moraines.

4.3.2.1 De Geer moraines

In sub-bottom profiles, ridges interpreted to be De Geer moraines show acoustically incoherent reflections typical of glacial diamicton. Gravelly sandy mud containing sub-rounded to sub-angular gravel (up to 15 cm) was observed in bottom photos and recovered from the surface of these ridges where they are exposed on the seafloor.

Together the acoustic character and sedimentological characteristics support the interpretation that these moraines are formed of glacial diamicton. The moraines also overlie glacial diamicton, which in places is in the form of drumlins. De Geer moraines may be overlain by glaciomarine silt which generally mimics the moraine surface. De Geer moraines appear either subdued or buried in deeper water and in seabed depressions where glaciomarine silt is thicker.

De Geer moraines occur in several fields in Placentia Bay in water depths of ~65-275 m. They are small, narrow, sharp-crested ridges that average 4 m high (SE: 0.25 m) and 79 m wide (SE: 6.2 m) (**Figure 4.17**). The length of the moraine ridges is variable; individual ridge crests can be traced horizontally from short segments of 108 m up to 1016 m. Individual moraines are generally symmetrical in cross-section. In planform, individual moraines display either linear or curved crestlines. The longer moraine crests are formed of multiple curved sections and may have more asymmetrical cross-sections, with their crests displaying a gentler slope to the north and a steeper slope to the south. The horizontal spacing between these ridges varies throughout the bay ranging from 20 to 276 m and averaging 75 m.

The orientation of the De Geer moraines varies throughout the bay but they generally follow the bathymetric contours. **Figure 4.18** shows the distribution of De Geer moraines throughout the bay. De Geer moraines typically occur on topographic highs, such as drumlin surfaces. Where they occur on drumlin surfaces, the crests of the De Geer moraines strike perpendicular or oblique to the drumlin orientations. Similar drumlin-De Geer moraine relationships have been mapped on German Bank offshore

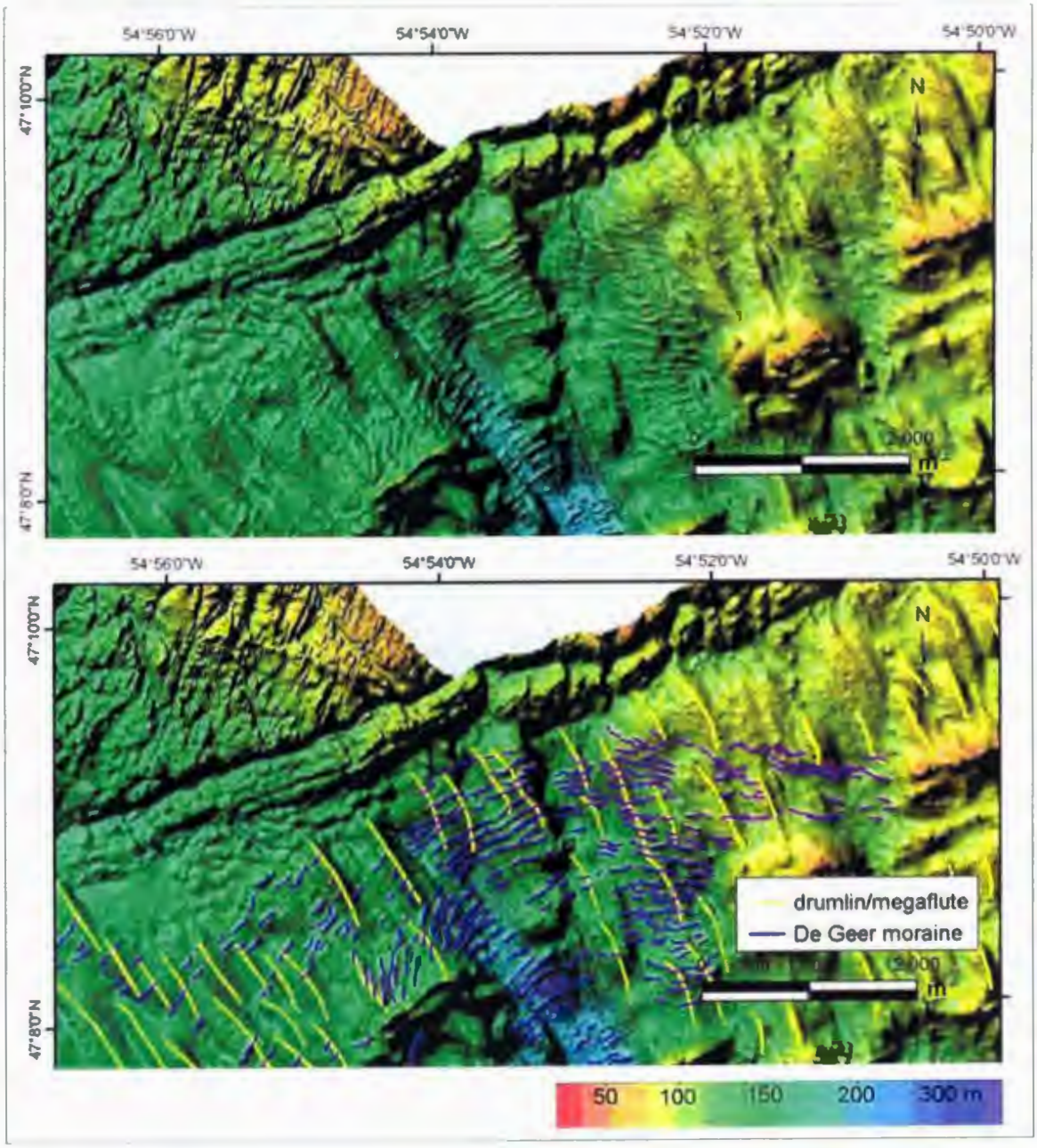

Figure 4.17 Multibeam shaded-relief image of De Geer moraines in southwestern Placentia Bay, interpretation shown in lower image. Image is sun-illuminated from the northeast (45°) with a vertical exaggeration of 10 times and a horizontal resolution of 5 m. See Figure 4.11 for location.

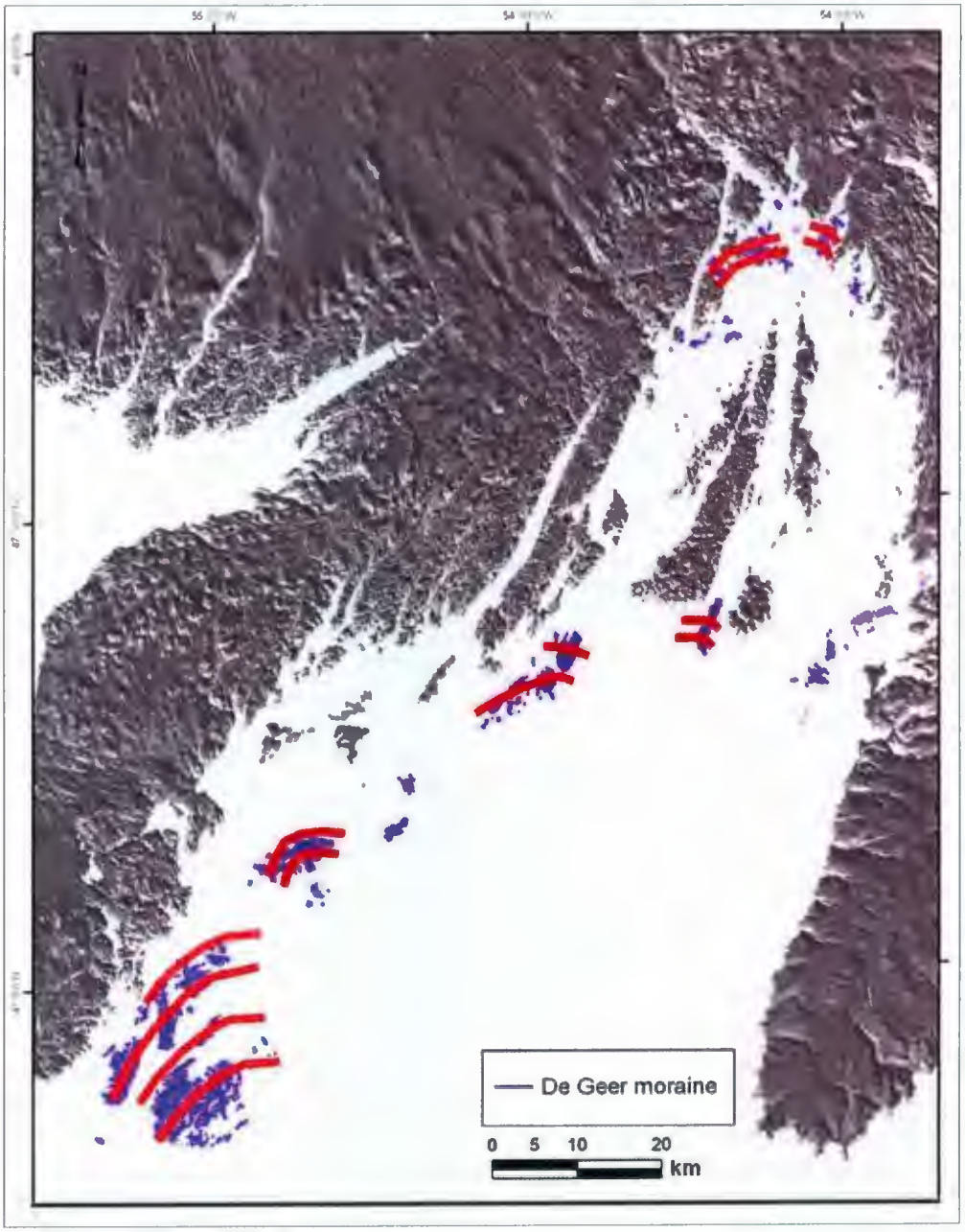

Figure 4.18 Distribution of De Geer moraines in Placentia Bay. Thick red lines show general orientation of the different fields (taken normal to ridge crests).

southern Nova Scotia (Todd *et al.*, 2007) and on Wollaston Island in the Canadian Arctic (Dyke and Savelle, 2000).

4.3.2.2 Grounding-line moraines

Moraine ridges identified in southwestern Placentia Bay are interpreted as grounding-line moraines (**Figure 4.19**). These moraines have similar composition and acoustic character as the De Geer moraines described above; however they display a more complex morphology and form a series of discontinuous sinuous ridges up to 7200 m long. Individual segments range from 110 m up to 1320 m and are crudely aligned. Arcuate lobes observed along the ridge crests average 150 m wide and are open to the northeast. They are larger than De Geer moraines in both height and width, averaging 158 m wide (SE: 19.6 m) and 9.7 m high (SE: 0.66 m). They are roughly parallel to each other and strike northeast-southwest (30-205°). These moraines are situated in a larger field that contains many smaller De Geer moraines where they all share a general northeast-southwest orientation.

4.4 Summary

A range of subglacial landforms is preserved on the Placentia Bay seabed which includes drumlins, flutes, megaflutes and crag and tails (summarized in **Table 4.2**). These landforms serve as palaeo ice-flow indicators that are used to reconstruct ice-flow history. Ice-marginal landforms (De Geer moraines, grounding-line moraines) provide evidence of the pattern of ice retreat in Placentia Bay. All identified subglacial landforms are primarily depositional and their spatial distribution is controlled by the presence of a

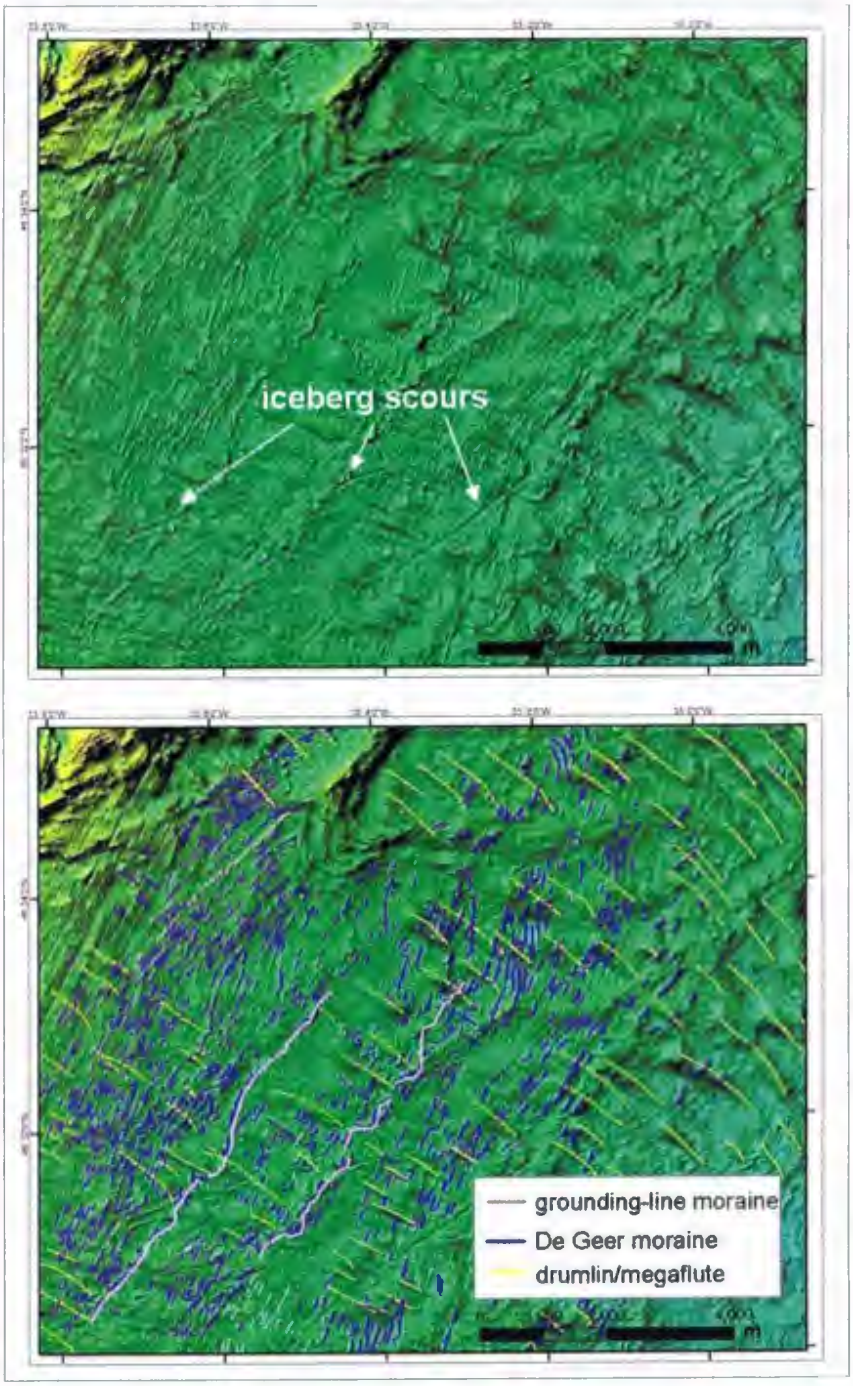

Figure 4.19 Multibeam shaded-relief image of grounding-line moraines, De Geer moraines and drumlins in southwestern Placentia Bay. Image is sun-illuminated from the northeast (45°) with a vertical exaggeration of 10 times and a horizontal resolution of 5 m. See Figure 4.11 for location.

Table 4.2 Summary of interpreted landforms.

Landform	Description	Association with other landforms	Location	Ice flow relationship	Formative Mechanism
Drumlin	Spindle, parabolic and modified forms with distinct stoss and lee sides	Part of flow-parallel landform continuum	Water depths of 20-320 m. Both sides of bay	parallel	Fast-flowing ice
Megaflute	Landforms more elongated with increasing depths	Part of flow-parallel landform continuum	Water depths of 150-320 m. Both sides of bay	parallel	Fast-flowing ice
Flute	Occur in one field of small linear, parallel ridges	Overprint drumlins, perpendicular to drumlins	Water depths of 20-100 m. Southeastern corner of bay	parallel	Deformation of sediments around obstacles on bed
Crag-and-tail	Trend NE-SW, converging into bay, distinct stoss and lee sides	With drumlins and megaflutes	Most prominent in northern and northeastern bay	parallel	Erosion by advancing ice
Grounding-line moraines	Lobate push features suggest ice readvances during northward ice retreat	Best developed on drumlin surfaces, surrounded by smaller De Geer moraines of same orientation	Water depths of 150-250 m. Southeastern bay	normal	Sediment deposition at or close to grounding-line during stillstands or readvances
DeGeer moraines	Small, numerous, sub-parallel ridges	Best developed on drumlin surfaces, less common in seabed depressions and bedrock highs	Water depths of 20-360 m. Commonly occur on drumlin surfaces Both sides of bay	normal	Sediment deposition at or close to grounding-line during minor stillstands or readvances

pre-existing substrate, mainly glacial diamicton. Landforms are concentrated on the seabed near the coast and extend out to water depths of ~275 m. They are not common on bedrock or where sediment cover is thin, such as in the northern part of the bay. These landforms are commonly draped by glaciomarine sediments which may either mimic the till surface or may conceal it. Landforms may also be locally covered by postglacial sediments.

Chapter 5: Discussion

5.1 Outline

In this chapter the study results are used to address the following research questions: 1) What do the morphology, orientation and spatial distribution of glacial landforms preserved on the seabed reveal about ice-flow events in Placentia Bay? 2) What was the style and timing of ice retreat from Placentia Bay? 3) Are the ice flow events and pattern of retreat consistent with glacial records from the surrounding terrestrial areas? 4) Is there landform evidence to support the concept of ice streaming as proposed by the conceptual model of Shaw *et al.* (2006a)? This is followed by a synthesis of the glacial history of Placentia Bay. The value and limitation of using this integrated onshore-offshore approach and suggestions for future work are also discussed.

5.2 Ice-flow events in Placentia Bay

Flow-parallel landforms preserved on the seabed of Placentia Bay demonstrate that ice extended well beyond the coast of both adjacent peninsulas. Flow-parallel landforms were identified on the seabed in water depths of ~55 to 200 m. Flow-parallel landforms were not identified in water depths greater than 200 m although sub-bottom profiles indicate that glacial diamicton is present at these depths. The superposition of flow-parallel landforms indicates that at least three discrete ice-flow events are preserved on the seabed and also provides a relative chronology for these events.

Evidence for the most regionally extensive ice-flow event comes from drumlins on both sides of the bay which exhibit progressive elongation with increasing water depths where they grade into megaflutes. These landforms show a general trend of convergent

flow down the axis of the bay (**Figure 5.1**). This convergence is observed in an extensive field of southeast-trending drumlins and megaflutes on the western side of the bay and from southwest-trending drumlins, megaflutes and crag-and-tails on the eastern side of the bay. These fields are interpreted as a contemporaneous flow set for it is unlikely that each flow tangentially into the bay without the adjacent flow to help steer it. Non-contemporaneous ice flows should typically show splaying in all directions as ice flowed from land into deeper water unhindered.

In southwestern Placentia Bay, a localized southwest-northeast trending fluting field is superimposed at right angles on top of a field of southeast-oriented drumlins (**Figure 5.2**). The drumlins are interpreted to be part of the regional convergent flow described above. The modification and fluting of the drumlins indicates that this fluting field postdates the drumlins. De Geer moraines do not appear to be preserved in this fluted field, but are seen adjacent to it (shown in **Figure 5.2**). There is no clear relative age relationship between the flutes and De Geer moraines. This ice-flow event is interpreted to be a later southwest-northeast flow that terminated in proximity to the small De Geer moraines observed near the limit of this field.

Based on the multibeam data, it is likely that this fluted flow could be a localized ice-flow originating from the northwest that became pinned by the shallow bedrock ridge (shown in **Figure 5.2**) and subsequently flowed in a southwest direction with grounded ice forming the observed flutes. This ice-flow did not heavily erode this area; it fluted the surface of the underlying drumlins suggesting that this ice flow was almost buoyant.

It may also be possible that the flutes are recording ice-flow that originated from an offshore source to the southwest, most likely from grounded ice that became isolated by

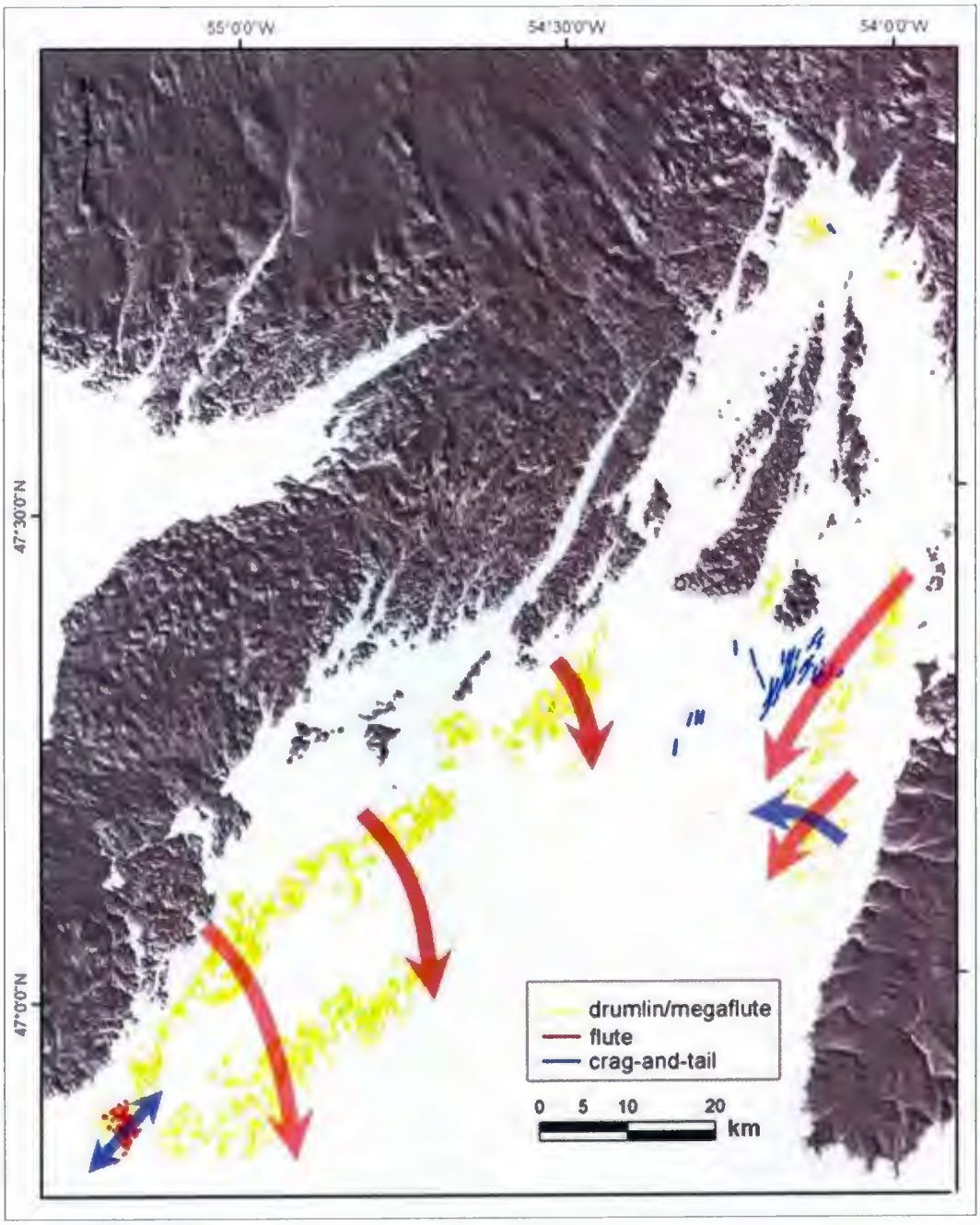

Figure 5.1 Convergent ice-flow patterns (shown by red arrows) shown on mapped flow-parallel landforms from both sides of Placentia Bay. Relatively younger ice-flow events (purple arrows) are also shown.

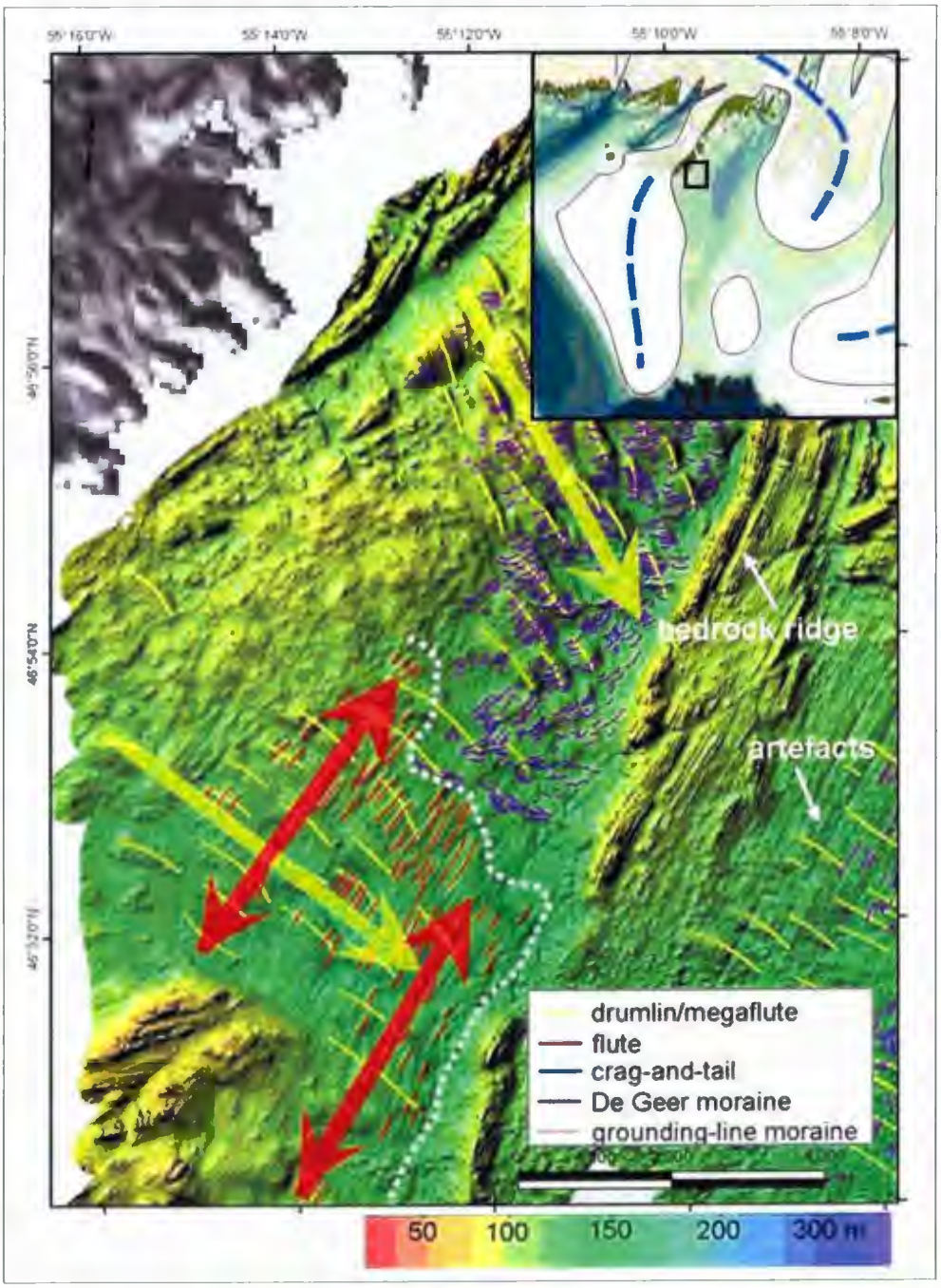

Figure 5.2 Fluted field in southwestern Placentia Bay. Here southeast-trending drumlins (flow lines shown by yellow arrow) have been overridden by flutes (red arrows). The extent of the fluted field is shown by the dotted white line. The location of this field is shown in the inset taken from the conceptual model of Shaw *et al.* (2006a) which depicts a lobe of ice south of the Burin Peninsula at 13 ka BP that could have been the source of this ice-flow.

calving southwest of Placentia Bay (Fader *et al.*, 1982; Shaw, 2003). This conclusion is consistent with an ice cap depicted in the conceptual model by Shaw *et al.* (2006a) which shows an ice cap extending down the Burin Peninsula and onto St. Pierre Bank (**Figure 5.2 inset**). While the existence of this ice cap is speculative, its presence provides a mechanism for the Burin Moraine (Fader *et al.*, 1982). Similarly, Tucker and McCann (1980) proposed that the last ice on the Burin Peninsula originated from an offshore source and it was thought likely that an ice cap, such as the one discussed by Fader *et al.* (1982) and Shaw *et al.* (2006a), was sustained for some time and grew in size. If this ice did originate from an offshore source to the southwest it would be expected that its extent would be identified by an ice-marginal moraine. This is not the case; no moraines were identified marking the extent of the fluted field. Also, no features were observed on adjacent land areas to support this northeastward ice-flow direction.

Another distinct ice-flow event is preserved on the eastern side of Placentia Bay. Here the imprint of small westward-trending drumlins on southwest-trending drumlins is interpreted to represent a relatively younger ice-flow event. The southeast-trending drumlins are interpreted as being part of the regional convergent flow into the bay whereas the westward-trending drumlins are interpreted as a later, possibly deglacial ice-flow, originating from the Avalon Peninsula. The flow lines of the westward-trending drumlins show a slight curvature but they do not converge into the bay as in the case for the larger southeast-trending drumlins (**Figure 5.3**).

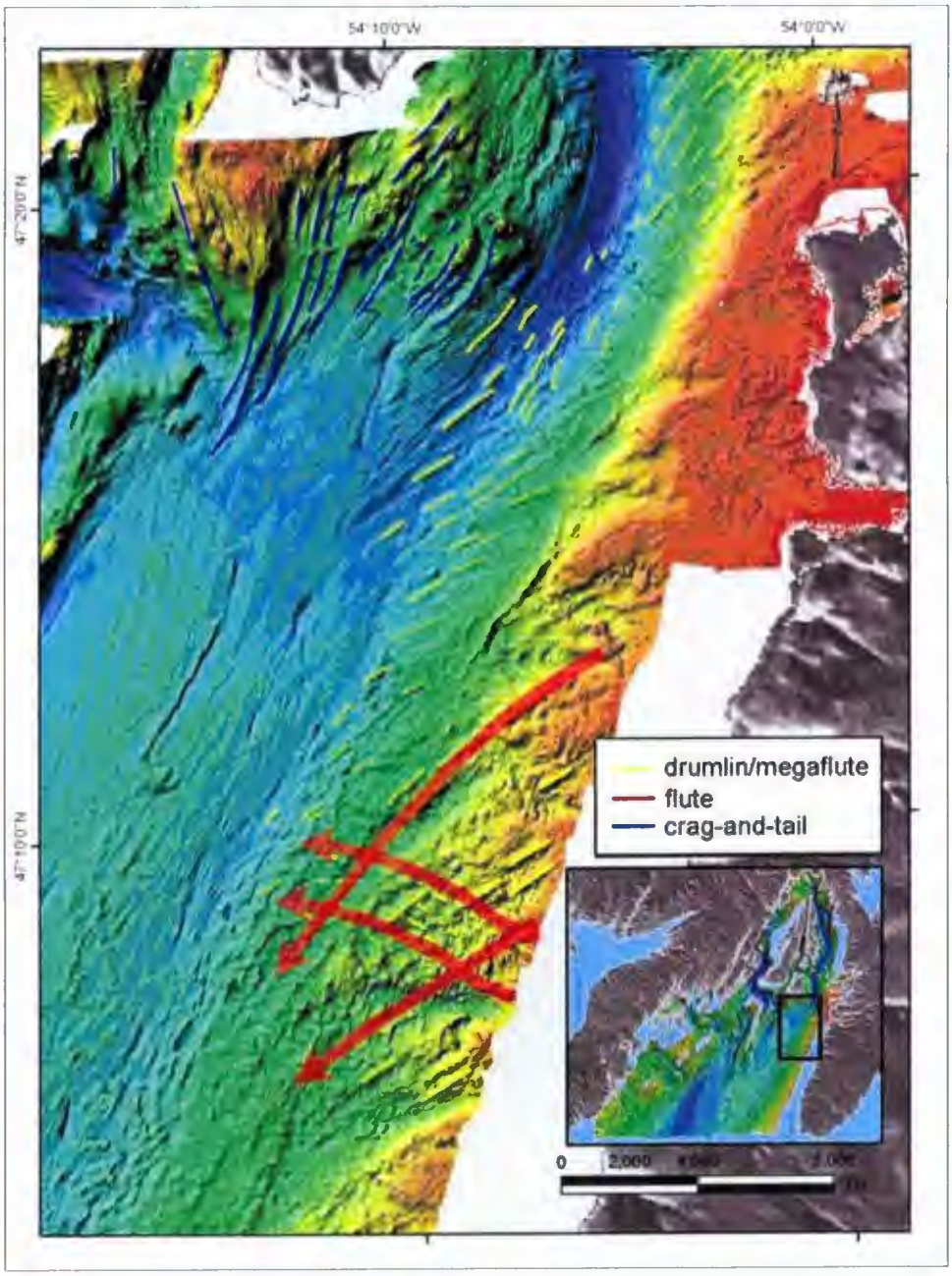

Figure 5.3 Ice-flow relationships in eastern Placentia Bay. Drumlins display two sets of orientations interpreted to represent different ice-flow events (indicated by red arrows). The imprint of the westward-trending drumlins on the southwestward-trending drumlins demonstrates that the westward ice-flow is relatively younger. Location of figure is shown in inset.

5.3 Style and timing of ice retreat from Placentia Bay

Ice-marginal landforms (De Geer moraines, grounding-line moraines) provide evidence of the pattern of ice retreat in Placentia Bay. These moraines record the active northwestward and northeastward retreat of tidewater ice margins. De Geer moraines generally occur in fields rather than as isolated individual landforms and occur in water depths of ~65 to 250 m. More sustained readvances or stillstands are marked by grounding-line moraines. In water depths greater than ~250 m, ice-marginal landforms were not observed and the seabed is dominated by glaciomarine and postglacial sediments. The absence of ice-marginal landforms in greater water depths suggests that either the ice margin was floating or landforms were buried by glaciomarine and postglacial sediments which thicken in deeper water depths.

The more widespread De Geer moraines display a linear to curvilinear pattern that generally follows the bathymetric contours. As shown in **Figure 4.17,** the deposition of De Geer moraines was greatest on seabed highs, such as drumlin crests, which likely acted as pinning points stabilizing the ice front.

The horizontal spacing between De Geer moraines in Placentia Bay varies, ranging from ~50 to 310 m, but is generally regular within individual fields. They likely formed during minor winter readvances of a tidewater ice front when iceberg calving was suppressed (Ottesen and Dowdeswell, 2006). Their distribution suggests a slow steady retreat with minor readvances during winter with a more stepwise retreat between the different fields of De Geer moraines, the distance between deglacial steps equal to the mean distance between the ridges (Linden and Möller, 2005).

The rate of calving and ice retreat is likely related to fast-moving ice flowing out of the bay and changes in relative sea level. Based on data from the Columbia Glacier, Alaska, van der Veen (1996) argued that calving rates and ice retreat is linked to increasing glacier speed and the associated thinning of the glacier. There are several other factors that may control ice-marginal fluctuations; for example, it may be a response to climatic forcing or to other factors that affect relative water depth such as eustasy, isostasy and sediment yield (Benn and Evans, 1998). It is also possible that the deposition of grounding-line systems can change relative water depth which alters the stability of the tidewater ice margin independent of sea level. Based on the distribution of De Geer moraines and grounding-line moraines in Placentia Bay, grounding-line retreat was likely driven by rapid calving, which was in turn enhanced by fast ice flow.

Chronological constraints on the retreat of ice from Placentia Bay come from ^{14}C ages from shells found in the glaciomarine silt. Around the mouth of the bay, ages closest to the base of the glaciomarine unit range from ~16.1 to 14.7 ka (see **Table 4.1**). These dates provide minimum ages for when ice retreated and indicate that glaciomarine sedimentation started before ~16.1 ka. Radiocarbon dates from the top of the glaciomarine unit range from ~12.7 to 12.0 ka providing minimum dates for the cessation of glaciomarine sedimentation.

5.4 Onshore-offshore correlations

The most pervasive ice-flow pattern preserved offshore is the regionally extensive convergent (southwestward to southeastward) ice-flow event. The orientation of drumlins and fluted terrain on the Burin and Avalon peninsulas is consistent with that of

the drumlins and megaflutes on the seabed. Drumlins and flutes on the Burin Peninsula have a southeastward orientation whereas drumlins and flutes on the Avalon Peninsula have a southwestward to westward orientation. Based on the orientations of landforms both on the seabed and on surrounding terrestrial areas, ice flow was directed into and subsequently down the axis of Placentia Bay. The continuation of strong southward flow is consistent with the hypothesis of Shaw *et al.* (2006a) that ice converged along the central axis of Placentia Bay. This convergent ice-flow can now be traced up-ice to regional ice dispersal centres (Catto, 1998; Catto and Taylor, 1998) (**Figure 5.4**).

The southwestward ice-flow set in eastern Placentia Bay is consistent with flutes, crag-and-tails and striations preserved along the western coast of the Avalon Peninsula; here several cross-cutting striation exposures have been interpreted to be different ice-flow events. One of these flow sets displays a southwestward orientation which is consistent with the southwestward drumlins seen on the seabed and is associated with the regionally extensive convergent flow, described above (see **Figures 4.15 and 4.16**). The second flow set on the Avalon Peninsula shows a westward orientation which is consistent with the orientation of the small westward-oriented drumlins present in eastern Placentia Bay (see **Figure 4.16**). Both the superposition of drumlins offshore and cross-cutting striation relationships on land provide a relatively younger age for the ice flow associated with the smaller westward-oriented drumlins (**Figure 5.5**).

There are areas where ice-flow patterns recorded on land were not observed offshore, and also where the ice-flow record preserved offshore was not observed on land. Evidence for the westward ice-flow documented by Batterson *et al.* (2006) on the Burin Peninsula was not observed on the adjacent seabed. The westward ice-flow is

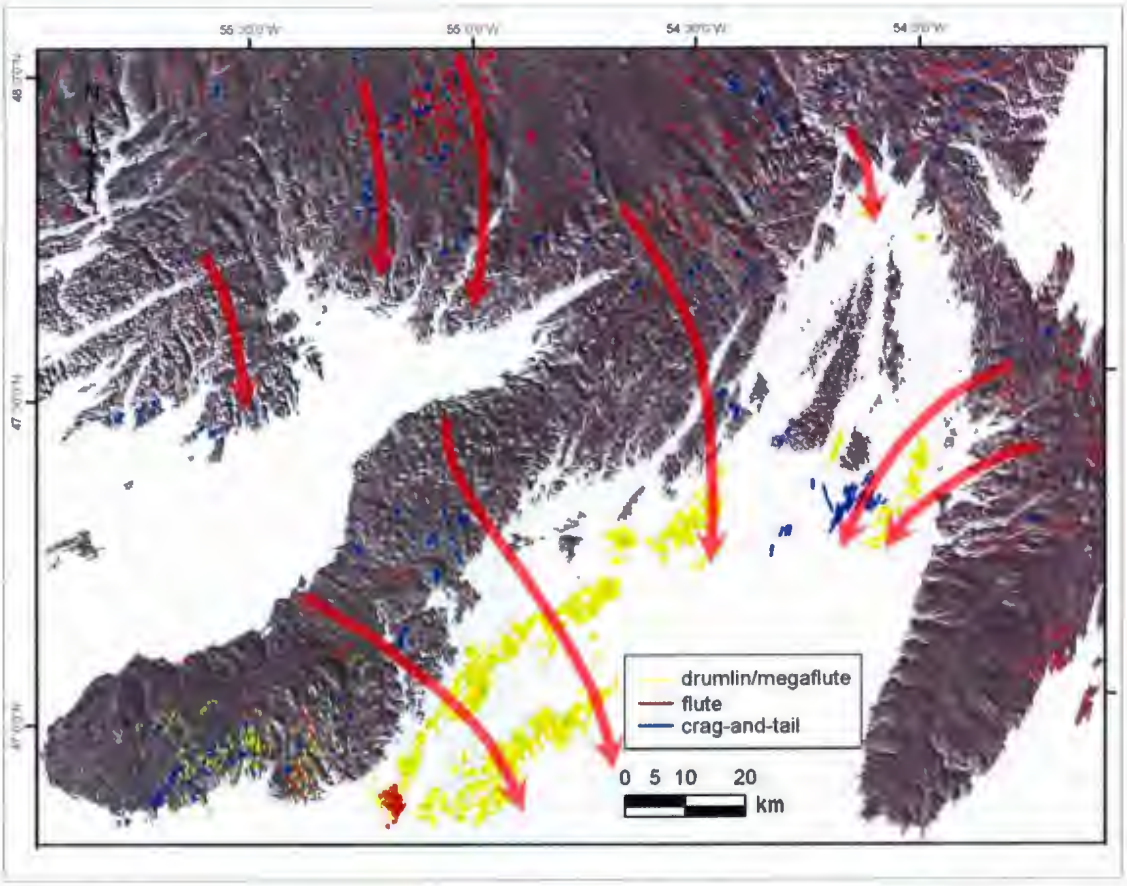

Figure 5.4 Convergent ice-flow patterns (indicated by red arrows) observed on the Placentia Bay seabed and surrounding peninsulas. The convergent ice flow on the seabed of Placentia Bay can be traced up-ice to regional ice dispersal centres on the surrounding Avalon and Burin peninsulas.

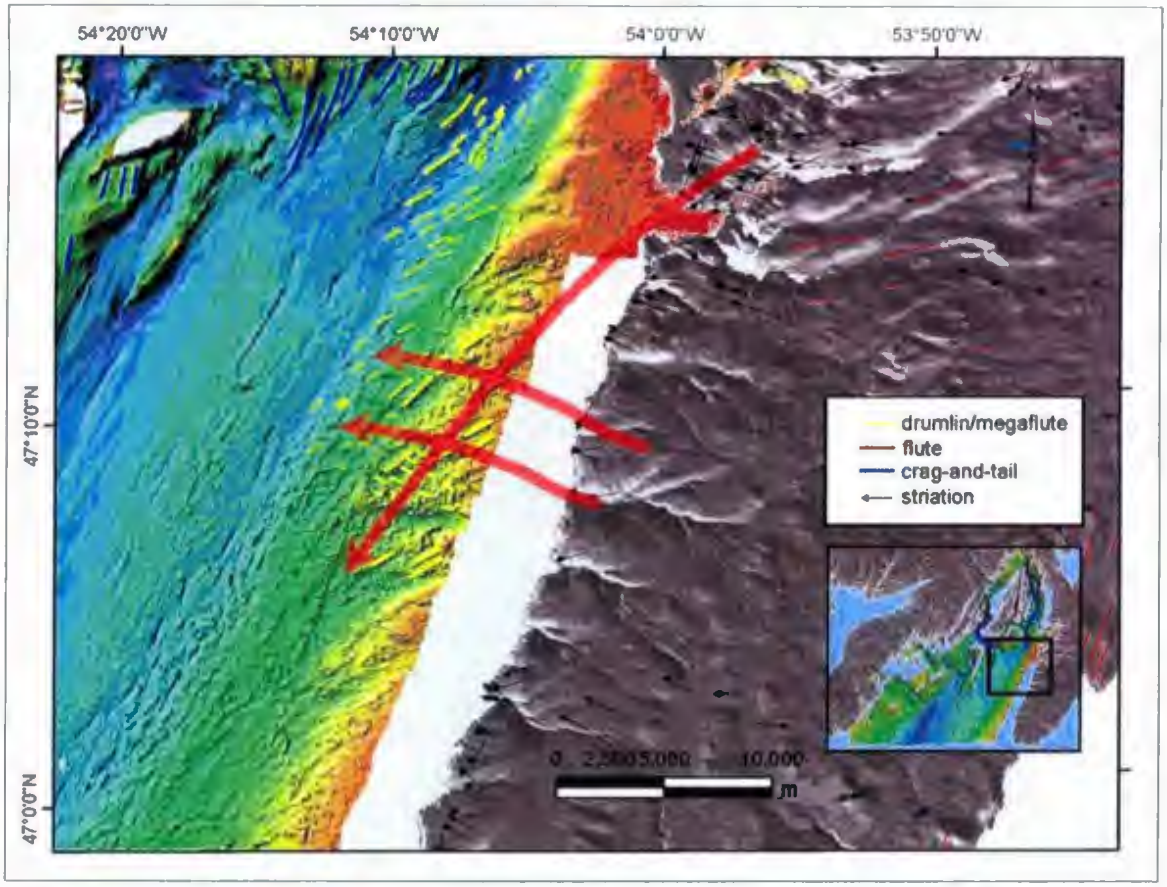

Figure 5.5 Ice-flow patterns (indicated by red arrows) observed on the eastern Placentia Bay seabed and adjacent Avalon Peninsula. The more limited westward to southwestward ice-flow set in eastern Placentia Bay is consistent with flow-parallel landforms and striations preserved along the western coast of the Avalon Peninsula.

younger than the regionally extensive southeastward flow and extends across the Burin Peninsula into Fortune Bay (Batterson *et al.*, 2006). There are no depositional features associated with this westward flow and only an erosional record is preserved. There is no evidence for the westward ice-flow on the seabed adjacent to the Burin Peninsula. The only seabed evidence for this westward ice-flow is along the eastern edge of the bay in a narrow zone southwest of Argentia (see **Figure 4.16**). If this ice-flow event is the eastward extension of a much larger westward ice-flow then it suggests an interesting glaciological dynamic during deglaciation of the bay. Alternatively, it may simply represent a local readvances of ice from an Avalon Peninsula ice source during overall deglaciation of the bay and is unrelated to ice-flow events on the Burin Peninsula.

Several hypotheses (detailed in 2.2.3) proposed for the origin of this ice-flow event necessitate ice being of sufficient thickness to cross the entire peninsula (over 170 m asl and up to ~320 m asl in the centre of the peninsula) (Batterson and Taylor, 2007). Striations from islands in Placentia Bay also record this westward ice-flow. Water depths surrounding these islands reach depths of ~ 350 m. It seems unlikely that ice would have been able to flow across these water depths and heights on land; however, similarly improbable ice-flow events have been documented elsewhere. For example, the Gold Cove Advance, recorded by ice-directional features and erratic lithologies, indicate that ice advanced over 300 km across the mouths of Hudson Strait and Frobisher Bay, onto Hall Peninsula of Baffin Island and well offshore into deep water (Miller and Kaufman, 1990) (**Figure 5.6**). This ice and has been described as a unique event with an ice-flow trajectory that is ice advance is the farthest known Pleistocene northward advance of

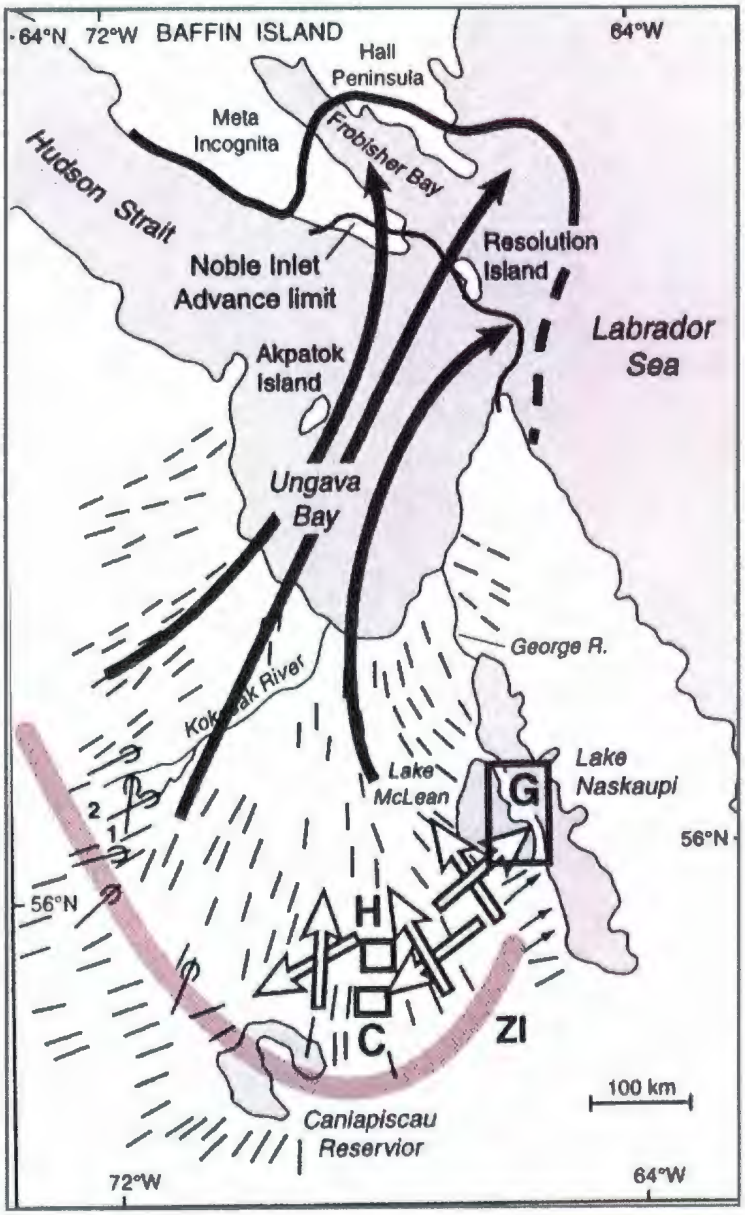

Figure 5.6 Location Map of Hudson Bay showing the advance of the Gold Cove ice-flow event onto Frobisher Island, Baffin Island (taken from Veillette *et al.*, 1999).

Labrador otherwise unexplained (Dyke *et al.*, 2002; Veillette *et al.*, 1999). The western ice-flow event documented on the Burin Peninsula is on a smaller scale but is similarly difficult to explain.

5.5 Evidence of ice streaming

Ice-flow convergence and increase in landform elongation are related to ice velocity (*e.g.*, Stokes and Clark, 2002, 2001; Briner, 2007). The elongated drumlins and megaflutes observed in Placentia Bay are therefore indicative of fast-flowing ice southward down the axis of Placentia Bay. According to the geomorphological criteria outlined by Stokes and Clark (1999; 2001) (see 2.2.1), the landform assemblage in Placentia Bay is typical of those characteristics associated with former ice streams, such as highly attenuated subglacial landforms and convergent flow pattern.

A conceptual model of a marine-based ice stream (**Figure 5.7a, b**) shows three zones that can be differentiated by characteristic landform assemblages found within them. Convergent landforms in the onset zone mark an increase in velocity that becomes more focused and elongated through the main trunk of the ice stream (Stokes and Clark, 2001). The main trunk of the ice stream shows elongated landforms that typically display abrupt lateral shear margins. The terminal zone of an ice stream may display diverging duck-foot-shaped features that terminate with abrupt lateral margins. These features are not preserved within Placentia Bay and data were not available for areas offshore of Placentia Bay. However, it is likely that there was a continuation of the palaeo-ice stream down Halibut Channel, which connects Placentia Bay with the continental shelf edge (Miller *et al.*, 2001). The landform assemblage in Placentia Bay is therefore interpreted

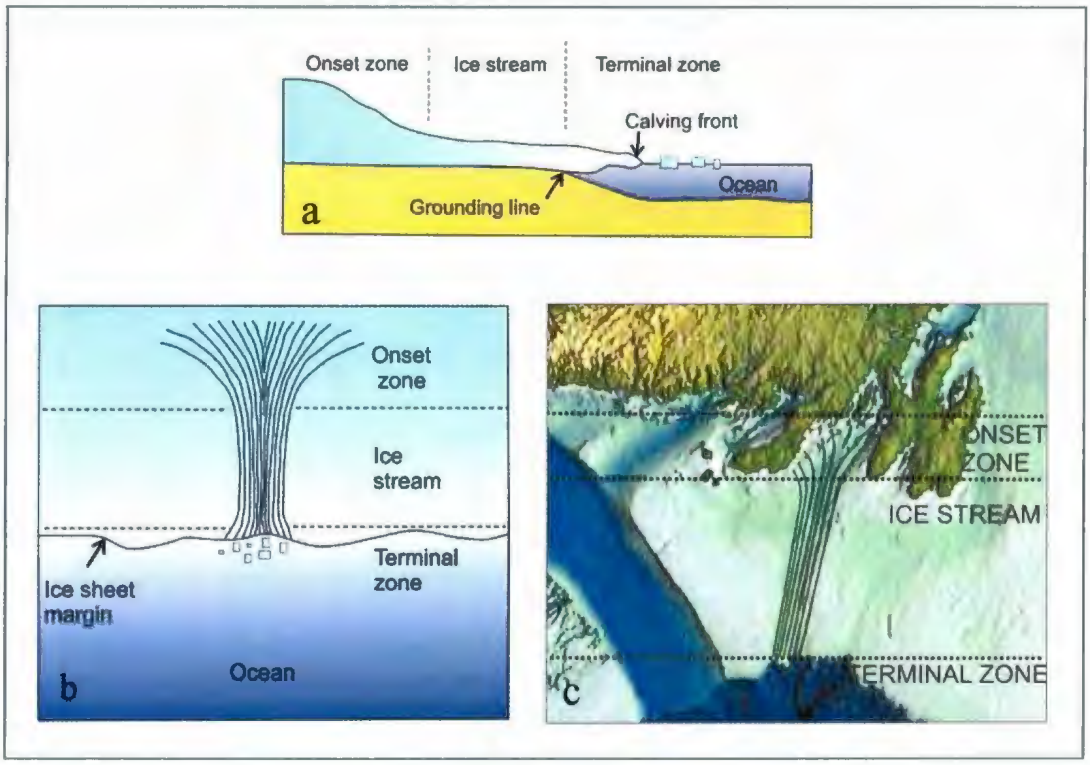

Figure 5.7 Conceptual model of marine-based ice stream (modified from Stokes and Clark, 2001) (a and b). The attenuated landforms and convergent flow pattern in Placentia Bay suggests that the bay falls within the onset zone of an ice stream that likely accelerated into an ice stream farther south in Halibut Channel and terminated at the shelf edge (c).

as recording ice-flow formed in the onset zone that accelerated into an ice stream farther south in Halibut Channel and terminated at the continental shelf edge supporting the model of Shaw *et al.* (2006a) (**Figure 5.7c**).

5.6 Synthesis: Glacial history of Placentia Bay region

Based on geomorphological evidence from both the Placentia Bay seabed and surrounding peninsulas, and ^{14}C dates from cores, a glacial history of Placentia Bay is discussed below.

During the late Wisconsinan, between 22 and 20 ka BP, Placentia Bay was covered by an ice sheet that terminated close to the edge of the continental shelf (Shaw *et al.*, 2006a). While there are no dates to confirm the timing of the maximum extent of ice in Placentia Bay, Shaw *et al.* (2006a) detail multiple sites near the shelf edges in Atlantic Canada that are consistent with this interpretation.

The oldest flow phase present on the Placentia Bay seabed is the convergent ice-flow down the bay shown by southward-trending drumlins and megaflutes that can be traced up-ice to regional ice dispersal centres (Catto, 1998; Catto and Taylor, 1998). The pattern of landforms suggests that they were formed in the onset zone of an ice stream that likely flowed southwestward out of the bay, southward through Halibut Channel towards the continental shelf edge. The existence of an ice stream in Placentia Bay has important implications for the glacial history of eastern Newfoundland as the location and behaviour of ice streams is one of the most important controls on ice sheet configurations. The majority of known palaeo-ice streams associated with the Laurentide Ice Sheet relate to the final stages of ice stream operation or conditions during or immediately prior to

deglaciation (Stokes and Clark, 2001). This flow is the oldest ice-flow phase recorded on the Burin Peninsula and is consistently the oldest flow when two or more ice-flow directions are present (Batterson *et al.*, 2006). This flow was assigned a late Wisconsinan age based on the continuity of striations and glacial features, the lack of moraines and the absence of surface weathering that would suggest a period of ice-free conditions. No divergent ice-flow patterns have been found, confirming that any ice divide is north of the peninsula, likely from the central Newfoundland divide (Shaw *et al.*, 2006a). Catto (1998) and Shaw (2003) suggested that this dominant ice-flow pattern post-dates maximum glacial conditions and is consistent with ice-flow from a central ice divide with offshore ice-flow convergence into prominent marine bays, including Placentia Bay, Trinity Bay, Notre Dame Bay, St. George's Bay and Bay D'Espoir. Ice was likely drawn down by active calving fronts in these bays.

This phase was followed by several smaller ice-flow events. No radiocarbon dates exist to constrain the age of these later ice-flow events; however, landforms imprinted on the surface of the older extensive southward-trending drumlins on the seabed and cross-cutting striation relationships on land suggest that these flow events are younger than the regional convergent southward ice-flow.

One of these is a generally westward flow recorded in the Burin Peninsula. Evidence for the westward ice-flow is found as striations on Merasheen Island and Jude Island in Placentia Bay, but no landforms were observed within the bay. Another westward flow originating from an Avalon ice centre is superimposed on southeast-trending drumlins in the eastern part of the bay. These drumlins are much smaller than those associated with the regional southward flow event. A third flow is recorded in the

fluted terrain on the seabed in the southwesternmost corner of the bay; however, this ice flow was not reflected in the terrestrial striation or landform records. This flow represents a small late ice-flow that originated either from the Burin Peninsula or from an offshore source in the southwest.

In the following deglacial phase, ice started to retreat from Placentia Bay. Ice retreat was punctuated by a fluctuating ice margin that resulted in the formation of De Geer and grounding-line moraines. The orientation of the moraines varies throughout the bay but shows a northward retreat of ice that is generally perpendicular to ice-flow direction and largely controlled by bathymetric relief. Ice marginal retreat was likely facilitated by calving embayments that formed when ice became buoyant and formed floating ice shelves. Ice became buoyant and glaciomarine sedimentation started outside of Placentia Bay (till tongue in the Burin Moraine) sometime before ~16.3 ka and at the mouth of the bay before ~16.1 ka, as indicated by ^{14}C dates from glaciomarine silt. Dates from samples closest to the top of the glaciomarine silt suggest that glaciomarine sedimentation had finished with open water conditions sometime after ~12.7 to 12.0 ka.

5.7 Summary of major findings and conclusions

One of the most important advances in our understanding of the glacial history of Atlantic Canada has resulted from the development of high-resolution multibeam bathymetry maps for offshore areas. This technique provides imagery of glacial landforms that are currently below sea level, enabling various terrestrial and marine records to be integrated. Multibeam surveys in Placentia Bay, augmented by seismic and groundtruthing surveys, reveal landform assemblages that are diagnostic of late

Wisconsinan glacial geomorphology and palaeo-ice dynamics. This landform assemblage consists of a convergent field of drumlins and megaflutes, interpreted as representing the onset zone of a palaeo-ice stream that extended to the south in Halibut Channel. Subsequent changes in ice-flow directions are marked by drumlins and fluted terrain. These flow-parallel landforms are overprinted by De Geer moraines and larger grounding-line moraines that record the retreat of grounded ice up the bay which according to ^{14}C dates from glaciomarine silt started before ~16.3 ka.

The reconstruction of palaeo-ice dynamics in Placentia Bay is consistent with a model showing Late Wisconsinan ice advance to the continental shelf edge with rapid retreat in deeper water and slower retreat in shallow water. This deglacial scenario likely reflects the deglaciation of other bays and inlets in Newfoundland that also would have preferentially channeled faster flowing ice.

The abundance of glacial landforms on the Placentia Bay seabed is much greater than those mapped on the surrounding peninsulas, demonstrating the wealth of information that can be gained through seabed mapping. However landforms are generally limited to shallow, gently sloping seabeds where a sediment source exists for deformation by the flow of ice; landforms were not generally preserved in areas where there are deep channels or complex and/or exposed bedrock. While there were fewer depositional landforms on land, the erosional striation record was essential in understanding the sequence of ice-flow events, particularly in areas where no offshore glacial record existed (*i.e.*, the westward flow on the Burin was not observed on adjacent seabed). Both seabed and terrestrial glacial records were integral to understanding the

glacial history of Placentia Bay and ice-sheet behaviour during the transition from marine-based to land-based glacial conditions.

5.8 Considerations for future research

This thesis has added many details to the glacial history of Placentia Bay. There still remain several areas where the regional glacial history is not well understood. There are two key areas where more multibeam data will resolve some important gaps in the glacial history of Placentia Bay. Additional multibeam data in the southwestern Placenta Bay onto the Burin Moraine will contribute to the further understanding of the extent of the flow represented by the small fluting field and its potential link with the Burin Moraine. Multibeam data farther out toward Halibut Channel will provide more details on the extent and terminus of the ice stream that initiates in the central part of the bay. There are also several cases where the onshore and offshore records do not correspond, particularly on the southern part of the Burin Peninsula. A reexamination of coastal exposures in this area will be essential to understanding the multiple ice-flow directions recorded by striation patterns and the small coast-parallel ice flow recorded offshore. Several exposures in the southern Burin Peninsula contain multiple till units (Tucker, 1979; Tucker and McCann, 1980). Further examination of these exposures may be important in trying to link the ice-flow events on land with those offshore.

References

Batterson, M.J. and Taylor, D.M., 2006. Till geochemistry of the northern Burin Peninsula and adjacent areas, Newfoundland. Department of Natural Resources. Open File 1M/0573, 145 pp.

Batterson, M.J. and Taylor, D.M., 2007. Till geochemical surveys and preliminary Quaternary mapping of the Burin Peninsula and adjacent areas. *In* Current Research. Newfoundland and Labrador Department of Natural Resources, Geological Survey, Report 07-1: 197-214.

Batterson, M., Taylor, D., Bell, T., Brushett, D. and Shaw, J., 2006. Regional Ice-flow mapping, surficial geology and till geochemistry of the northern Burin Peninsula and adjacent Placentia Bay. *In* Current Research. Newfoundland and Labrador Department of Natural Resources, Geological Survey, Report 06-01: 161-176.

Bell, T., Liverman, D.G.E. and Sheppard, K., 1999. Stratigraphy and age of Quaternary sediments exposed along the coast of southern St. Georges Bay. *In* Current Research. Newfoundland and Labrador Department of Natural Resources, Geological Survey, Report 99-01: 1-13.

Bell, T., Liverman, D.G.E., Batterson, M.J. and Sheppard, K., 2001. Late Wisconsinan stratigraphy and chronology of southern St. George's Bay, Newfoundland: a reappraisal. Canadian Journal of Earth Sciences, 38: 851-869.

Benn, D.I. and Evans, D.J.A., 1998. Glaciers and Glaciation. Arnold: London, 734 pp.

Blake, K.P., 2000. Common origin for De Geer moraines of variable composition in Raudvassdalen, northern Norway. Journal of Quaternary Science, 15: 633-644.

Bonifay, D. and Piper, D.J.W., 1988. Probable late Wisconsinan margin on the upper continental shelf off St. Pierre Bank, eastern Canada. Canadian Journal of Earth Sciences, 25: 853-865.

Briner, J.P., 2007. Supporting evidence from the New York drumlin field that elongate subglacial bedforms indicate fast flow. Boreas, 36: 143-147.

Brushett, D., Bell, T., Batterson, M., and Shaw, J., 2007. Ice-flow history of Placentia Bay, Newfoundland: Multibeam seabed mapping. *In* Current Research. Newfoundland and Labrador Department of Natural Resources, Geological Survey, Report 07-1: 215-228.

Canadian Centre for Marine Communications, 2004. Placentia Bay Information Seaway Project, 47 pp.

Canadian Hydrographic Service. Newfoundland Southeast Coast Chart # 4016. Canadian Hydrographic Service, Department of Fisheries and Oceans, Ottawa.

Catto, N.R., 1992. Quaternary Geological Mapping, Southwestern Avalon Peninsula. *In* Current Research. Newfoundland and Labrador Department of Natural Resources, Geological Survey, Report 92-1: 23-26.

Catto, N.R., 1998. The pattern of glaciation on the Avalon Peninsula of Newfoundland. Geographie Physique et Quaternaire, 52: 1-24.

Catto, N.R. and Taylor, D.M., 1998. Landforms and surficial geology of the Argentia map sheet (NTS 1N/05), Newfoundland. Newfoundland Department of Mines and Energy, Geological Survey, Open File 001N/05/0637, scale 1:50 000.

Colman-Sadd, S.P., Hayes, J.P. and Knight, I., 1990. Geology of the Island of Newfoundland. Newfoundland Department of Mines and Energy, Geological Survey, Map 90-01, scale 1:500 000.

Courtney, R. and Shaw, J., 2000. Multibeam bathymetry and backscatter imaging of the Canadian Continental Shelf. Geoscience Canada, 27: 31-42.

Cumming, E.H., Aksu, A.E. and Mudie, P.J., 1992. Late Quaternary glacial and sedimentary history of Bonavista Bay, northeast Newfoundland. Canadian Journal of Earth Sciences, 29: 222-235.

Dyke, A.S. and Prest,V.K., 1987. Late Wisconsinan and Holocene history of the Laurentide Ice Sheet. Geographie Physique et Quaternaire, 41: 237-263.

Dyke, A.S. and Savelle, J.M., 2000. Major end moraines of Younger Dryas Age on the Wollaston Peninsula, Victoria Island, Canadian Arctic. Canadian Journal of Earth Sciences, 37: 601-619.

Dyke, A.S., Andrews, J.T., Clark, P.U., England, J.H., Miller, J.H., Shaw, J. and Veillette, J.J., 2002. The Laurentide and Innuitian ice sheets during the last glacial maximum. Quaternary Science Reviews, 21: 9-31.

Evans, D.J.A., 2003. Glaciers. Progress in Physical Geography, 27: 261-274.

Fader, G.B.F., King, L.H., and Josenhans, H.W., 1982. Surficial geology of the Laurentian Channel and the western Grand Banks of Newfoundland. Marine Sciences Paper 21, Geological Survey of Canada Paper 81-22. Department of Energy, Mines and Resources, Ottawa, 37 pp. and map.

Fader, G.B.F. and Miller, R.O., 1986. A reconnaissance study of the surficial and bedrock geology of the southern Grand Banks of Newfoundland. In Current Research, Part B, Geological Survey of Canada, Paper 86-1B: 591-604.

Fader, G.B.F., Miller, R.O., and Pecore, S.S., 1991. The marine geology of Halifax Harbour and adjacent areas. Geological Survey of Canada, Open File Report 2384, 22 pp.

Geosciences Resource Atlas, Newfoundland and Labrador Department of Natural Resources, available at http://gis.geosurv.gov.nl.ca (November 21, 2007).

Gipp, M.R., 2000. Lift-off moraines: markers of last ice-flow directions on the Scotian Shelf. Canadian Journal of Earth Sciences, 37: 1723-1734.

Gordon, J.E., Darling, W.G., Whalley, W.B. and Gellatly, A.F., 1992. The formation of glacial flutes: assessment of models with evidence from Lyngsdalen, north Norway. Quaternary Science Reviews, 11: 709-731.

Gosse, J., 2002. Atlantic Canada glacier ice dynamics workshop. Geoscience Canada, 29: 183-186.

Gosse, J.C., Grant, D.R., Klein, J. and Lawn, B., 1995. Cosmogenic ^{10}Be and ^{26}Al constraints on weathering zone genesis, ice cap basal conditions, and Long Range Mountains (Newfoundland) glacial history. CANQUA-CGRG Joint meeting 1995, Programme, Abstracts and Field Guides. Department of Geography, Memorial University of Newfoundland, p. CA19.

Grant, D., 1975. Glacial Features of the Hermitage-Burin Peninsula area, Newfoundland. Geological Survey of Canada, Paper 75-1C, Report of Activities, Part C: 333-334.

Grant, D., 1989. Quaternary Geology of the Applachian region of Canada. *In*: R.J. Fulton (Editor), Quaternary Geology of Canada and Greenland. Geological Survey of Canada, Geology of Canada, pp. 393-440.

Grant, D. and Batterson, M., 1988. Guidebook for CIM field trip to the Burin Peninsula, November 6th and 7th, 1988, 17 pp.

Henderson, E.P., 1972. Surficial Geology of Avalon Peninsula, Newfoundland. Geological Survey of Canada, Memoir 368, 121 pp.

Hughen K.A., Baillie, M.G.L., Bard, E., Bayliss, A., Beck, J.W., Bertrand, C., Blackwell, P.G., Buck, C.E., Burr, G., Cutler, K.B., Damon, P.E., Edwards, R.L., Fairbanks, R.G., Friedrich, M., Guilderson, T.P., Kromer, B., McCormac, F.G., Manning, S., Bronk Ramsey, C., Reimer, R.W., Remmele, S., Southon, J.R., Stuiver, M., Talamo, S., Taylor, F.W., van der Plicht, J. and Weyhenmeyer, C.E., 2004. Marine04 marine radiocarbon age calibration, 0-26 Cal Kyr BP. Radiocarbon, 46: 1059-1086.

Hughes, T., 2002. Calving bays. Quaternary Science Reviews, 21: 267-282.

Hughes Clarke, J.E., Mayer, L.A. and Wells, D.E., 1996. Shallow-water imaging multibeam sonars: A new tool for investigating seafloor processes in the coastal zone and on the continental shelf. Marine Geophysical Research, 18: 607-629.

Jenness, S.E., 1960. Late Pleistocene glaciation of eastern Newfoundland. Bulletin of the Geological Society of America, 71: 161-180.

King, A.F., 1990. Geology of the St. John's Area. Newfoundland Department of Mines and Energy. Geological Survey Branch, Report 90-2, 88 pp.

King, L.H., 1970. Surficial geology of the Halifax-Sable Island map area. Canadian Hydrographic Service, Marine Sciences Paper 1, 16 pp.

King, L.H., 1980. Aspects of regional surficial geology related to site investigation requirements, in Ardus D.A. (Eds.) Offshore site investigation, London, Graham and Trotman, Society for Underwater Technology, pp. 37-60.

King, L.H., 1996. Late Wisconsinan ice retreat from the Scotian Shelf. Geological Society of America Bulletin, 108: 1056-1067.

King, L.H. and Fader, G.B.J., 1986. Wisconsinan glaciation of the Atlantic continental shelf of southeast Canada. Geological Survey of Canada, Bulletin 363: 72 pp.

King, E.L. and Fader, G.B.J., 1992. Quaternary geology of southern northeast Newfoundland Shelf. In: Abstracts, Wolfville, 1992, GAC/AGC joint annual meeting, May 25-27, Acadia University, Wolfville, p. A57.

King, L.H., Rokoengen, K., Fader, G.B.F., and Gundleiksrud, T., 1991. Till-tongue stratigraphy. Geological Society of America Bulletin, 103: 637-659.

King, E.L. and Sonnichsen, G.V., 2000. New insights into glaciation and sea-level fluctuation on northern Grand Bank, offshore Newfoundland. *In* Current Research, Geological Survey of Canada, Paper 2000-D6: 1-10.

Kongsberg Maritime AS. 2006a. Product Specification: Simrad EM1002 multibeam echo sounder. Available from http://www.km.kongsberg.com/ (December 10, 2006).

Kongsberg Maritime AS. 2006b. Product Specification: Simrad EM1000 multibeam echo sounder- The obvious choice for shallow water surveys and ROV and AUV use. Available from http://www.km.kongsberg.com/ (December 10, 2006).

Kongsberg Maritime AS. 2006c. Product Specification: Simrad EM3000 multibeam echo sounder. Available from http://www.km.kongsberg.com/ (December 10, 2006).

Linden, M. and Möller, P. 2005. Marginal formation of De Geer moraines and their implication on the dynamics of grounding-line recession. Journal of Quaternary Science, 20: 113-133.

Liverman, D.G.E. and St. Croix, L., 1989. Ice flow indicators on the Baie Verte Peninsula. Newfoundland Department of Mines and Energy, Open File map 89-36.

Liverman, D.G.E., Batterson, M., Bell, T., Nolan, L., Marich, A., and Putt, M., 2006. Digital Elevation Models from Shuttle Radar Topography Mission Data - New Insights into the Quaternary History of Newfoundland. *In* Current Research. Newfoundland and Labrador Department of Natural Resources, Geological Survey, Report 06-01: 177-189.

Loncarevic, B.D., Courtney, R.C., Fader, G.B.F., Giles, P.S., Piper, D.J.W., Costello, G., Hughes Clarke, J.E., and Stea, R.R., 1994. Sonography of a glaciated continental shelf. Geology, 22: 747-750.

Lundqvist, J., 1989. Rogen (ribbed) moraine – identification and possible origin. Sedimentary Geology, 62: 281-292.

Lurton, 2002. An Introduction to underwater acoustics: principles and applications. Praxis Publishing Ltd. Chichester, UK, 347 pp.

MacLean, B. and King, L.H., 1971. Surficial geology of the Banquereau and Misiane Bank map area. Marine Sciences, Paper 20, Ottawa, 11 pp.

Marich, A., Batterson, M. and Bell, T., 2005. The morphology and sedimentology analyses of Rögen moraines, Central Avalon Peninsula, Newfoundland. *In* Current Research. Newfoundland and Labrador Department of Natural Resources, Geological Survey, Report 05-1: 1-14.

Menzies, J., 2001. The Quaternary Sedimentology and stratigraphy of small, ice-proximal, subaqueous grounding-line moraines in the central Niagara Peninsula, southern Ontario. Geographie Physique et Quaternaire, 55: 75-86.

Miller, A.A.L., Fader, G.B.F. and Moran, K., 2001. Late Wisconsinan ice advances, ice extent, and glacial regimes interpreted from seismic data, sediment physical properties, and foraminfera: Halibut Channel, Grand Banks of Newfoundland. In: Weddle, T.K., Retelle, M.J. (Eds.), Deglacial History and Relative Sea-level Changes, Northern New England and Adjacent Canada: Boulder, Colorado. Geological Society of America Special Paper, 351: 51-107.

Miller, G.H. and Kaufman, D.S., 1990. Rapid Fluctuations of the Laurentide Ice Sheet at the mouth of Hudson Strait: new evidence for ocean/ice-sheet interactions as a control on the younger dryas. Paleooceanography, 5: 907-919.

Miller, R. and Fader, G.B.F., 1995. The bottom of Halifax Harbour, Geological Survey of Canada (Atlantic), Open File 3154.

Moran, K. and Fader, G.B.J., 1997. Glaciomarine seismic features and groundtruth: Halibut Channel, Grand Banks of Newfoundland. In: Davies, T.A., Bell, T., Cooper, A.K., Josenhans, H., Polyak, L., Solheim, A., Stoker, M.S. and Stravers, J.A. (Eds.) Glaciated Continental Margins: An Atlas of Acoustic Images. Chapman & Hall, England, pp. 217-220.

Ottessen, D. and Dowdeswell, J.A., 2006. Assemblages of submarine landforms produced by tidewater glaciers in Svalbard. Journal of Geophysical Research. 111: 1-16.

Rose, J. 1987. Drumlins as part of a glacier landform continuum. In Menzies, J.and Rose, J. (eds.) *Drumlin Symposium*. Balkema, Rotterdam, 103-116.

Scott, D.B., Baki, V., and Younger, C.D., 1989. Late Pleistocene-Holocene paleoceanographic changes on the eastern Canadian Margin: stable isotopic evidence. Palaeogeography, Palaeoclimatology, Palaeoecology, 74: 279-295.

Shaw, J., 2003. Submarine moraines in Newfoundland coastal waters: implications for the deglaciation of Newfoundland and adjacent areas. Quaternary International, 99-100: 115-134.

Shaw, J., Johnston, L., and Wile, B., 1989. Navicula Operations in Placentia Bay, Newfoundland. Geological Survey of Canada, Open File 2029.

Shaw, J. and Courtney, R.C., 1997. Multibeam bathymetry of glaciated terrain off southwest Newfoundland. Marine Geology, 143: 125-135.

Shaw, J., Courtney, R.C. and Currie, J., 1997. Marine geology of St. George's Bay, Newfoundland, as interpreted from multibeam bathymetry and back-scatter data. Geomarine Letters, 17: 188-194.

Shaw, J., Cranston, R., Girouard, P., Asprey, K., Murphy, R., and Wile, B., 1999. Ground truthing of multibeam bathmetry data in southern Newfoundland: White Bear Bay, Ramea Islands region, Bay d'Espoir, and the Argentia area. Cruise Report 99020.

Shaw, J., Grant, D.R., Guilbault, J.P., Anderson, T.W. and Parrot, D.R., 2000. Submarine and onshore end moraines in southern Newfoundland: implications for the history of late Wisconsinan ice retreat. Boreas, 29: 295-314.

Shaw, J., Piper, D.J.W. Fader, G.B., King, E.L., Todd, B.G., Bell, T., Batterson, M., and Courtney, R.C., 2006a. A conceptual model of the deglaciation of Atlantic Canada. Quaternary Science Reviews, 25: 2059-2081.

Shaw, J., Ward, B., Bell, T., Brushett, D., Robertson, A., Atkinson, A., Standen, G., and Murphy, R., 2006b. Cruise report 2005-051, CCGS Matthew. Surveys in Placentia Bay, Newfoundland. Unpublished cruise report, Geological Survey of Canada (Atlantic), Dartmouth, NS.

Shaw, J., Jarrett, K., Brushett, D., Asprey, K., Wile, B., Standen, G., Middleton, G. and Murphy, R., 2006c. Cruise Report 2006-039, CCGS Hudson. Surveys in Placentia Bay, Newfoundland. Unpublished cruise report, Geological Survey of Canada (Atlantic), Dartmouth, NS.

Shaw, J., Courtney, R. C., and Todd, B. J., 2006d. Backscatter strength and surficial geology and sun-illuminated seafloor topography, inner St. George's Bay, Newfoundland and Labrador. Geological Survey of Canada, Map 2090A, scale 1:50 000.

Shaw, J., Courtney, R. C., and Todd, B. J. 2006e. Surficial geology and sun-illuminated seafloor topography, inner St. George's Bay, Newfoundland and Labrador. Geological Survey of Canada, Map 2084A, scale 1:50 000.

Shaw, J., Courtney, R.C., and Todd, B.J., 2006f. Sun-illuminated seafloor topography, inner St. George's Bay, Newfoundland and Labrador. Geological Survey of Canada, Map 2089A, scale 1: 50 000.

Stea, R.R., 2004. The Appalachian Glacier Complex in Maritime Canada. *In* Ehlers, J., Gibbard, P.L. (eds.), Quaternary Glaciations – Extent and Chronology, Part II. Developments in Quaternary Science, vol. 2b. Elsevier, Amsterdam, pp. 213-232.

Stea, R.R., Piper, D.J.W., Fader, G.B.J., and Boyd, R., 1998. Wisconsinan glacial and sea-level history of Maritime Canada and the adjacent continental shelf: A correlation of land and sea events. Geological Survey of America Bulletin, 110(7): 821-845.

Stokes, C.R. and Clark, C.D., 1999. Geomorphological criteria for identifying Pleistocene ice streams. Annals of Glaciology, 28: 67-75.

Stokes, C.R. and Clark, C.D., 2001. Palaeo-ice streams. Quaternary Science Reviews, 20: 1437-1457.

Stokes, C.R. and Clark, C.D., 2002. Are long subglacial bedforms indicative of fast ice flow? Boreas, 31: 239-249.

Stokes, C.R., Clark, C.D. and Winsborrow, M.C.M., 2006. Subglacial bedform evidence for a major palaeo-ice stream and its retreat phases in Amundsen Gulf, Canadian Arctic Archipelago. Journal of Quaternary Science, 21: 399-412.

Taylor, D.M., 2001. Newfoundland Striation Database. Newfoundland Dept. of Mines and Energy, Geological Survey Branch, Open File NFLD/2195, version 4.

Todd, B.J., Fader, G.B.J., Courtney, R.C. and Pickrill, R.A., 1999. Quaternary geology and surficial sediment processes, Browns Bank, Scotian Shelf, based on multibeam bathymetry. Marine Geology, 162: 165-214.

Todd, B.J., Valentine, P.C., Longva, O. and Shaw, J., 2007. Glacial landforms on German Bank, Scotian Shelf: evidence for Late Wisconsinan ice sheet dynamics. Boreas, 36: 1-23.

Tucker, C.M., 1979. Late Quaternary events on the Burin Peninsula, Newfoundland. Unpublished Ph.D. thesis, McMaster University, Ontario, 282 pp.

Tucker, C.M. and McCann, S.B. 1980. Quaternary Events on the Burin Peninsula, Newfoundland, and the islands of St. Pierre and Miquelon, France. Canadian Journal of Earth Sciences, 17: 1462-1479.

Van der Veen, C.J. 1996. Tidewater calving. Journal of Glaciology, 42: 375-385.

Vaughan, D.G., 2006. The Antarctic Ice Sheet. *In* P.G. Knight (ed.) Glacier science and environmental change, Blackwell Science, pp. 209-221.

Veillette, J.J., Dyke, A.S. and Roy, M., 1999. Ice-flow evolution of the Labrador Sector of the Laurentide Ice Sheet: a review with new data from northern Quebec. Quaternary Science Reviews, 18: 993-1019.

Appendix A: Sample Descriptions

Table A.1 Grab samples from cruise 2005-051 (modified from Shaw *et al.*, 2006b).

Sample	Depth (m)	Latitude	Longitude	Description
2005-051-001	96.2	47 45.1023	54 10.5845	Dark gray gravelly sandy mud.
2005-051-002	122.5	47 45.1741	54 09.8054	Dark olive gray soft silty mud.
2005-051-003	137.4	47 44.3512	54 07.3412	Dark gray gravelly sandy mud with worm tubes, fine angular gravel, a few pebbles and one rounded cobble.
2005-051-004	36.2	47 42.5462	54 09.8945	First attempt failed – some fine red seaweed. Second attempt failed – some fine red seaweed. Third attempt: several rounded gravel clasts (up to 7 cm) thickly coated with *Lithothamnion sp.*, red seaweed attached to clasts, small sea urchin and four brittlestars.
2005-051-005	50.8	47 42.1396	54 11.6110	Gravelly sand: surface pavement of closely-packed rounded gravel clasts (up to 15 cm), coated on top with red Lithothamnion, overlying brown gravelly sand with numerous shell fragments, brittlestars and red seaweed attached to gravel.
2005-051-006	99.3	47 41.3872	54 12.8545	Gravelly sandy mud with a few worm tubes. Gravel clasts (up to 15 cm) are sub-rounded to sub-angular - possible surficial gravel lag. Area of De Geer moraines.
2005-051-007	105.4	47 40.0350	54 14.9378	Dark brownish gray gravelly sandy mud with a surficial veneer of gravel (sub-rounded to sub-angular clasts up to 14 cm) and no coralline algae. Area of subdued De Geer moraine topography.
2005-051-008	200.5	47 38.9460	54 16.0512	Black silty clay with worm tubes and a brown surface veneer.
2005-051-017	398.3	47 26.9373	54 21.2045	Very dark olive gray clayey mud with a brown surface veneer.
2005-051-018	379.5	47 28.6241	54 20.1678	Very dark olive gray clayey mud with a brown surface veneer. Small (1 cm) half bivalve, small (2 cm) angular gravel clasts.
2005-051-019	194.5	47 32.9276	54 19.3882	Very dark olive gray silty mud with worm tubes and numerous angular (2-3 cm) clasts.
2005-051-020	126.0	47 33.7769	54 19.6310	Three attempts: 1st a small pebble; 2nd empty; 3rd two gravel clasts: one sub-rounded pebble (bare) and one cobble (25 cm) with sponge encrustations and other unidentified encrustations. Lower part of cobble is bare, suggesting it is part of an immobile pavement.
2005-051-021	232.5	47 36.5935	54 17.5215	Very dark olive gray silty mud with worm tubes and a few small shell fragments.
2005-051-022	137.5	47 08.8671	54 53.9531	Very dark to black gravelly sandy mud with a surface veneer of scattered sub-rounded red pebbles, worm tubes and light brown surface veneer.

2005-051-024	87.4	47 09.2220	54 50.9458	Two attempts. 1st dark olive gray sandy gravelly mud with several red sub-rounded clasts (up to 10 cm). The main sample was dark brown gravelly sand with shell fragments and red gravel clasts (up to 10 cm).
2005-051-025	109.3	47 10.3096	54 44.4875	Dark olive brown muddy sandy gravel: poorly sorted – perhaps with a concentration of gravel at surface. Shell fragments, worm tubes, reddish clasts (up to 10-15 cm), no Lithothamnion, a few small bio-encrustations.
2005-051-026	105.4	47 11.5168	54 43.2298	Sub-angular, clean gravel (5-10 cm) with shell fragments and one sea urchin.
2005-051-029	238.0	47 14.2524	54 36.7354	Very dark olive gray mud, slightly pungent.
2005-051-030	170.3	47 19.2700	54 29.8158	A large (20-30 cm) sub-angular boulder - 50% embedded in olive gray gravelly (angular) sandy mud.
2005-051-033	182.5	47 21.0424	54 27.5194	Coarse angular gravel, forms a veneer over gravelly sandy mud. Bare clasts except for some sponge patches.
2005-051-034	169.4	47 21.6423	54 26.7321	
2005-051-036	250.5	47 18.0614	54 05.3632	1st attempt: a sub-rounded clast (20 cm) with organic encrustation on the top only and some gravelly sandy mud, part of a gravel pavement. 2nd attempt: sandy muddy gravel (angular to sub-rounded) in a matrix of dark olive gray sandy mud with a few worm tubes.
2005-051-039	201.4	47 18.3062	54 04.4432	Dark olive gray sandy silty stiff mud with a few worm tubes and several sub-rounded pebbles.
2005-051-040	173.4	47 19.2833	54 03.4926	Olive gray silty sand, perhaps up to 40% mud with worm tubes and small bivalves.
2005-051-043	90.5	47 20.1491	54 02.1611	Light brownish gray poorly sorted medium sand with high content of shell fragments and a few small bivalves.
2005-051-044	27.8	47 29.4612	54 00.9678	2 attempts – a piece of wrack each time. No sample retained.
2005-051-046	49.3	47 18.3755	53 57.7847	

Note: Bottom photographs were not considered to be of scientific quality and were not used.

Table A.2 Grab samples, bottom photographs and core details from cruise 2006-039 (modified from Shaw *et al.*, 2006c).

Sample	Depth (m)	Latitude	Longitude	Type	Seismic daytime	Description
2006-039-004	184.0	46 15.5997	-54 58.9288	G	78012-1390022	Olive gray gravelly sandy mud with a surface veneer of sub-rounded and sub-angular pebbles (up to 12 cm diameter) embedded in sandy mud. Pebbles are mainly bare except for a few small attached sponges. Same site as core 005.
2006-039-005	184.0	46 15.6122	-54 58.9238	PC	78012-1390022	Cutter has reddish gray clay. Same site as grab 004. Length ~ 5.09 m.
2006-039-006	231.0	46 26.7592	-54 51.7118	G	78012-1380850	Dark olive gray stiff silty mud with scattered small shell fragments. Same site as core 007.
2006-039-007	231.0	46 26.7530	-54 51.7316	PC	78012-1380850	Cutter has stiff, buttery, red clay. Same site as grab 006. Length ~6.19 m.
2006-039-008	185.0	46 15.5389	-54 58.8045	PC	78012-1390023	No grab at this station. Cutter has buttery, reddish gray clay. Length ~ 4.20 m.
2006-039-009	184.0	46 15.4799	-54 58.7161	PC	78012-1390024	No grab at this station. Nose of cutter has buttery red clay. Length ~5.56 m.
2006-039-010	183.0	46 15.6571	-54 59.0286	PC	78012-1390021	No grab at this station. Length ~ 4.87 m.
2006-039-011	243.0	46 15.5997	-54 58.9288	G	78012-1362047	Very dark gray silty mud with a few worm tubes, one large sub-rounded pebble and one brittlestar. Same location as camera 012 and core 013.
2006-039-012	243	46 52.0171	-54 49.0243	C	78012-1362047	Same location as grab sample 011 and core 013. Photo 1.
2006-039-012	243	46 52.0146	-54 49.0195	C	78012-1362047	Photo 2.
2006-039-012	242	46 52.0121	-54 49.0143	C	78012-1362047	Photo 3.
2006-039-012	242	46 52.0136	-54 49.0105	C	78012-1362047	Photo 4.
2006-039-012	243	46 52.0155	-54 49.0131	C	78012-1362047	Photo 5.
2006-039-013	243	46 52.0187	-54 48.9949	PC	78012-1362047	Same location as camera 011 and grab 012. Trigger-weight core was empty.
2006-039-014	188	46 52.8716	-54 30.1645	C	78012-1361818	Eleven camera stations – drifting north from the SDT location. Photo 1.
2006-039-014	188	46 5.8764	-54 30.1640	C	78012-1361818	Photo 2.
2006-039-014	188	46 52.8780	-54 30.1565	C	78012-1361818	Photo 3.
2006-039-014	187	46 52.8835	-54 30.1562	C	78012-.15721361818	Photo 4.
2006-039-014	189	46 52.8967	-54 30.1572	C	78012-	Photo 5.

					1361818	
2006-039-014	188	46 52.9050	-54 30.1546	C	78012-1361818	Photo 6.
2006-039-014	188	46 52.9114	-54 30.1438	C	78012-1361818	Photo 7.
2006-039-014	188	46 52.9159	-54 30.1278	C	78012-1361818	Photo 8.
2006-039-014	186	46 52.9201	-54 30.1968	C	78012-1361818	Photo 9.
2006-039-014	189	46 52.9216	-54 30.0877	C	78012-1361818	Photo 10.
2006-039-014	189	46 52.9163	-54 30.0782	C	78012-1361818	Photo 11.
2006-039-015	174.0	46 52.8722	-54 30.1719	PC	78012-1361818	Same location as camera station 014 and grab station 016.
2006-039-016	191.0	46 52.8510	-54 30.1761	G	78012-1361818	Dark olive gray muddy fine sand. Same location as camera 014 and core 015.
2006-039-017	196.0	46 52.7721	-54 32.2030	G	78012-1361832	Olive gray muddy fine sand. Same location as camera 018 and core 019.
2006-039-018	199.0	46 52.7793	-54 32.1847	C	78012-1361832	Photo 1 – part of a series of 5 photos, same site as grab 017 and core 019.
2006-039-018	199.0	46 52.7777	-54 32.1880	C	78012-1361832	Photo 2
2006-039-018	199.0	46 52.7716	-54 42.1927	C	78012-1361832	Photo 3
2006-039-018	199.0	46 52.7713	-54 32.1979	C	78012-1361832	Photo 4
2006-039-018	199.0	46 52.7789	-54 32.1940	C	78012-1361832	Photo 5
2006-039-019	199.0	46 52.7649	-54 32.1889	PC	78012-1361832	Length 5.37 m.
2006-039-027	403.0	47 25.5237	-54 22..7331	PC	2005051-3021750	Western Channel. Same location as 025 and 026.
2006-039-028	221.0	47 24.9839	-54 03.2545	G	2005051-3051652	Eastern Channel. Dark olive gray silty clay with a few shell fragments.
2006-039-029	224.0	47 24.9756	-54 03.2844	PC	2005051-3051652	Eastern Channel – same site as grab 028. Trigger weight core was empty.
2006-039-030	298.0	47 25.0636	-54 03.9323	G	99020-1852029	Eastern Channel. Dark olive gray gravelly sandy mud with a surficial veneer of sub-angular to sub-rounded gravel (see deck photos) with attached fauna. Same site as core 031.
2006-039-031	296.8	47 25.0545	-54 03.8777	PC	99020-1852029	Eastern Channel – same site as grab 030. Trigger-weight core length 0.58 m.
2006-039-032	211.0	47 17.9275	-54 07.7828	PC	2005051-3051443:30	Eastern Channel-site of old submarine slide. Trigger weight empty. Core length 565 cm.
2006-039-033	212.0	47 29.1594	-54 02.6368	212.0	2005051-3051756	Dark olive gray silty mud with a light brown surface.
2006-039-034	204.7	47 29.1691	-54 02.6429	C	2005051-3051756	Photo 1 – poor quality.
2006-039-034	204.7	47 29.1720	-54 02.6479	C	2005051-	Photo 2– poor quality.

					3051756	
2006-039-034	210.0	47 29.1709	-54 02.6517	C	2005051-3051756	Photo 3– poor quality.
2006-039-034	203.8	47 29.1703	-54 02.6509	C	2005051-3051756	Photo 4– poor quality.
2006-039-034	201.9	47 29.1698	-54 02.6487	C	2005051-3051756	Photo 5– poor quality.
2006-039-035	212.0	47 29.1602	-54 02.6435	PC	2005051-3051756	Same site as camera 034 and grab 033. Length = 7.6 m.
2006-039-036	184.0*	47 10.9049	-54 15.8849	C	2005051-298170450	Depth may be too deep. Photo 1.
2006-039-036	175.0	47 10.9054	-54 15.8822	C	2005051-298170450	Photo 2.
2006-039-036	177.0	47 10.9046	-54 15.8812	C	2005051-298170450	Photo 3.
2006-039-036	174.0	47 10.9056	-54 15.8838	C	2005051-298170450	Photo 4.
2006-039-037	184.0	47 10.9102	54 15.8932	G	2005051-298170450	Gravelly sandy mud. Same location as camera 036
2006-039-038	201.0	47 09.2019	-54	G		Dark olive gray muddy very fine sand, light brown on surface. Same location as camera 039.
2006-039-039	202.0	47 09.2023	54 15.3211	C	2006039-	Same location as 038. Photo 1.
2006-039-039	196.0	47 09.2026	54 15.3207	C	2006039-	Photo 2.
2006-039-039	196.0	47 09.2067	54 15.3196	C	2006039-	Photo 3.
2006-039-039	196.8	47 09.2030	54 15.3229	C	2006039-	Photo 4.
2006-039-039	202.0	47 09.2085	54 15.3238	C	2006039-	Photo 5.
2006-039-040	83.7	47 07.6141	54 11.5562	C	2005051-298130750	Photo 1.
2006-039-040	84.9	47 07.6144	54 11.5541	C	2005051-298130750	Photo 2.
2006-039-040	84.9	47 07.6109	54 11.5565	C	2005051-298130750	Photo 3.
2006-039-040	84.9	47 07.6163	54 11.5487	C	2005051-298130750	Photo 4.
2006-039-040	83.9	47 07.6130	54 11.5561	C	2005051-298130750	Photo 5.
2006-039-041	84.9	47 07.6111	-54 11.5527	G	2005051-298130750	Same location as camera 040. Morainal area in shallow water: Yellow brown poorly-sorted coarse shelly gravelly sand with sub-rounded gravel clasts and bivalves.
2006-039-042	200.8	47 03.8347	-54 21.3833	G	2006039-	'scalloped' sea floor. Olive gray muddy fine sand.
2006-039-043	201.0	47 03.8364	-54 21.4051	C	2006039-	Photo 1.
2006-039-043	200.0	47 03.8389	-54 21.4156	C	2006039-	Photo 2.
2006-039-043	199.9	47 03.8385	-54 21.4044	C	2006039-	Photo 3.
2006-039-043	199.9	47 03.8331	-54 21.4003	C	2006039-	Photo 4.
2006-039-043	200.8	47 03.8337	-54 21.4073	C	2006039-	Photo 5.
2006-039-044	92.9	46 52.2897	-54 21.9380	C	78012-1361717	Hard sea floor close to coast. Photo 1.
2006-039-044	90.7	46 52.2858	-54 21.9164	C	78012-1361717	Photo 2.
2006-039-044	92.0	46 52.2863	-54 21.9250	C	78012-1361717	Photo 3.
2006-039-044	92.0	46 52.2897	-54 21.9397	C	78012-1361717	Photo 4.

2006-039-044	92.0	46 52.2914	-54 21.9467	C	78012-1361717	Photo 5.
2006-039-045	88.0	46 52.2955	-54 21.9554	G	78012-1361717	Hard sea floor close to coast.
2006-039-046				G		In megaflute. Dark olive gray fine sand with some mud and a few small shrimp.
2006-039-047	198.0	46 54.3239	-54 29.2143	C		Photo 1.
2006-039-047	198.0	46 54.3212	-54 29.2162	C		Photo 2.
2006-039-047	198.0	46 54.3252	-54 29.2167	C		Photo 3.
2006-039-047	192.0	46 54.3273	-54 29.2219	C		Photo 4.
2006-039-047	191.0	46 54.3286	-54 29.2205	C		Photo 5.
2006-039-047	195.0	46 54.3273	-54 29.2195	C		Photo 6.
2006-039-047	191.0	46 54.3242	-54 29.2146	C		Photo 7.
2006-039-047	196.8	46 54.3297	-54 29.2183	C		Photo 8.
2006-039-047	191.0	46 54.3268	-54 29.2280	C		Photo 9.
2006-039-047	196.8	46 54.3207	-54 29.2362	C		Photo 10.
2006-039-047	192.0	46 54.3136	-54 29.2423	C		Photo 11.
2006-039-047	192.0	46 54.3079	-54 29.2489	C		Photo 12.
2006-039-047	196.0	46 54.3022	-54 29.2582	C		Photo 13.
2006-039-047	196.0	46 54.2968	-54 29.2704	C		Photo 14.

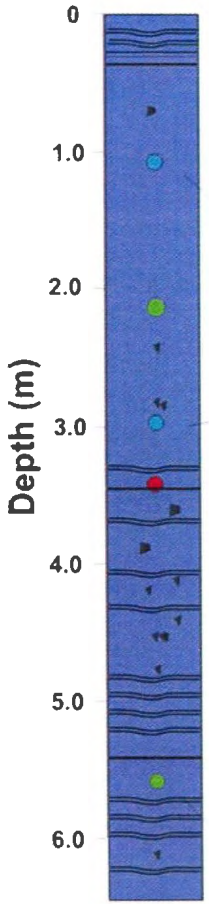

0-28 Olive gray clayey silt, minor fine sand

28-30 Reddish gray clay

30-36 Dark reddish gray clay; pebbles and granules;

36-343 shell fragments.

Reddish gray clay; black bioturbation mottles; shell fragments and bivalves; scattered angular gravel and granules.

109 cm; both valves of a specimen of Nucula tenuis. Gastropod hole in one valve.

300 cm; both valves of a bivalve, Yoldia sp.. Perhaps Yoldia lucida

343-540 Reddish gray clay witth red bands, 2-30 mm; black bioturbation mottles; shell fragments and bivalves; scattered angular gravel and granules, concentrated in bands in places.

540-644.5 Reddish gray clay with black silty laminae; several thin sand layers; red bands, 2-30 mm; black bioturbation mottles; shell fragments and bivalves; scattered angular gravel and granules.

558 cm; single valve of Portlandica arctica

LEGEND

- **Glaciomarine unit**
- **Postglacial unit**
- **Shell fragment**
- **Half bivalve**
- **Complete bivalve**
- **Gastropod**
- **Angular dropstones**
- **Rounded clast**
- **Silty laminae**
- **Bioturbation mottles**
- **Gas escape cracks**

Note: Trigger weight core in bag: soft, olive gray mud.

Figure B.1 Core description for piston core 2006-039-007

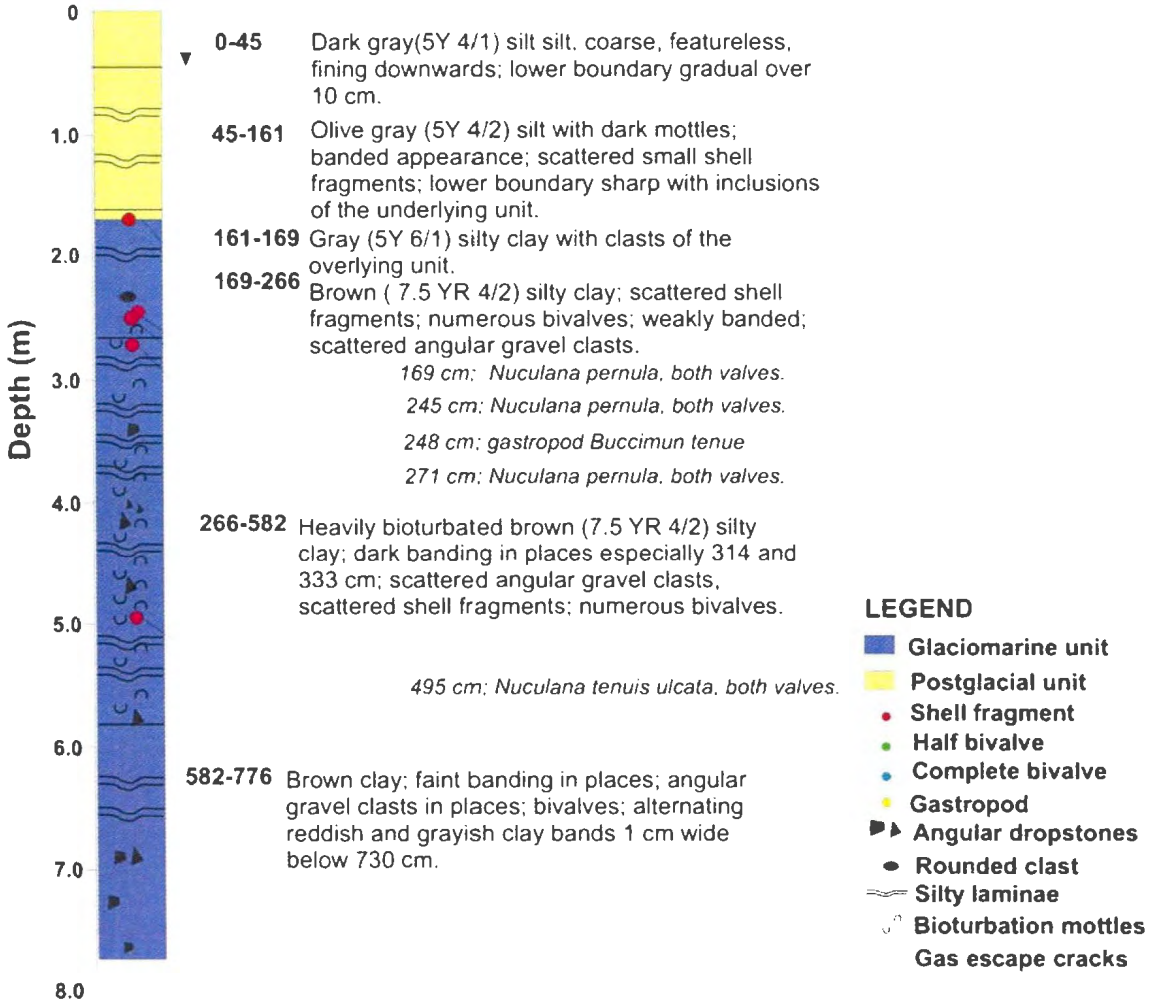

Figure B.2 Core description for piston core 2006-039-013

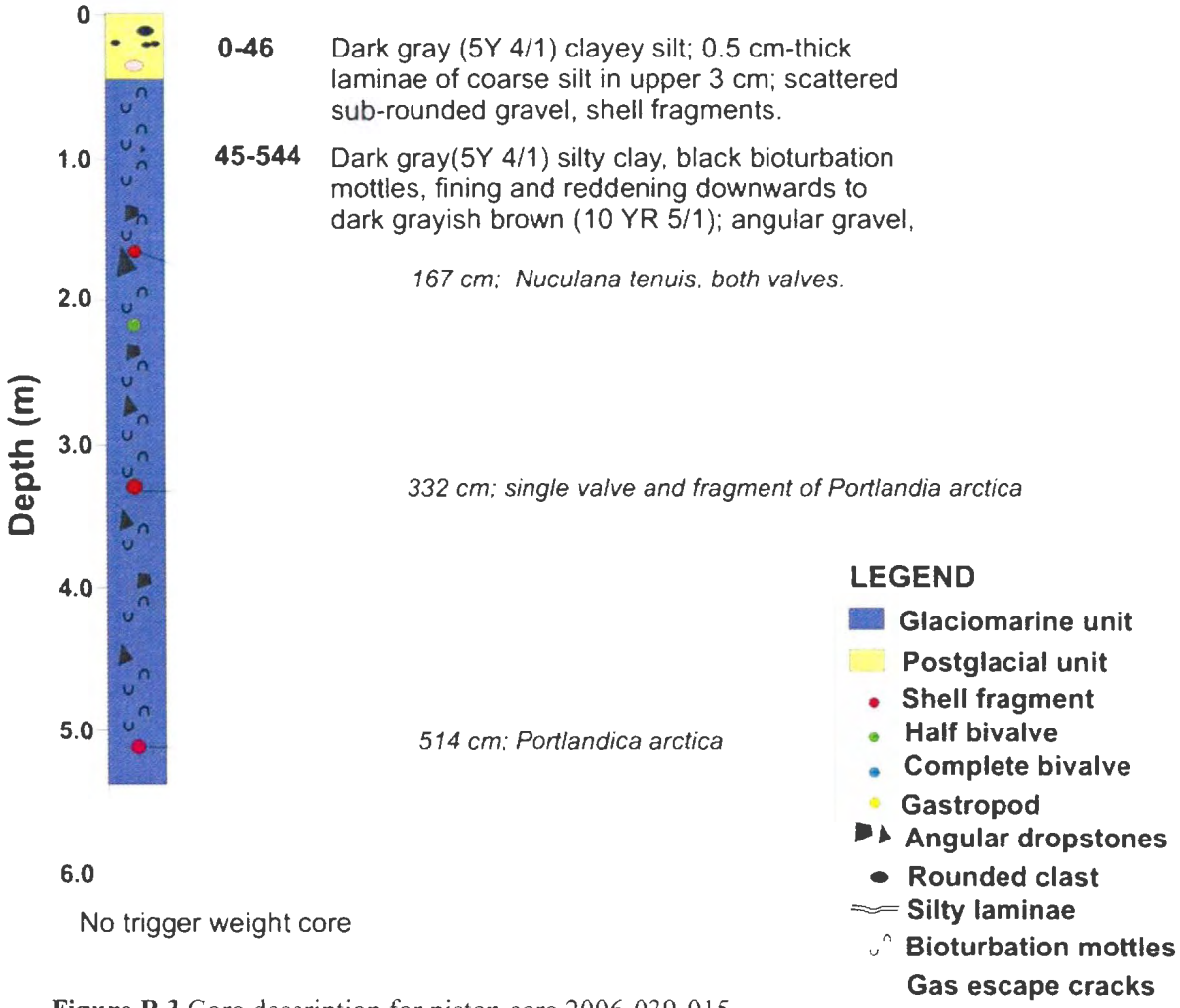

Figure B.3 Core description for piston core 2006-039-015

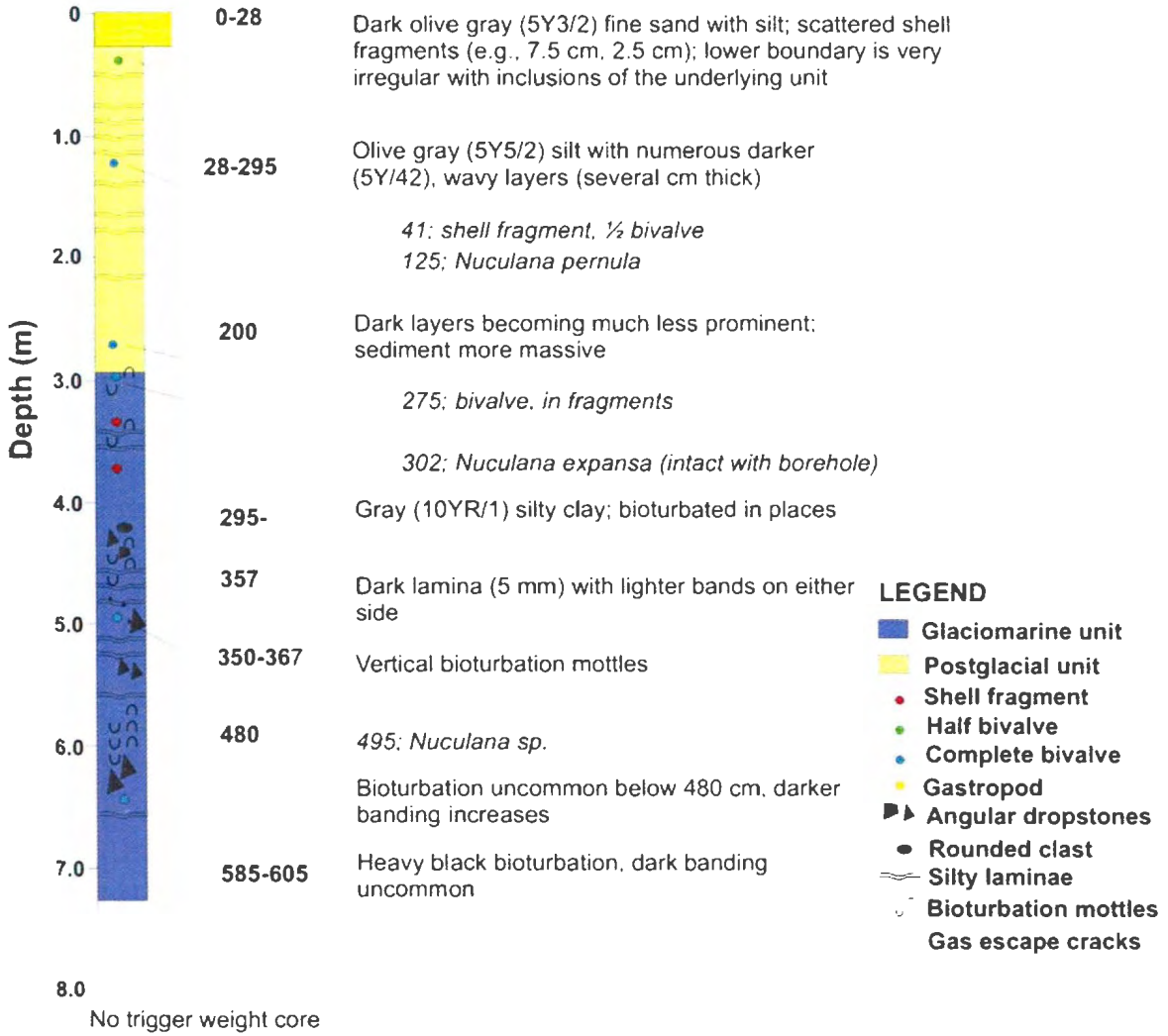

Figure B.4 Core description for piston core 2006-039-019

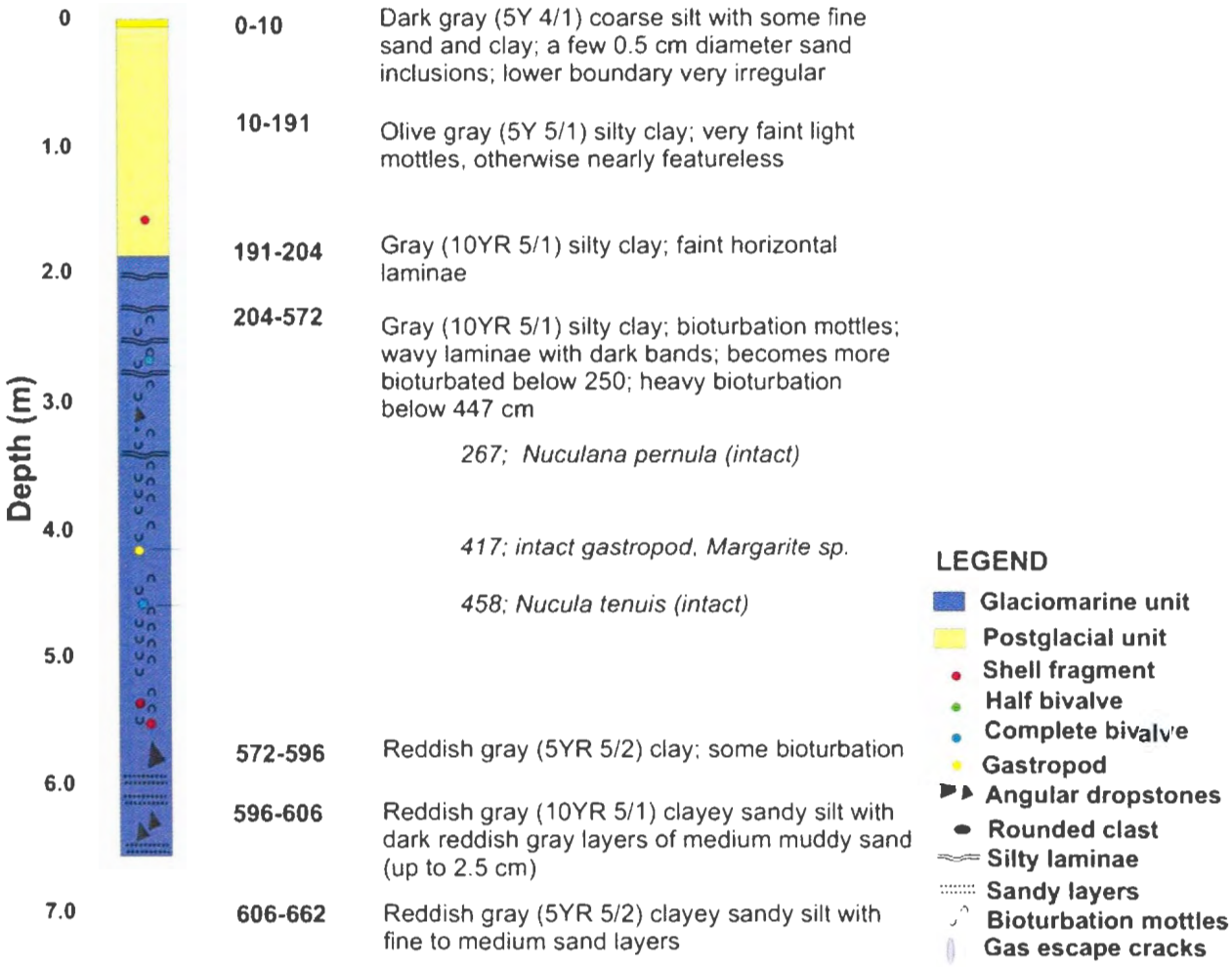

Figure B.5 Core description for piston core 2006-039-032

Appendix C: Seabed landform dimensions

Table C.1 Drumlin dimensions from southwestern Placentia Bay

Drumlins: Southwestern Placentia Bay	length (m)	width (m)	E (l/w)	height (m)	orientation (deg)	landform
1	658	218	3.0	13	134	drumlin
2	521	168	3.1	7	158	drumlin
3	518	190	2.7	14	142	drumlin
4	516	140	3.7	7	138	drumlin
5	527	144	3.7	7	144	drumlin
6	622	203	3.1	12	151	drumlin
7	988	209	4.7	9	146	drumlin
8	569	244	2.3	12	145	drumlin
9	487	159	3.1	8	156	drumlin
10	873	242	3.6	5	157	drumlin
11	597	249	2.4	7	152	drumlin
12	955	284	4.4	17	151	drumlin
13	794	243	3.3	8	160	drumlin
14	874	178	4.9	16	168	drumlin
15	791	236	3.4	25	168	drumlin
16	766	241	3.2	13	165	drumlin
17	848	220	3.9	10	160	drumlin
18	834	242	3.4	6	151	drumlin
19	992	241	4.1	15	145	drumlin
20	1042	265	3.9	11	144	drumlin
21	692	242	2.9	5	134	drumlin
22	908	206	4.4	6	138	drumlin
23	845	295	2.9	11	142	drumlin
24	691	224	3.1	9	145	drumlin
25	695	226	3.1	17	138	drumlin
26	803	214	3.8	17	137	drumlin
27	768	160	4.8	9	151	drumlin
28	1084	288	3.8	18	146	drumlin
29	1054	332	3.2	15	142	drumlin
30	1224	292	4.2	16	132	drumlin
Average dimensions:						
average	795	227	3.5	10	145	
standard deviation	207	46	0.7	2.9	7	
standard error	38	8.4	0.13	0.55	1.3	

Note:
landforms occur in water depths of ~55 -140 m

Table C.2 Megaflute dimensions from southwestern Placentia Bay

Megaflutes: Southwestern Placentia Bay	length (m)	width (m)	E (l/w)	height (m)	orientation (deg)	landform
1	1326	289	4.6	5	124	megaflute
2	1088	211	5.2	12	122	megaflute
3	1255	284	4.4	17	126	megaflute
4	1451	316	4.6	9	127	megaflute
5	1069	229	4.7	8	115	megaflute
6	1386	256	5.4	8	110	megaflute
7	1248	219	5.7	8	124	megaflute
8	1307	243	5.4	14	120	megaflute
9	1610	271	5.9	7	126	megaflute
10	1369	229	6.0	16	124	megaflute
11	1215	226	5.4	20	131	megaflute
12	1990	277	7.2	16	127	megaflute
13	3021	221	13.7	16	144	megaflute
14	2007	274	7.3	16	140	megaflute
15	1442	266	5.4	11	141	megaflute
16	2639	285	9.3	13	137	megaflute
17	1902	338	5.6	17	140	megaflute
18	2874	280	10.3	12	151	megaflute
19	2143	313	6.8	5	144	megaflute
20	1910	242	7.9	5	158	megaflute
21	2538	320	7.9	8	156	megaflute
22	2204	289	7.6	6	161	megaflute
23	2131	311	6.9	12	164	megaflute
24	3264	347	9.4	18	164	megaflute
25	2357	326	7.2	11	158	megaflute
26	2796	334	8.4	8	162	megaflute
27	2371	314	7.6	11	159	megaflute
28	2364	372	6.4	8	164	megaflute
29	2166	351	6.2	10	165	megaflute
30	2724	343	7.9	16	172	megaflute
Average dimensions:						
average	1972	286	6.9	11	142	
standard deviation	634	45	2.0	4.3	18	
standard error	116	8.2	0.37	0.79	3.3	

Note:
All landforms occur in water depths of ~140 -200 m

Table C.3 Drumlin dimensions from southwesternmost Placentia Bay

Drumlins: Southwesternmost Placentia Bay	length (m)	width (m)	E (l/w)	height (m)	orientation (deg)	landform
1	784	254	3.1	10	138	drumlin
2	684	259	2.6	8	122	drumlin
3	541	198	2.7	6	124	drumlin
4	510	132	3.9	12	132	drumlin
5	716	333	2.2	7	126	drumlin
6	560	329	1.7	5	131	drumlin
7	985	204	4.8	5	134	drumlin
8	759	269	2.8	6	134	drumlin
9	634	224	2.8	7	144	drumlin
10	539	261	2.1	7	127	drumlin
11	558	208	2.7	11	132	drumlin
12	665	246	2.7	7	140	drumlin
13	889	203	4.4	7	135	drumlin
14	518	185	2.8	11	136	drumlin
15	954	282	3.4	10	134	drumlin
16	729	189	3.9	7	131	drumlin
17	777	183	4.2	9	142	drumlin
18	592	271	2.2	11	135	drumlin
19	751	209	3.6	8	153	drumlin
20	473	176	2.7	6	154	drumlin
21	856	321	2.7	11	152	drumlin
22	638	206	3.1	5	152	drumlin
23	948	220	4.3	8	149	drumlin
24	802	325	2.5	9	158	drumlin
25	710	196	3.6	4	150	drumlin
26	495	180	2.8	7	140	drumlin
27	682	188	3.6	6	149	drumlin
28	662	242	2.7	5	163	drumlin
29	860	278	3.1	9	154	drumlin
30	649	237	2.7	7	144	drumlin
Average dimensions:						
average	697	234	3.1	8	141	
standard deviation	142	50	0.74	2	11	
standard error	26	9.1	0.13	20	2.0	

Note:
All landforms occur in water depths of ~55-125 m

Table C.4 Flow-parallel landform dimensions from eastern Placentia Bay

Drumlins, megaflutes and crag-and-tails: Eastern Placentia Bay (south of Red Island)						
	length (m)	width (m)	E (l/w)	height (m)	orientation (deg)	landform
1	1044	302	3.5	5	210	drumlin
2	1717	519	3.3	21	222	drumlin
3	1081	300	3.6	11	234	drumlin
4	1001	274	3.7	4	226	drumlin
5	979	485	2	14	223	drumlin
6	841	219	3.8	18	208	drumlin
7	830	259	3.2	13	201	drumlin
8	988	284	3.5	4	241	drumlin
9	813	248	3.3	7	234	drumlin
10	1093	285	3.8	11	245	drumlin
11	1727	431	4	12	242	megaflute
12	1093	257	4.3	9	206	megaflute
13	1732	266	6.5	9	230	megaflute
14	1499	298	5	6	233	megaflute
15	1860	486	3.8	5	241	megaflute
16	1951	358	5.4	4	236	megaflute
17	1152	282	4.1	11	220	megaflute
18	1684	328	5.1	9	224	megaflute
19	1758	352	5	4	246	megaflute
20	2011	567	3.5	18	228	megaflute
21	4783	534	9	5	205	crag-and-tail
22	2187	345	6.3	35	214	crag-and-tail
23	1346	280	4.8	24	218	crag-and-tail
24	1068	272	3.9	18	205	crag-and-tail
25	1223	722	1.7	11	187	crag-and-tail
26	2227	417	5.3	20	192	crag-and-tail
27	2065	505	4.1	40	163	crag-and-tail
28	974	264	3.7	18	173	crag-and-tail
29	1206	531	2.3	15	242	drumlin
30	1433	365	3.9	17	238	drumlin
31	1410	408	3.5	20	238	drumlin
32	1358	422	3.2	7	242	drumlin
33	358	169	2.1	7	304	drumlin
34	212	171	1.2	6	302	drumlin
35	365	165	2.2	8	305	drumlin
36	388	147	2.6	9	298	drumlin
37	397	160	2.5	9	269	drumlin
38	519	189	2.7	12	293	drumlin
39	467	206	2.3	22	227	drumlin
40	456	227	2	11	300	drumlin

Note: All landforms found between water depths of 75 to 230 m Fewer landforms were found here as compared to the western side of the bay and fewer measurements were possible Landforms 1 through 27 are from an area just south of Red Island, at the mouth of Eastern Channel Landforms 29 through 40 are from an area to the south where drumlins of different orientations are present					
drumlin dimensions:					
average	1039	318	3.4	11	224
standard deviation	259	101	0.5	5.9	15
standard error	72	28	0.14	1.64	4.2
crag-and-tail dimensions:					
average	1984	417	4.9	21	195
standard deviation	1241	162	2.1	12	20
standard error	439	57	0.7	4.2	7.1
megaflute dimensions:					
average	1647	363	4.7	8.7	231
standard deviation	311	102	0.9	4.3	13
standard error	98.4	32.3	0.28	1.36	4.1
westward drumlin dimensions:					
average	502	206	2.3	10	285
standard deviation	332	85	0.6	4.9	29
standard error	111	28	0.2	1.63	1.6
southwestward drumlin dimensions:					
average	1352	432	3.2	15	240
standard deviation	102	71	0.7	5.6	2.3
standard error	51	36	0	3	1.2

Table C.5 De Geer moraine and grounding-line moraine dimensions from southwesternmost Placentia Bay

De Geer and grounding-line moraines: Southwesternmost Placentia Bay						
	length (m)	width (m)	height (m)	spacing (m)	orientation (degrees)	landform
1	395	68	3	91	~26	De Geer moraine
2	222	58	3	57	~26	De Geer moraine
3	264	79	4	43	~26	De Geer moraine
4	466	91	5	41	~26	De Geer moraine
5	774	63	4	160	~26	De Geer moraine
6	215	65	3	147	~26	De Geer moraine
7	1871	141	9	74	~26	grounding-line moraine
8	222	49	4	62	~26	De Geer moraine
9	134	42	3	49	~26	De Geer moraine
10	179	40	6	42	~26	De Geer moraine
11	151	65	3	32	~26	De Geer moraine
12	190	50	4	46	~26	De Geer moraine
13	131	55	4	34	~26	De Geer moraine
14	155	52	6	56	~26	De Geer moraine
15	180	95	4	72	~26	De Geer moraine
16	330	89	3	116	~26	De Geer moraine
17	315	64	3	86	~26	De Geer moraine
18	320	135	11	70	~26	grounding-line moraine
19	397	112	3	195	~26	De Geer moraine
20	394	104	3	46	~26	De Geer moraine
21	1832	197	9	100	~26	grounding-line moraine
22	412	74	6	190	~26	De Geer moraine
23	292	65	5	98	~26	De Geer moraine
24	502	73	6	30	~26	De Geer moraine
25	593	81	4	124	~54	De Geer moraine
26	276	276	4	276	~54	De Geer moraine
27	196	90	2	79	~54	De Geer moraine
28	211	82	3	47	~54	De Geer moraine
29	510	75	4	147	~54	De Geer moraine
30	531	64	3	89	~54	De Geer moraine
average	422	86	4.5	90		
standard deviation	418	49	2.1	58		
standard error	76	9.0	0.38	10.6		

Note:
Moraine measurements were made along transects perpendicular to the ridge crests. Lengths of ridges were variable and ridges may be formed of discontinuous elements. Lengths reported here are for the length of the segment that intersected the transect. Moraines 1-25 were measured from transect 1 (**Figure C.1**). Moraines 25-30 were measured from transect 2 (**Figure C.1**). Orientations of ridges were taken along ridge crests.

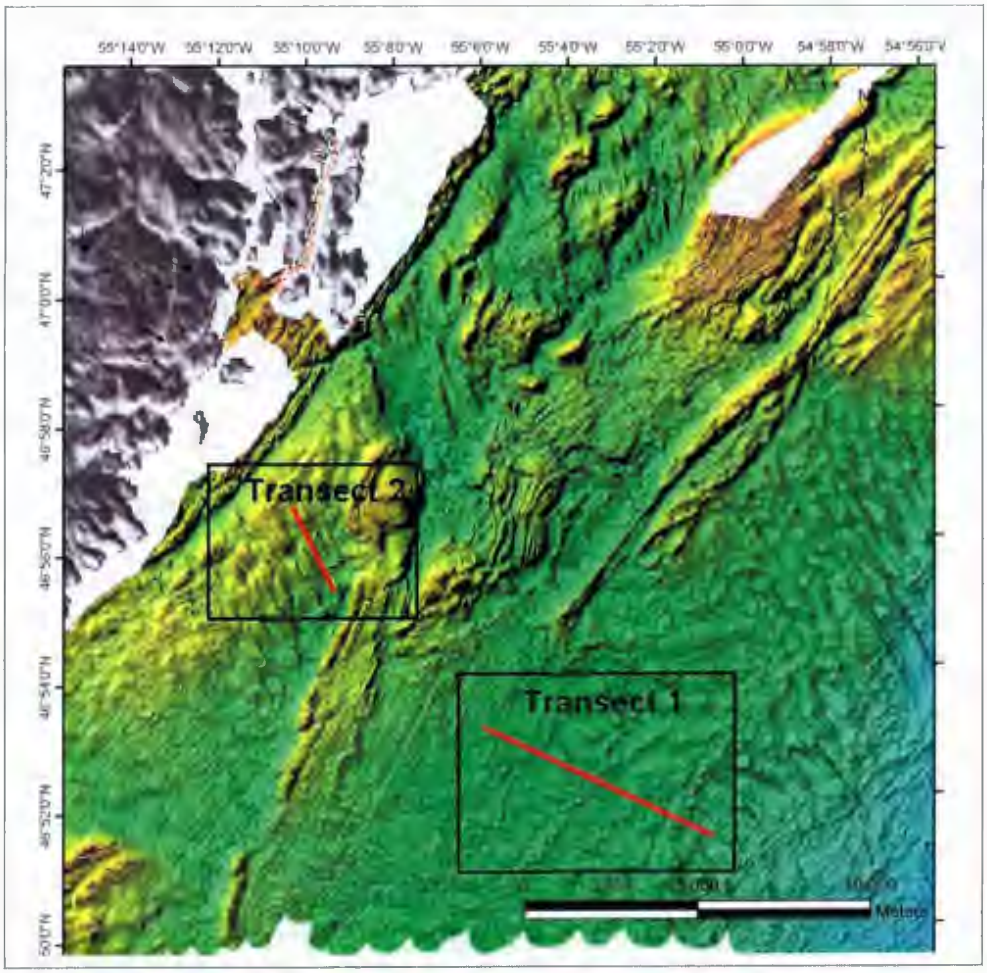

Figure C.1 Transects through De Geer moraine fields in southwestern Placentia Bay.

Table C.6 De Geer moraine dimensions from western Placentia Bay

De Geer moraines: Western Placentia Bay	length (m)	width (m)	height (m)	spacing (m)	orientation (degrees)
1	232	74	2	35	~38
2	227	69	2	163	~38
3	192	75	3	61	~38
4	198	89	2	44	~38
5	226	62	4	74	~75
6	267	74	5	55	~75
7	136	52	3	34	~75
8	336	66	4	20	~75
9	356	51	5	29	~75
10	720	54	4	78	~75
11	357	69	3	64	~75
12	495	48	5	54	~75
13	476	65	6	122	~62
14	687	121	5	71	~62
15	978	62	3	82	~62
16	1016	65	3	41	~62
17	984	78	4	29	~62
18	747	97	4	86	~62
19	850	61	5	81	~62
20	178	52	2	61	~98
21	108	34	3	44	~98
22	340	55	3	45	~98
23	611	72	4	70	~98
24	907	49	4	68	~98
25	736	54	5	20	~98
26	660	56	4	30	~98
27	438	55	5	22	~98
28	478	46	4	69	~98
29	411	59	4	65	~98
30	469	64	3	44	~98
average	494	64	3.8	59	
standard deviation	276	17	1.1	31	
standard error	51	3.1	0.18	5.7	

Note:
Moraines 1-4 were measured from transect 1 (**Figure C.2**). Moraines 5-12 were measured from transect 2. Moraines 13-19 were measured from transect 3. Moraines 20-30 were measured from transect 4.

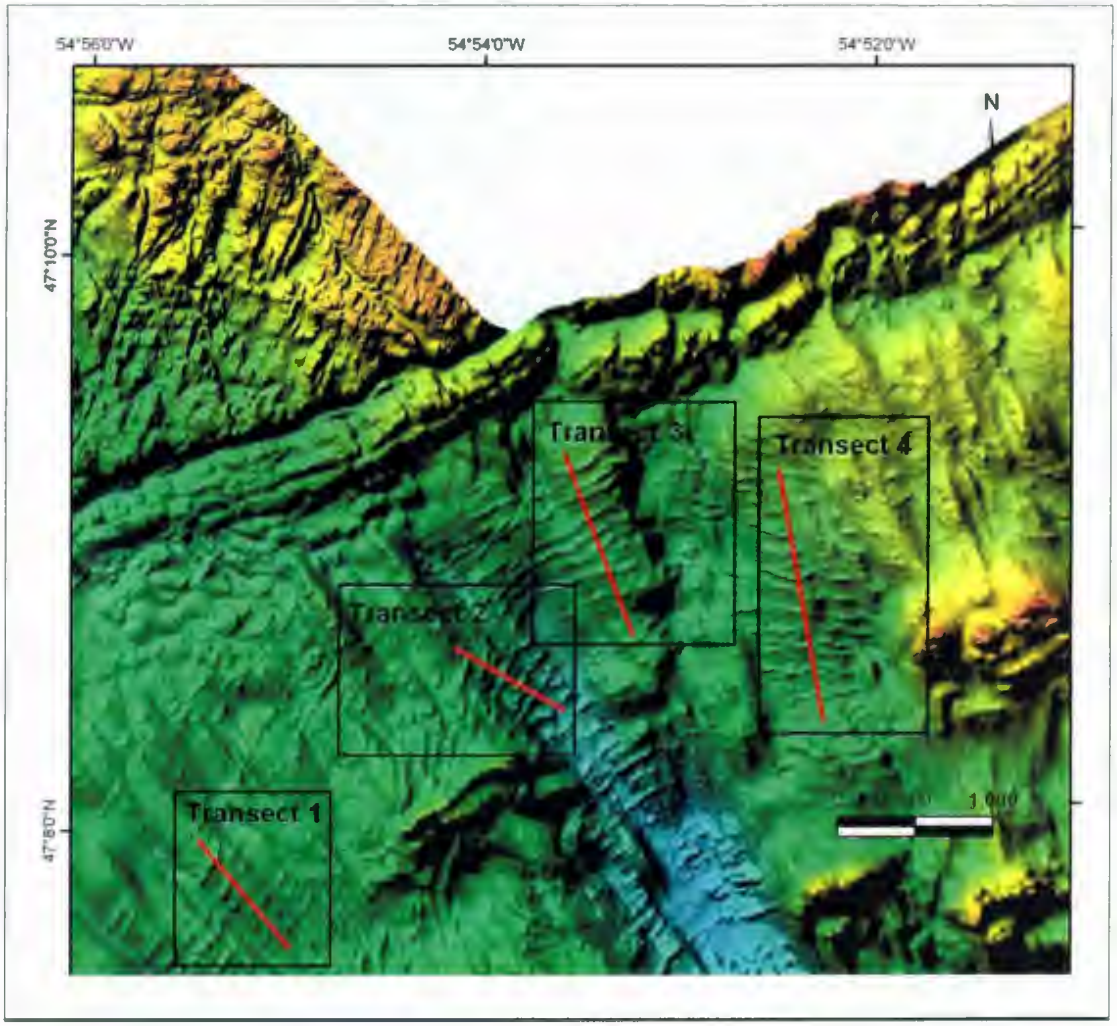

Figure C.2 Transects through De Geer moraine fields in western Placentia Bay.

Table C.7 De Geer moraine dimensions from Western and Central channels, western Placentia Bay.

De Geer moraines Western and Central channels					
	length (m)	width (m)	height (m)	spacing (m)	orientation (degrees)
1	509	85	5	197	~106
2	396	96	3	85	~106
3	399	70	3	53	~106
4	259	84	3	80	~106
5	500	177	4	74	~106
6	919	88	3	78	~106
7	489	116	4	99	~106
8	303	162	3	45	~106
9	866	107	4	205	~106
10	680	87	4	165	~106
11	795	123	5	45	~106
12	859	136	4	157	~106
13	727	144	3	106	~106
14	860	74	6	53	~114
15	675	79	3	43	~114
16	662	61	3	59	~114
17	442	51	3	54	~114
18	628	34	4	75	~114
19	450	49	3	80	~114
20	467	62	2	51	~114
21	489	65	3	21	~114
22	439	49	4	37	~114
23	402	57	2	34	~114
24	606	79	3	57	~114
25	362	95	3	58	~114
26	387	98	2	88	~114
27	312	53	6	40	~114
28	406	57	5	43	~114
29	248	87	3	53	~114
30	309	94	2	61	~114
average	528	87	3.5	77	
standard deviation	196	35	1.1	47	
standard error	36	6.4	0.20	8.6	

Note:
Moraines 1-13 were measured from transect 1 (**Figure C.3**). Moraines 14-30 were measured from transect 2.

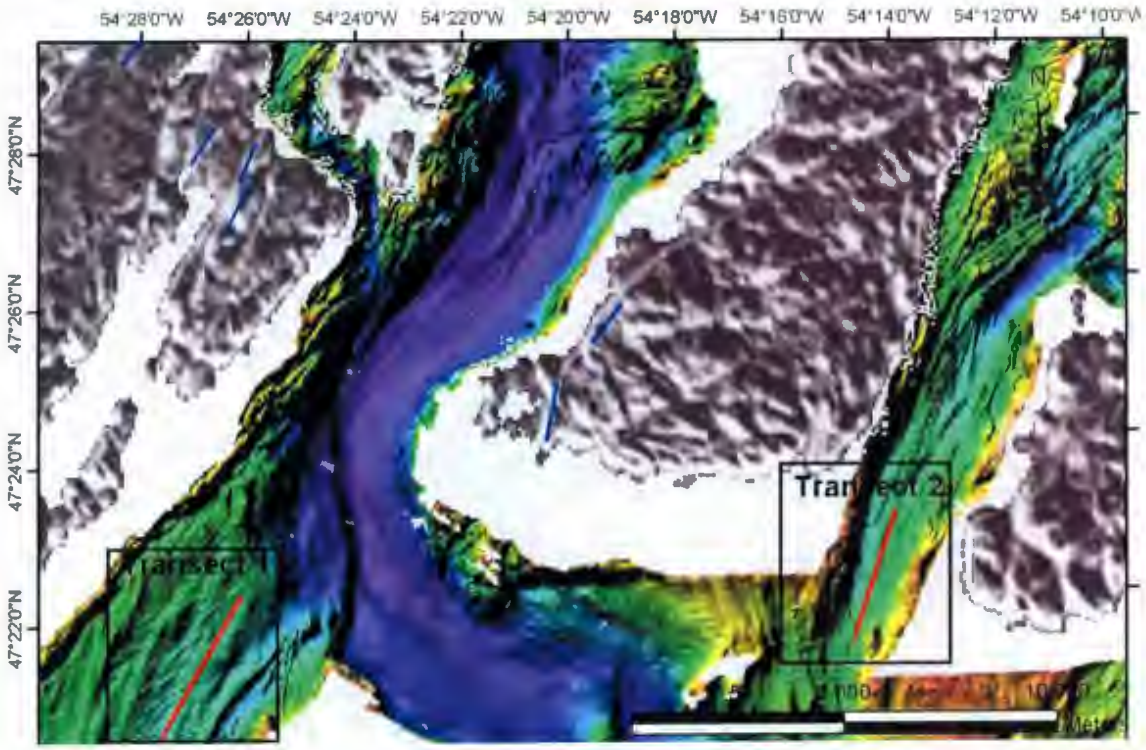

Figure C.3 Transects through De Geer moraine fields in Western and Central channels, western Placentia Bay.